

MOLECULAR AND CELLULAR PROPERTIES OF THE HUMAN BRAIN Na^+/H^+ EXCHANGER ISOFORM 5

by

Elöd Zala Szabó

Department of Physiology
Faculty of Medicine
McGill University
Montréal

March 2002

A thesis submitted to the Faculty of Graduate Studies and Research in partial fulfilment
of the requirements for the degree of Doctor of Philosophy.

© Elöd Z. Szabó 2002



National Library
of Canada

Acquisitions and
Bibliographic Services

395 Wellington Street
Ottawa ON K1A 0N4
Canada

Bibliothèque nationale
du Canada

Acquisitions et
services bibliographiques

395, rue Wellington
Ottawa ON K1A 0N4
Canada

Your file Votre référence

Our file Notre référence

The author has granted a non-exclusive licence allowing the National Library of Canada to reproduce, loan, distribute or sell copies of this thesis in microform, paper or electronic formats.

The author retains ownership of the copyright in this thesis. Neither the thesis nor substantial extracts from it may be printed or otherwise reproduced without the author's permission.

L'auteur a accordé une licence non exclusive permettant à la Bibliothèque nationale du Canada de reproduire, prêter, distribuer ou vendre des copies de cette thèse sous la forme de microfiche/film, de reproduction sur papier ou sur format électronique.

L'auteur conserve la propriété du droit d'auteur qui protège cette thèse. Ni la thèse ni des extraits substantiels de celle-ci ne doivent être imprimés ou autrement reproduits sans son autorisation.

0-612-78779-6

Canada

ABSTRACT

Na^+/H^+ exchangers (NHE) are transmembrane proteins that mediate the electroneutral exchange of Na^+ and proton across the plasma membrane. There are seven mammalian isoforms of the gene family identified to date. The recently cloned isoform NHE5 seems to be the most highly cell type-specific being probably expressed only in neurons. The objective of my research was to describe the basic biochemical and some of the regulatory characteristics of NHE5 in an effort to understand its *in vivo* function. To this end, the full-length cDNA of NHE5 was reconstructed and transfected into the NHE-deficient Chinese hamster ovary cell line AP1.

Pharmacological analyses demonstrated that H^+ -activated $^{22}\text{Na}^+$ influx mediated by NHE5 was inhibited by several classes of drugs at half-maximal concentrations that were intermediate to those determined for the high-affinity NHE1 and the low-affinity NHE3 isoforms. Kinetic analyses showed that the extracellular Na^+ -dependence of NHE5 activity followed a simple hyperbolic relationship and, unlike other NHE isoforms, the intracellular H^+ -dependence also exhibited first-order kinetics. Extracellular monovalent cations, such as H^+ and Li^+ , but not K^+ , acted as effective competitive inhibitors of $^{22}\text{Na}^+$ influx by NHE5.

To find novel interacting proteins that are involved in NHE5 regulation, a yeast two-hybrid screen of human brain cDNA library was conducted using NHE5 as bait. A clone encoding the AMP-activated protein kinase (AMPK) $\alpha 2$ subunit was further analyzed. AMPK is a serine/threonine kinase that is activated by elevated ratios of $[\text{AMP}]/[\text{ATP}]$, regulating various biological processes in response to hypoxia or exercise. AMPK $\alpha 2$ binds NHE5 *in vitro* and *in vivo*, and directly phosphorylates it *in vitro*. Activation of endogenous AMPK by AICAR, a membrane permeable AMP analogue, as well as heterologous expression of the full-length and constitutive active forms of $\alpha 2$ subunit increased the transporter activity measured by $^{22}\text{Na}^+$ influx.

The regulatory protein arrestin3 was also found to interact with NHE5 in the yeast two-hybrid screen. Arrestins were previously shown to associate with and regulate transmembrane proteins of the G protein-coupled receptor family. We demonstrate that NHE5 binds arrestin3 both *in vitro* and *in vivo*; and the binding is phosphorylation-dependent. When co-expressed in CHO cells, arrestin3 and NHE5 co-localize, and arrestin3 expression seems to attenuate the basal activity of the transporter. The data presented in this thesis reveals new aspects of both NHE regulation, and AMPK and arrestin function.

RÉSUMÉ

Les échangeurs d'ions Na^+/H^+ (NHE) sont des protéines transmembranaires qui médient l'échange électroneutral de Na^+ et des protons à travers la membrane plasmique. Sept isoformes de mammifère de cette famille génique ont été identifiées à ce jour. L'isoforme récemment clonée NHE5 semble avoir l'expression la plus spécifique à un type cellulaire, étant probablement exprimée seulement au niveau des neurones. L'objectif de ma recherche consistait à décrire la base biochimique de NHE5 et certaines caractéristiques concernant sa régulation en vue de comprendre sa fonction *in vivo*. À cette fin, l'ADNc pleine longueur de NHE5 a été reconstruit et transfecté dans des cellules AP1, qui représente une lignée de cellules ovariennes de hamster chinois déficiente en NHE.

Des analyses pharmacologiques ont démontré que l'influx de $^{22}\text{Na}^+$ activé par H^+ , qui est médié par NHE5 était inhibé par plusieurs classes de composés à des concentrations semi-maximales qui sont intermédiaires à celles déterminées pour les isoformes de haute affinité NHE1 et de faible affinité NHE3. Des analyses cinétiques ont montré que la dépendance de l'activité NHE5 aux niveaux de Na^+ extracellulaires suivait une relation hyperbolique simple et, au contraire des autres isoformes NHE, la dépendance aux H^+ intracellulaires a aussi présenté une cinétique de premier ordre. Les cations monovalents extracellulaires, tels que H^+ et Li^+ , mais pas K^+ , ont agi efficacement en tant qu'inhibiteurs compétitifs de l'influx de $^{22}\text{Na}^+$ produit par NHE5.

Afin de trouver des nouvelles protéines interagissant avec NHE5 et qui seraient impliquées dans sa régulation, un criblage par un système de "yeast two-hybrid" à partir d'une banque d'ADNc de cerveau humain a été mené en utilisant NHE5 comme cible. Un clone encodant la sous-unité $\alpha 2$ de la protéine kinase activée par l'AMP (AMPK) a ensuite été analysé. AMPK est une kinase sérine/thréonine qui est activée par des ratios élevés de $[\text{AMP}]/[\text{ATP}]$, régulant des processus biologiques variés en réponse à l'hypoxie ou à l'exercice. AMPK $\alpha 2$ lie NHE5 *in vitro* et *in vivo*, et mène à sa phosphorylation *in vitro*. L'activation de AMPK endogène par AICAR, un analogue de l'AMP perméable à la membrane, ainsi que l'expression hétérologue de la forme pleine longueur et

constitutivement active de la sous-unité $\alpha 2$, ont provoqué une augmentation de l'activité de transport mesurée par l'influx de $^{22}\text{Na}^+$.

La protéine de regulation arrestin3 a aussi été déterminée pour son interaction avec NHE5 dans le criblage par "yeast two-hybrid". Il a été montré précédemment que les arrestines peuvent s'associer avec, et réguler, les protéins transmembranaires faisant partie de la famille des récepteurs couplés à des protéines G. Nous avons démontré que NHE5 lie arrestin3 à la fois *in vitro* et *in vivo*, et que la liaison était dépendante de l'état de phosphorylation. Lorsque co-exprimée dans les cellules CHO, arrestin3 et NHE5 colocalisent, et l'expression de arrestin3 semble réduire l'activité basale du transporteur. Les données présentées dans cette these révèlent des nouveaux aspects de la regulation des NHE, ainsi que dans les fonctions de l'AMPK et des arrestines.

ACKNOWLEDGEMENTS

I would like to express my sincere gratitude to my supervisor, Dr. John Orlowski, for the support, advice and inspiration that was invaluable in the preparation of this thesis. His guidance and encouragement helped me through difficult times, personal and professional alike, during the years I spent in his laboratory. I would like to thank him for being a fair and helpful “boss” and friend. His good judgement in choosing members for his team has created a most enjoyable family-like environment, working in which was an exceptional experience. The dedication and enthusiasm for research I have acquired through his exemplar will be my treasures wherever I will get in the future.

I am indebted and grateful to Masayuki Numata, whose help, advice and precious time was immeasurable, not to mention his patience for my never-ending questions; and Pietro Iannuzzi, my right hand and Italian teacher, supplier of boost and froosh inspiration, and whose family was a shrine and shelter for my family. I am grateful to Frank Yu whose friendship helped me through the tough beginning; Annie Boucher, my consultant in kids’ stuff, for being the long-time only girl in the lab keeping all of us in balance; and Hans Zaun for his altruism and music.

I would also like to acknowledge the rest of the Olab family past and present members alike. Amole Khadilkar, my first comrade and inventor of epidemic OCD, for his sincere help; Colin Josephson, for his English and shared interest in history; Armin Akhavan, the almost-Olab-member; Preet Virdee and Caroline Girard for their amazing enthusiasm.

I also wish to thank Drs. Ursula Stochaj and John Hanrahan for their support and guidance in my research; and Dr. Norma Lake for her tutoring, and generosity in helping my family.

During my years at the Physiology Department, I have learnt a great deal about basic research, lab-work, values and friendship. I apologize for not being able to thank everyone who has been a part of this experience and also contributed in my thesis.

Finally, I would like to thank my wife and family without whose support this thesis would not have been possible and who all made it worthwhile.

I am dedicating this thesis to my Parents.

PREFACE¹

As an alternative to the traditional thesis format, the dissertation can consist of a collection of papers of which the student is an author or co-author. These papers must have a cohesive, unitary character making them a report of a single program of research. The structure for the manuscript-based thesis must conform to the following:

1. Candidates have the option of including, as part of the thesis, the text of one or more papers submitted, or to be submitted, for publication, or the clearly-duplicated text (not the reprints) of one or more published papers. These texts must conform to the "Guidelines for Thesis Preparation" with respect to font size, line spacing and margin sizes and must be bound together as an integral part of the thesis. (Reprints of published papers can be included in the appendices at the end of the thesis.)
2. The thesis must be more than a collection of manuscripts. All components must be integrated into a cohesive unit with a logical progression from one chapter to the next. In order to ensure that the thesis has continuity, connecting texts that provide logical bridges between the different papers are mandatory.
3. The thesis must conform to all other requirements of the "Guidelines for Thesis Preparation". In addition to the manuscripts the thesis must include a table of contents; an abstract in English and French; an introduction which clearly states the rational and objectives of the research; a comprehensive review of the literature (in addition to that covered in the introduction to each paper); and a final conclusion and summary.
4. As manuscripts for publication are frequently very concise documents, where appropriate, additional material must be provided (e.g., in appendices) in sufficient detail to allow a clear and precise judgement to be made of the importance and originality of the research reported in the thesis.
5. In general, when co-authored papers are included in a thesis the candidate must have made a substantial contribution to all papers included in the thesis. In addition, the candidate is required to make an explicit statement in the thesis as to who contributed to such work and to what extent. This statement should appear in a single section entitled "Contributions of Authors" as a preface to the thesis. The supervisor must attest to the accuracy of this statement at the doctoral oral defence. Since the task of the examiners is made more difficult in these cases, it is in the candidate's interest to clearly specify the responsibilities of all the authors of the co-authored papers.

¹ quoted from the "Guidelines for Thesis Preparation", Faculty of Graduate Studies and Research

CONTRIBUTIONS OF AUTHORS

Chapter 1: This study was designed and all experiments were carried out by E.Z. Szabó. M. Numata helped in the construction of the plasmid pNHE5, and G.E. Shull provided the original partial cDNAs and RACE products of NHE5. The study was coordinated and supervised by J. Orlowski.

The text and figures of this chapter were published in the *Journal of Biological Chemistry* (2000) 275: 6302–6307.

Chapter 2: The authors M. Numata and E.Z. Szabó contributed equally to this study. More specifically, the design of this study was a collaborative effort of M. Numata and E.Z. Szabó. With the exception of AMPK $\alpha 2$ cloning performed by M. Numata, and GST pull-down and $^{22}\text{Na}^+$ influx assays performed by E.Z. Szabó, all experiments were carried out by both authors. P. Iannuzzi helped in DNA sequencing, tissue culture and $^{22}\text{Na}^+$ influx assays. The study was coordinated and supervised by J. Orlowski.

This manuscript is in preparation for submission to the *Journal of Biological Chemistry*.

Chapter 3: The authors E.Z. Szabó and M. Numata contributed equally to this study. More specifically, the design of this study was a collaborative effort of E.Z. Szabó and M. Numata. With the exception of cloning and *in vivo* phosphorylation experiments performed by M. Numata, and GST pull-down and $^{22}\text{Na}^+$ influx assays performed by E.Z. Szabó, all experiments were carried out by both authors. P. Iannuzzi helped in DNA sequencing, tissue culture and $^{22}\text{Na}^+$ influx assays. The study was coordinated and supervised by J. Orlowski.

This manuscript is in preparation for submission to the *Journal of Biological Chemistry*.

STATEMENT OF CONTRIBUTION TO ORIGINAL KNOWLEDGE

1. Human NHE5 cDNA encodes a functional Na^+/H^+ exchanger when expressed in NHE-deficient Chinese hamster ovary AP1 cells.
2. NHE5 displays distinct pharmacological properties, half-maximal inhibitory values for several classes of drugs that are intermediate to those determined for the high-affinity NHE1 and the low-affinity NHE3 isoforms.
3. Like other isoforms, NHE5 exhibits first order dependence on the extracellular Na^+ concentration. Its intracellular H^+ -dependence, contrary to the other isoforms, conforms to simple Michaelis-Menten kinetics.
4. NHE5 is competitively inhibited by extracellular H^+ and Li^+ , and only slightly affected by K^+ .
5. NHE5, like NHE1-3, is inhibited by cellular ATP-depletion.
6. The AMP-activated protein kinase (AMPK) $\alpha 2$ subunit binds NHE5 cytoplasmic tail in the yeast two-hybrid system. The interaction was confirmed by both GST pull-down and co-immunoprecipitation experiments.
7. The predominant binding domain in AMPK $\alpha 2$ resides between amino acid residues 386 and 421. AMPK $\alpha 2$ binds to two independent regions in NHE5 cytoplasmic tail, G543-I654 and G789-L896. AMPK directly phosphorylates these regions *in vitro*.
8. Co-transfection of AMPK $\alpha 2$ with NHE5 in CHO cells caused pronounced redistribution of AMPK $\alpha 2$ to the plasma membrane with patchy appearances co-localizing with the NHE5 signal.
9. The transport activity of NHE5 is enhanced by the activation of AMPK by the AMP analogue AICAR and by overexpression of constitutive active mutants of the kinase.
10. Arrestin3 binds NHE5 cytoplasmic tail in the yeast two-hybrid system. The interaction was confirmed by both GST pull-down and co-immunoprecipitation experiments. The binding region in arrestin3 resides between the residues L291 and E339.
11. NHE5 is a phosphoprotein *in vivo*. The association of arrestin3 and NHE5 is phosphorylation dependent and is confined to region G689-G789 in NHE5.
12. When co-expressed, NHE5 and arrestin3 display nearly perfect co-localization in CHO cells.
13. Co-expression of arrestin3 and NHE5 in NHE-deficient AP1 cells seems to attenuate the basal activity of the transporter.

ABBREVIATIONS

AICAR	5-aminoimidazole-4-carboxamide riboside
AMPK	adenosine monophosphate-activated protein kinase
AP1	CHO-derived NHE-deficient cell line
BCECF	2',7'-bis(carboxyethyl)-5(6)-carboxyfluorescein
CHO	Chinese hamster ovary cells
CMV	cytomegalovirus
CNS	central nervous system
ECS	extracellular space
EIPA	5-(<i>N</i> -ethyl- <i>N</i> -isopropyl)amiloride
GPCR	G-protein coupled receptor
GRK	GPCR Kinase
HA	influenza virus hemagglutinin epitope
MAPK	mitogen-activated protein kinase
NHE	Na ⁺ /H ⁺ exchanger
NHE5-36HA3	NHE isoform 5 HA tagged at the first extracellular loop
pH _i	intracellular pH
pH _o	extracellular pH
PBS	phosphate buffered saline
PKA	adenosine 3',5'-cyclic monophosphate-dependent protein kinase A
PKC	diacylglycerol-dependent protein kinase C
PS120	NHE-deficient Chinese hamster lung fibroblast cell line
TM	membrane-spanning segment

TABLE OF CONTENTS

ABSTRACT	i
RÉSUMÉ	iii
ACKNOWLEDGEMENTS.....	v
PREFACE	vii
CONTRIBUTIONS OF AUTHORS	viii
STATEMENT OF CONTRIBUTION TO ORIGINAL KNOWLEDGE	ix
ABBREVIATIONS	x
TABLE OF CONTENTS	xi
INTRODUCTION.....	1
1.2 Mechanisms of pH _i regulation.....	4
1.3 pH regulation in the Central Nervous System.....	12
1.4 Na ⁺ /H ⁺ Exchangers.....	18
1.5 Rationale and Objectives.....	31
<i>Preamble to Chapter1</i>	33
CHAPTER 1	36
INTRODUCTION.....	38
EXPERIMENTAL PROCEDURES	41
RESULTS	45
DISCUSSION.....	49
<i>Preamble to Chapter2 and Chapter3</i>	55
CHAPTER 2	56
INTRODUCTION.....	59
EXPERIMENTAL PROCEDURES	61
RESULTS AND DISCUSSION.....	68
CHAPTER 3	75
INTRODUCTION.....	77
EXPERIMENTAL PROCEDURES	79
RESULTS AND DISCUSSION.....	88
GENERAL DISCUSSION AND CONCLUSION	97
REFERENCE LIST	106

INTRODUCTION

1.1.1 Intracellular pH

Most participants of the multitude of aqueous chemical reactions that characterize life are ionizable. Ionization is pH dependent and can greatly vary at physiological pH levels (pH 6.5 - 7.5). Proteins, by virtue of their composition, contain a large number of ionizable groups both on their surface as well as within their folded structure. The ionization status of a protein can influence its tertiary and quaternary structure, which in turn may perturb the function of the protein. (1;2)

Consequently, it is not surprising that cells try to tightly control their intracellular pH by several mechanisms (see Introduction 1.2). This is not to say that pH_i is stationary; rather, it should be viewed as a regulated parameter, which can also serve as a medium of signal transduction (3-5). The control of extracellular pH in multicellular organisms is mediated by neurohormonal mechanisms not discussed further in the current thesis.

1.1.2 Distribution of H^+ across the plasma membrane, quantity of pH_i

The Nernst equation predicts the steady state distribution of H^+ ions across the cell membrane at a given membrane potential

$$E_m = E_{H^+} = \frac{RT}{F} \ln \frac{[H^+]_o}{[H^+]_i} ,$$

where E_m is the membrane potential, E_{H^+} is the equilibrium potential for H^+ , R is the gas constant, T is the absolute temperature, and F is the Faraday constant. Assuming a membrane potential of -60mV , and a pH_o of 7.3, the equation yields a pH_i of about 6.35

at 37°C. However, the intracellular pH of virtually all cell types is ordinarily 7.1-7.2, necessitating the existence of active acid extruding mechanisms within the cell. (6;7)

1.2 Mechanisms of pH_i regulation

The thermodynamic process of passive H^+ accumulation within the cell has several sources. The major component is passive ion flux, influx of H^+ , egress of OH^- , and HCO_3^- driven by the substantial electrochemical gradient; and cellular metabolism (8;9). Transmembrane fluxes of non-ionized weak bases and acids can also contribute to intracellular acidification.

The mechanisms by which the cell counteracts acidification and achieves pH homeostasis include the following:

- 1) the fundamental physicochemical buffering,
- 2) transfer of H^+ or OH^- equivalents between the cytosol and organelles, and
- 3) active extrusion of acid-equivalents by transmembrane proteins. (7;10)

1.2.1 Physicochemical buffering, buffer systems

Physicochemical buffering is the inherent property of the aqueous solution of a weak acid and its salt form (or a weak base and its salt equivalent) to dampen pH changes of the solution induced by the admixture of strong acid or base. The major buffer systems of the body fluids are the bicarbonate, phosphate, and protein buffer systems (10).

The **bicarbonate buffer system** operates according to the chemical reaction



Although this buffer system is not very strong (the pK_a of the reaction is 6.1, far from the extracellular pH of 7.4 at $[HCO_3^-] = 28$ mM, $P_{CO_2} = 46$ mmHg), it is especially important as both constituents can be regulated at the systemic level. P_{CO_2} is regulated by the respiratory system on a timescale of minutes to hours, while $[HCO_3^-]$ is regulated by the kidneys on a timescale of hours to days.

The reaction $H_2PO_4^- = H^+ + HPO_4^{2-}$ comprises the **phosphate buffer system** ($pK_a = 6.8$). This system has a better efficiency at pH_o 7.4 than the bicarbonate buffer. The total concentration of phosphate intracellularly (75 mM) is considerably greater than extracellularly (4 mM), rendering the buffer substantially effective only within the cell, where the pH (7.1) is actually closer to its pK_a .

The **protein buffer system** is responsible for about three quarters of all chemical buffering, due to the high concentration of intracellular proteins (16 g/dl) and the great number of ionizable groups on them.

Physicochemical buffering is instantaneous, and for the most part (protein buffer) not regulated at the cellular level. With continuous intracellular loading of acid-equivalents saturating the buffer systems, the cell must possess means that will mediate removal of excess intracellular protons. This crucial step in long-term pH homeostasis is achieved by pH_i regulatory ion transporters.

1.2.2 Ion transporters in pH_i regulation

Eukaryotic cells express transmembrane proteins that actively regulate intracellular pH. These ion transporters are the Na^+ -independent $\text{Cl}^-/\text{HCO}_3^-$ exchanger, the Na^+ -dependent $\text{Cl}^-/\text{HCO}_3^-$ exchanger, the Na^+/H^+ exchanger (discussed in more detail in 1.4), the $\text{Na}^+/\text{HCO}_3^-$ cotransporter, and the Cl^-/OH^- exchanger (Fig. In.1). Recently, the distinction between the different bicarbonate-transporting proteins is becoming blurred with the characterization of atypical transporters (see below), and a new, bicarbonate transporter superfamily with members resembling each other about 30-50% is emerging (11).

The Na^+ -independent $\text{Cl}^-/\text{HCO}_3^-$ exchangers, better known as **anion exchangers** (AE) execute the electroneutral exchange of Cl^- and HCO_3^- across the plasma membrane. Given the physiological gradients of the respective anions, these transporters serve as an acidifying mechanism. Their activity is characteristically inhibited by stilbene drugs, such as DIDS (4,4'-diisothiocyanatodihydrostilbene-2,2'-disulphonate) or SITS (4-acetamido-4'-isothiocyano-2,2'-stilbenedisulfonate) (12;13).

Classically, there are three genes in the anion exchanger family: AE1 is the erythrocyte Band3 protein, AE2 is expressed in most tissues, while AE3 is expressed in brain and heart. Alternative splicing of each gene product gives rise to more isoforms, and may provide a molecular basis for the diversity of functions exhibited by AEs. These functions include the $\text{Cl}^-/\text{HCO}_3^-$ exchange in erythrocytes (Band3), pH_i regulation (13), Cl^- and HCO_3^- homeostasis in kidney (12;14), cell volume regulation (15), flexibility of the erythrocyte cytoskeleton (16-18), regulation of glycolysis in erythrocytes (19), and generation of senescent cell antigen (20;21). A newly cloned atypical transporter, termed

AE4, possessing greater identity to NBCs than to AEs is closing the functional gap between these ion transporter families. It is expressed in β -intercalated cells of the cortical collecting duct of kidney, and exhibits a sodium-independent and DIDS-insensitive $\text{Cl}^-/\text{HCO}_3^-$ exchange (22). There are two more ion transporters that are structurally unrelated to AEs (homology <15%), but can function in $\text{Cl}^-/\text{HCO}_3^-$ exchange mode. Pendrin (23), deficient in Pendred's syndrome, is highly expressed in thyroid, inner ear, and kidney proximal tubule and cortical collecting duct. While DRA (*down regulated in adenoma*), deficient in congenital chloride diarrhea, is highly expressed in colon and cecum, and probably performs the majority of $\text{Cl}^-/\text{HCO}_3^-$ exchange in intestinal epithelium (24).

Carbonic anhydrase (CA) accelerates the chemical process of $\text{CO}_2 + \text{H}_2\text{O} = \text{H}_2\text{CO}_3 = \text{H}^+ + \text{HCO}_3^-$ over 5000-fold (CAII has a turnover rate of $10^6/\text{s}$) providing substantial amount of substrate for bicarbonate transporters (25). Recently, the importance of this enzyme in bicarbonate transport has been further emphasised by the description of a transport metabolon (26). Metabolons are functional units of physically associated complex of proteins in a sequential metabolic pathway; known examples include enzymes of glycolysis, citric acid and urea cycles (27-29). The transport metabolon is formed by the C-terminal cytoplasmic tail of AE1 binding carbonic anhydrase isoform II (CAII). The association potentiates bicarbonate transport by coupling CAII enzymatic activity and AE1 anion exchange activity. The existence of bicarbonate transport metabolons might be a more general phenomenon, as sequence

alignment identifies putative CAII binding motifs in the extreme C-terminus of other bicarbonate transporters (26).

Na⁺-driven Cl/HCO₃⁻ exchanger (NDCBE) was the first pH regulatory ion transporter described (30;31). This mechanism is nearly as widespread as Na⁺/H⁺ exchange (7), and in many cell types more important in pH_i homeostasis (32-39). NDCBEs mediate the electroneutral exchange of intracellular Cl⁻ and H⁺ to extracellular HCO₃⁻ and Na⁺, thereby increasing pH_i. The transport activity is reversible and inhibited by the stilbene drugs DIDS and SITS.

According to the classical description, **Na⁺-HCO₃⁻ cotransporters (NBC)** are ion transporters that are *i)* electrogenic, *ii)* Na⁺ dependent, *iii)* HCO₃⁻ dependent, *iv)* Cl⁻ independent, and *v)* inhibited by stilbene drugs. Depending on the Na⁺:HCO₃⁻ coupling ratio and the membrane potential, they are either moving Na⁺ and HCO₃⁻ out of the cell at 1:3 stoichiometry, or they work in the other direction as an alkalizing mechanism at a stoichiometry of 1:2 or 1:1. Their functions include bulk reabsorption of filtered HCO₃⁻ in kidney proximal tubules, HCO₃⁻ secretion in pancreas and salivary ducts, and pH homeostasis in non-epithelial cells (reviewed in (11;40)). The functional versatility of NBCs is enhanced by several mechanisms. First, there are multiple isoforms with several spliced variants of the transporter (11). Second, the transporter is driven by three gradients, the concentration gradients for Na⁺ and HCO₃⁻, as well as the membrane potential, each of which can be controlled separately by other tissue specific mechanisms. Third, the direction of transport at a given membrane potential depends on the

stoichiometric ratio (q) of the transported ions. q is not a fixed attribute of an NBC isoform or variant. The stoichiometric ratio of the same isoform can be switched by phosphorylating the protein (41), changing $[Ca^{2+}]_i$ (42), or switching the cellular background (43).

Recent identification of several atypical bicarbonate transporters challenges the previous classification of bicarbonate transporters. The “prototype” Na^+ -driven Cl^-/HCO_3^- exchanger, NDCBE1, cloned from human brain (44), is actually a variant of the earlier cloned electroneutral human NBC3 (45), which does not seem to transport Cl^- . The reason for their conflicting transport properties is not clear. Another Na^+ -driven Cl^-/HCO_3^- exchanger, NCBE, cloned from a mouse insulinoma cell line, bears the highest amino acid identity to NBC2 and NBC3. NCBE has peculiar functional properties; it depends on extracellular Cl^- even in the forward mode exchanging extracellular HCO_3^- for intracellular Cl^- (46). AE4, as mentioned earlier, is structurally closer to NBCs than to anion exchangers. It is possible, that some of the functional differences between the members of this emerging bicarbonate transporter superfamily reflect differences in the actual experimental cell system.

The **Cl^-/OH^- exchanger** (CHE) is a recently described ion transporter that mediates the intracellular pH recovery of guinea-pig ventricular myocytes from an alkali load. It operates by electroneutrally exchanging intracellular OH^- to extracellular Cl^- ions. The exchanger is not sensitive to DIDS, but is inhibited by another stilbene derivative DBDS (dibenzamidostilbene-disulphonic acid) (47).

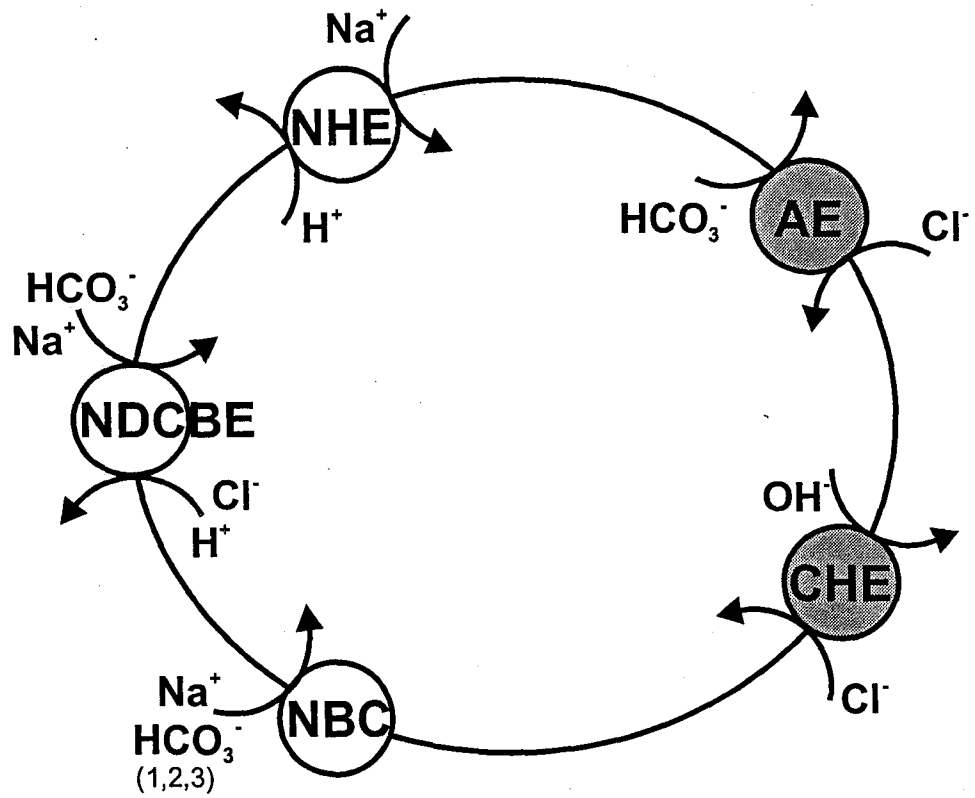


Fig. In.1. pH_i regulatory ion transporters.

Empty symbols represent acid recovery mechanisms, grey symbols indicate acid-loading transporters.

1.2.3 Other transmembrane proteins

Under certain conditions, the **vacuolar H^+ -ATPases**, a family of ATP-dependent proton pumps that are responsible for the acidification of intracellular compartments in eukaryotic cells (48) may play a role in pH homeostasis. In mitochondrion-rich cells, such as the intercalated cells of kidney cortical collecting duct, or the urinary epithelial cells in turtles, CO_2 induced intracellular acidification results in a transient $[Ca^{2+}]_i$ increase, which then causes exocytosis of V-ATPases containing vesicles into the plasma membrane, where they help to restore pH_i (49). V-ATPases, being constitutively present in the plasma membrane, mediate a portion of pH_i regulation of certain tumor cell lines (50), some glial cells (51;52), macrophages (53), and osteoclasts (54). In hepatocytes, the organellar V-ATPases are partly responsible for alkalization of the cytosol upon intracellular acid loading (55).

Voltage-gated H^+ channels represent a special type of facilitated diffusion. These channels are highly selective for H^+ , are activated by membrane depolarization, and their threshold voltage is strongly dependent on the pH gradient across the cell membrane. The combined result is that they only open when there is an outward gradient for H^+ ions. In human neutrophils, mononuclear phagocytes (56), and microglia (57), they are activated during respiratory burst. In snail neurons, they open during action potentials, probably to compensate for the metabolic cost of excitation (58;59). They are also abundant in alveolar epithelial cells, where they probably expedite CO_2 elimination

by working in parallel with carbonic anhydrase and either a $\text{Cl}^-/\text{HCO}_3^-$ exchanger or a presumed anion channel (56).

1.3 pH regulation in the Central Nervous System

Because of the many cellular processes sensitive to pH, all mammalian cells closely regulate their intracellular pH (7). Some of the general cellular and biochemical processes that are influenced by pH are cell metabolism, contractile function of muscle cells, Ca^{2+} homeostasis, cytoskeletal organization, membrane permeability, cell cycle, and cell proliferation (reviewed in (8;60-62)). A frequently cited example in cell metabolism is the extremely pH-sensitive enzyme phosphofructokinase 1, a major controller of glycolysis, which can be fully activated or arrested by 0.1 unit changes in pH within the physiological range (63).

Although it is obviously very important to control pH_i in every tissue, it is inevitably even more so in the central nervous system (CNS), where special considerations add another dimension to pH_i regulation. First, the blood-brain barrier (BBB) sealing off acid-base equivalents, with the exception of CO_2 , and the choroid plexus actively producing cerebrospinal fluid with reasonably constant constituents provide a stable overall extracellular pH only changed under pathological conditions (e.g. ischemia, status epilepticus). Second, the extracellular space (ECS) in CNS has a special structure comprising only 20% of the total volume of the brain and being often as narrow as 20 nm between a neuron and a glial cell (64). This distance defines such a small volume, that neuronal electrical activity, ordinarily unable to significantly alter extracellular fluid, can change its ionic composition tremendously. Extracellular K^+ concentration during repetitive action potentials can reach otherwise lethal values had it not been for the glial syncytium to control this key determinant of membrane potential.

Similar reasoning is applicable to the transport of polarized acid-base equivalents, such as H^+ , across plasma membranes of these closely adjacent cells.

Considering the tight control of extracellular pH (BBB, choroid plexus) in the central nervous system, and the fact that neuronal activity causes well-defined pH transients (reviewed in (4;65)) it is straightforward to postulate a signaling role for H^+ in between CNS cells (5;66;67).

1.3.1 Processes influenced by pH in CNS

In general, neural excitability of the CNS is suppressed by acidosis, and enhanced by alkalosis. This dependence is generated as a sum of a large number of pH-sensitive processes. Intrinsic neuronal excitability is altered by pH-sensitive voltage-gated ion channels, while both excitatory and inhibitory synaptic transmission is influenced by pH-sensitive ligand-gated ion channels (reviewed in (68-70)).

Voltage-gated Na^+ channel conductance is blunted by extracellular H^+ in all cells examined (reviewed in (69)). By contrast, K^+ currents are only slightly affected by pH change (71) with the notable exception of the inward rectifier K^+ channel HIR/IRK3, which is depressed by external H^+ with a pK around 7.4 (72). High-voltage activated (HVA) Ca^{2+} currents are enhanced by external alkaline shifts. They are particularly sensitive to pH; only 0.1 unit pH shifts near presynaptic HVA Ca^{2+} channels can, in principal, lead to functional changes in synaptic transmission (71;73).

Not all ion channels are sensitive to changes in pH. Interestingly, even within one ligand-gated ion channel family, there are pH-sensitive and non-sensitive channels. For example, in the case of $GABA_A$ receptors, pH sensitivity is controlled by the subunit

composition. Receptors comprised of $\alpha 1\beta 1$ subunits are enhanced by low pH, while the $\alpha 1\beta 1\gamma 2S$ receptor is pH insensitive (74). Another example is the glutamate-gated excitatory cation channel, the NMDA receptor. The NMDA receptor is tonically inhibited at physiological pH. The presence or absence of the 21 amino acid residues encoded by exon 5 in the NR1 subunit determines the proton inhibition of the receptor (75).

In addition to the above-mentioned pH-sensitive ion channels, there are also H^+ -gated channels in both central and peripheral neurons. At the molecular level, these channels are formed as heteromultimeric complexes of three different subunits (ASIC1-3, for acid-sensing ion channel), and belong to the amiloride-sensitive Na^+ channel family. They have kinetic and ion selectivity properties similar to other ligand-gated cation channels (e.g. NMDA receptor), and require acidic pH fluctuations for activation (76).

Finally, gap junctions of the glial syncytium are also particularly pH-sensitive. Cytoplasmic acidification decreases the open probability of junctional channels formed by Cx43 and Cx32 subunits, and thereby reduces inter-glial communication (77).

The fact that members within a gene family, such as GABA receptors, display considerable variation in their pH sensitivity suggests that proteins influenced by changes in ambient pH indeed have evolved to sense these changes and respond in a functionally significant way. Certainly, having domains that are allosterically regulatable by pH in a protein without a practical purpose would only confer instability onto a highly-organized system such as the brain.

1.3.2 Mechanisms of activity-induced changes in pH

The relationship between neural activity and pH is reciprocal. pH transients influence neural activity, and conversely, transmembrane fluxes of acid-base equivalents can be elicited by neural activity.

For instance, postsynaptic neuronal depolarizations large enough to activate voltage-gated Ca^{2+} channels lead to a rise in $[\text{Ca}^{2+}]_i$. This increase, in turn, will activate the plasmalemmal $\text{Ca}^{2+}/\text{H}^+$ -ATPase generating a large sustained decrease in pH_i and a simultaneous increase in pH_o (65).

Another type of acid load is caused by inhibitory synaptic transmission. The activation of GABA- and glycine-gated anion channels leads to an efflux of HCO_3^- through the anion conductance, thereby acidifying the interior of the neuron (78).

The widespread mechanism of glutamate uptake into neurons and glial cells is essential for terminating the excitatory synaptic transmission of this neurotransmitter. Glutamate uptake carriers mediate a Na^+ -dependent electrogenic transport, which also generates pH changes across cell membranes. The carrier transports 2 Na^+ ions along with glutamate into, and a K^+ ion out of, the cell. Additionally, there is movement of an acid-base equivalent that acidifies the interior in the form of either a H^+ moving in or a OH^- moving out of the cell (79;80).

It seems likely that the main role of acid extruding pH_i regulatory transporters in both neurons and glia is to reestablish intracellular pH after activity-evoked changes.

1.3.3 pH_i control mechanisms in mammalian CNS

Studies on CNS primary cell cultures, neural and glial cell lines, as well as *in situ* experiments demonstrated that neurons and glia possess a variety of pH regulatory

transporters with cell-specific patterns of expression (reviewed in (81;82)). Na^+/H^+ exchangers and Na^+ -driven $\text{Cl}^-/\text{HCO}_3^-$ exchangers are the most abundant acid-extruders in both neurons and glia, while some cells (e.g. hippocampal astrocytes (51)) harness the vacuolar-type H^+ -ATPase in intracellular pH regulation, though at limited capacity. Acid-loaders are the plasma membrane $\text{Ca}^{2+}/\text{H}^+$ pump and the anion exchanger. The anion exchanger is an acid-loader present in both neurons (AE3) and glia, while the plasma membrane $\text{Ca}^{2+}/\text{H}^+$ pump is found in neurons. The $\text{Ca}^{2+}/\text{H}^+$ pump removes moderate loads of Ca^{2+} entered during neuronal excitation and simultaneously decreases neuronal pH_i (83).

Interestingly, electrogenic $\text{Na}^+/\text{HCO}_3^-$ cotransporter has been functionally demonstrated only in glia, where it is an abundant pH regulatory protein (81). Its presence in glia provides a mechanistic basis for the interesting phenomenon of depolarization-induced alkalinization (DIA, see below). However, recent evidence demonstrates that not only the electroneutral NBC3 (44;45), but also the electrogenic NBC1 protein is, in fact, expressed in neurons. Its localization is apparently restricted to neuronal processes explaining the lack of physiological confirmation by common techniques such as the pH-sensitive dye (BCECF) loading of the cell soma (84).

1.3.4 Depolarization-induced alkalinization (DIA)

The remarkable paradigm of DIA illustrates the tight functional coupling of glia and neurons in pH regulation. During neuronal activity, extracellular K^+ levels are sufficiently elevated to depolarize the adjacent glial cells. The increase in $[\text{K}^+]_o$, as discussed above, is further enhanced by the proximity of glial and neuronal cell

membranes. Depolarization drives HCO_3^- into the glial cell through the electrogenic NBC producing an alkaline pH shift. Inevitably, the intracellular alkaline shift is accompanied by an acidic shift in the extracellular space of at least the same magnitude owing to spatial constraints and limited buffering capacity. During intense neuronal activity, such as epileptic seizures, the magnitude of the acidic pH transients can theoretically reach values that would dampen the electrical activity by suppressing neuronal excitability, and thereby limit the expansion of epileptic focus. In essence, DIA constitutes an intrinsic safety mechanism in the brain demonstrating the functional co-dependence of glia and neurons. (5;67;82;85-87)

1.4 Na⁺/H⁺ Exchangers

Na⁺/H⁺ exchangers (NHE) are a functionally diverse group of ubiquitous transmembrane proteins that mediate the electroneutral exchange of Na⁺ and H⁺ across the membrane. With seven mammalian isoforms (NHE1 – NHE7) identified to date, they form the largest gene family of the pH_i regulatory ion transporters. Their function encompasses not only the maintenance of pH_i homeostasis, but also cell volume regulation, (re)absorption of Na⁺, and indirectly HCO₃⁻, across epithelia, promotion of cell proliferation, regulation of actin cytoskeleton dynamics (cell adhesion and motility), and organellar ion and volume homeostasis. (88-93)

1.4.1 Structural features

Based on their amino acid sequence, hydropathy analysis of all isoforms predicts a similar structure with two distinct domains; a hydrophobic *N*-terminal transmembrane region containing 12 putative membrane-spanning segments (TM), and a large hydrophilic *C*-terminal cytoplasmic region that contains numerous recognition motifs for various protein kinases and other regulatory molecules.

The amino acid identity amongst the isoforms in the transmembrane domain is 45 to 65%, while in the cytoplasmic domain it is only 25 – 35%. The organellar isoforms (NHE6 and NHE7) constitute a disparate group, sharing an overall amino acid identity of ~70%, while resembling the other isoforms to a much smaller extent (20 – 25%) (89-91). Most of the shared identity of the isoforms resides in TM3 – TM12. TM6 and TM7, being 95% identical between the plasma membrane isoforms, likely participate in cation

translocation, whereas TM4 and TM9 are responsible for pharmacological antagonist binding (94;95).

Several recent topological studies have refined our understanding of the secondary and tertiary structure of NHEs. Wakabayashi *et al.* (96) used substituted cysteine accessibility analysis to provide a more precise model of the secondary structure of NHE1. Their results largely support the previously predicted structure with some notable differences. Namely, parts of the second and fourth intracellular loop are accessible to external SH-directed reagents, suggesting that they may form part of the ion translocation pore. The originally predicted TM10 seems to be entirely embedded in the lipid bilayer, while the last extracellular loop forms an intracellular loop, a new TM (TM11), and an extracellular loop. Recently, Biemersderfer *et al.* (97) found the extreme C-terminus of NHE3 extracellularly accessible in brush border membrane vesicles and apical region of proximal tubule to monoclonal antibodies directed to the last 131 amino acids of NHE3. However, the analyses of Wakabayashi indicated that the entire C-terminal tail of NHE1 is cytoplasmic (96). The basis for these differences is unclear. Our own data using C-terminal epitope-tagged isoforms (NHE1_{HA} and NHE3_{HA}) in AP1 cells affirms the generally accepted view of the C-terminal tail being cytoplasmic. Recently, Williams (98) defined the three-dimensional structure of the Na⁺/H⁺ antiporter of the inner membrane of *E. coli* (NhaA) by electron cryo-microscopy, giving the first accounts on the architecture of an ion-coupled transport protein. In this study, NhaA is depicted as a protein with 12 tilted transmembrane spanning helices.

The quaternary structure of NHEs is not well defined. Homodimerization is suggested by immunological data (99) in case of NHE1 and NHE3, and NhaA has been

shown to form homodimers by electron cryo-microscopy (98). Dimerization is possibly mediated through formation of disulfide bonds in the *N*-terminal transmembrane domain (99;100). Nevertheless, the monomer seem to represent the minimal functional unit for Na^+/H^+ exchange, demonstrated by the failure of a null-mutant (NHE1-E262I) to exert dominant negative effect on transporter function when co-expressed with the wild-type in NHE-deficient PS120 cells (99).

NHE1 contains both *N*- and *O*-linked oligosaccharides (101), while NHE2 exhibits only *O*-linked glycosylation (102). In contrast, NHE3 seems not to be glycosylated (101). The glycosylation status of the other isoforms is not yet determined.

1.4.2 Biochemical features

Kinetics – Under physiological conditions NHEs mediate the exchange of extracellular Na^+ for intracellular H^+ at 1:1 stoichiometry. The extracellular Na^+ dependence of the transport activity exhibits a simple Michaelis-Menten kinetics. The apparent affinity constant ($K_{0.5}$) for external Na^+ of the different isoforms is 3 – 50 mM, well below physiological values of $[\text{Na}^+]_o$, excluding external Na^+ as a regulatory substrate. (88;91;103;104)

The external cation-binding site is not selective for Na^+ . Other monovalent cations, such as H^+ , Li^+ , NH_4^+ can compete with Na^+ for binding, sometimes with substantially higher affinity for the exchanger (105;106). For instance, the half-maximal inhibitory value (K_i) of NHE2 for Li^+ is 2.2 mM, whereas $K_{0.5}$ of Na^+ for this isoform is 50 mM. However, the actual turnover rate for these other transported cations is much slower, than it is for Na^+ (103;104;107), indicating that Na^+/H^+ exchange is the favoured mode of transport. K^+ , another physiologically relevant cation, does not seem to be

translocated in isoforms NHE1 – NHE3, but competes with Na^+ for the external binding site of NHE1 (103;104).

Na^+/H^+ exchange is normally quiescent at physiological pH, and becomes allosterically activated by intracellular H^+ when pH_i drops below a threshold level (103;106;108).

Pharmacology – Initially, inhibitors of Na^+/H^+ exchange fell into three categories. The diuretic compound amiloride, and its 5-*N* alkyl substituted derivatives formed the primary set, and were used to divide the isoforms into amiloride-sensitive and amiloride-resistant classes. While amiloride is not a very specific antagonist, inhibiting other Na^+ transport proteins (e.g. the epithelial Na^+ channel ENaC) as well, its derivatives such as ethylisopropyl- (EIPA), dimethyl- (DMA), or methylpropyl-amiloride (MPA) are both more potent and more selective (95;103;109-112).

The acylguanidine compounds HOE694 and HOE642 (cariporide) bind NHEs more selectively, particularly NHE1, and in fact are proposed as NHE1 specific therapeutic agents in ischaemia/reperfusion injury of the heart (113;114).

The third group was formed by other unrelated pharmacological agents, such as cimetidine, clonidine, and harmaline. These drugs block NHE activity at generally lower efficiency (103;104). While being structurally distinct, they all have either a pyrazine, an imidazoline, or a guanidine moiety, therefore bearing some similarity to each other (Fig. In.2). The general order $\text{NHE1} > \text{NHE2} \gg \text{NHE3}$ characterizes most drugs listed above in their isoform specificity.

Recently, propelled by clinical interest (113;115), a new generation of NHE antagonists is emerging. EMD 84021, EMD 94309, EMD 96785 (eniporide) are further

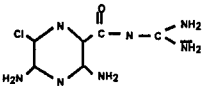
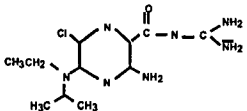
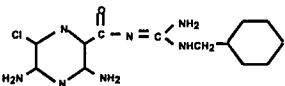
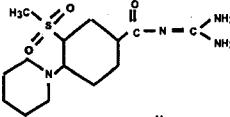
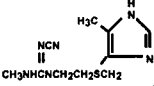
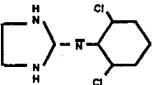
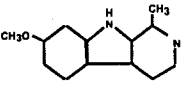
Pharmacological Agent	Structural Formula	Inhibition Constants (IC ₅₀ , M)	
		NHE1	NHE3
Amiloride		1.6×10^{-6}	1.0×10^{-4}
Ethylisopropylamiloride		1.5×10^{-8}	2.4×10^{-6}
Benzamil		1.2×10^{-4}	1.0×10^{-4}
HOE694		1.6×10^{-7}	6.5×10^{-4}
Cimetidine		2.6×10^{-5}	6.2×10^{-3}
Clonidine		2.1×10^{-4}	6.2×10^{-4}
Harmaline		1.4×10^{-4}	1.0×10^{-3}

Fig. In.2. **Chemical structures and relative affinities of NHE antagonists.** The half-maximal inhibitory values for NHE1 and NHE3 were obtained from Orłowski, *JBC* (1993) **268**:16369-77.

derivatives of the HOE family (116), while SL 59.1227 is a novel imidazolyloypiperidine NHE inhibitor (117), zoniporide is a carbonylguanidine based compound (118), and T-162559 is an aminoguanidine derivative (119). These drugs are at least as potent as HOE642 in inhibiting NHE1. Another drug, S3226, a bismethacryloyl guanidine derivative, was identified as a novel potent NHE3 inhibitor (120).

According to several studies, the mechanism of inhibition by amiloride compounds is competitive, suggesting a common binding site for both Na^+ and the drug (107;110). However, recent site-directed mutagenesis (121;122) and chimera analyses (112) have demonstrated that residues in TM4 and TM9 contribute to drug sensitivity without affecting Na^+ affinity. Another recent study illustrates the complex involvement of TM4 in both Na^+ and drug binding. Touret *et al.* (123) describe that a single mutation in TM4 (F162S) results in both low Na^+ and drug (cariporide) affinity; and this low Na^+ affinity can be reverted without changing the drug affinity by mutations at distant locations (I169S or I170T) within the same transmembrane segment.

1.4.3 Tissue distribution and physiology

NHE1 is expressed at the plasma membrane of virtually all cells and tissues, and is directed to the basolateral membrane of polarized epithelial cells. It most likely fulfills the general function of intracellular pH and cell volume homeostasis (91;92). Recently, a novel role in the maintenance of cell shape has been proposed for NHE1. Independent of cation translocation, NHE1 has been found to regulate the cortical cytoskeleton organization through its direct binding to ezrin/radixin/moesin (ERM) proteins. The

ERM family of proteins can directly bind both actin and certain plasmalemmal proteins, thereby linking the actin cytoskeleton to the plasma membrane (124).

A spontaneous mutation, as well as targeted disruption of the *Nhe1* locus has provided surprising results on its importance in mammalian physiology (125;126). Although the null mutation of *Nhe1* caused significant mortality before weaning, surviving mice had no gross developmental defects and displayed a CNS restricted phenotype. The novel seizure phenotype, slow-wave epilepsy, and the ataxia exhibited by NHE1-knockout mice demonstrate the vulnerability of certain CNS cell-types and the delicate balance of pH-dependent neuroexcitability and neuron survival.

NHE2 is expressed predominantly in the gastrointestinal tract and, to lesser extent, in kidney, brain, testis, uterus and lung (127-129). Although the expression in kidney and the targeting of the exchanger is somewhat controversial (88;91), it seems likely that NHE2 is localized to the apical membrane of epithelial cells. Recently, two unique proline-rich motifs resembling SH3 binding domains in the cytoplasmic tail of NHE2 have been implicated in apical sorting of the transporter (130).

The tissue and subcellular distribution of NHE2 implies a major physiologic role in Na⁺ absorption of colon. However, the *Nhe2* null mutant mice do not exhibit any obvious defects in intestinal function. Instead, they show a deficiency in gastric acid secretion and a loss of parietal cells after weaning, proving an essential role of NHE2 in the long-term viability of these cells (131).

NHE3 is predominantly expressed in the epithelial cells of the gastrointestinal tract and kidney. It is directed exclusively to the apical membrane of these cells, where it has been shown to mediate the (re)absorption of Na^+ and, indirectly, HCO_3^- ; conclusions derived largely from the use of pharmacological antagonists (91;92;132). The physiology of NHE3 has recently been confirmed by the targeted disruption of the gene. NHE3-knockout mice show severe absorptive defects in both intestine and proximal convoluted tubules, are mildly acidotic, have reduced blood pressure, and have slight diarrhea (133).

NHE4 mRNA is expressed abundantly in stomach epithelium and kidney inner medullary collecting duct, with lower levels in uterus, skeletal muscle, and pancreas (127;132). The protein was detected at the basolateral membrane of different epithelial cells of pancreas, kidney, and stomach (134;135), and NHE4 activity was demonstrated in the basolateral membrane of macula densa and thick ascending limb cells (136;137). The physiological role of NHE4 remains unclear, but it may mediate NH_4^+ transport across the basolateral membrane of distal nephron segments (136).

1.4.5 Regulation of NHEs

The activity of NHEs is regulated by a variety of signaling pathways and other stimuli including the PKA and PKC pathways, Ca^{2+} /calmodulin, certain accessory proteins (CHP, NHERF), and cell volume (reviewed in (88;91;93)). A brief summary of the regulation of NHE1 and NHE3 is presented below.

In general, the regulation of a transmembrane transporter involves changes in its kinetic properties, either the maximal velocity (v_{max}) of the reaction or the substrate

affinity (K_M or pK) of the enzyme. The first usually represents a change in the number of active transporters in the membrane, while the second represents a functional change at the level of individual transporters (*i.e.* being more or less active under a given condition).

The regulation of NHE1 activity by various cell-surface receptors converge on a limited number of NHE1-interacting proteins that mediate conformational changes in the C-terminal cytoplasmic tail of the transporter altering the affinity of the internal H^+ transport site (93).

Three serine/threonine kinases directly phosphorylate and activate NHE1. $p90^{RSK}$ phosphorylates Ser703 in the cytoplasmic tail of NHE1, and plays a key role in growth factor mediated activation of the transporter through the MEK1-ERK1/2- $p90^{RSK}$ pathway (138-140). Activation of NHE1 by lysophosphatidic acid and the G protein $G\alpha_{13}$ is mediated through the low molecular weight GTPase RhoA. The downstream effector, the RhoA target kinase p160-ROCK, directly phosphorylates NHE1 in the cytoplasmic tail (62). Integrin receptor signaling also couples to the activation of NHE1 through the RhoA-ROCK cascade (141). The adaptor protein Nck through its downstream effector, the Nck-interacting kinase (NIK), mediates platelet-derived growth factor activation of NHE1. NIK directly binds to NHE1 and phosphorylates it at a distinct site in the cytoplasmic tail (142).

There are two binding sites, a low-affinity and a high-affinity, for calmodulin in the cytosolic tail of NHE1. The regulation of NHE1 activity in response to Ca^{2+} -mediated signaling mechanisms is realized through Ca^{2+} /calmodulin binding to the high-

affinity domain (residues 636-656). Deletion of this region results in constitutive activation of NHE1, suggesting that in the absence of Ca^{2+} signaling it may function as an autoinhibitory domain (143-145).

The ubiquitous calcineurin B homologous protein (CHP), a Ca^{2+} -binding phosphoprotein, binds to NHE1-3 at the juxtamembrane region of their C-terminal cytoplasmic tail (residues 515-530 in NHE1), and serves as an essential cofactor in Na^+/H^+ exchange activity. The CHP-binding domain is conserved among NHE1-5, suggesting that CHP-binding is a common requirement for exchange activity of all plasma membrane-type NHEs (146).

In the regulation of NHE3, both changes in v_{\max} as well as K_M occur depending on the stimulus. The transport activity of NHE3 is potently inhibited by the elevation of cAMP concentration. This inhibition is only partially explained by direct phosphorylation of the exchanger, since abolition of serine 605, the only serine exhibiting PKA-dependent phosphorylation, does not completely abrogate cAMP-mediated inhibition (147). This finding predicts the presence of accessory proteins in cAMP-mediated regulation of NHE3. Indeed, several proteins have been found to associate with NHE3 (146;148). Most notably, Na^+/H^+ exchanger regulatory factors, NHERF1 and NHERF2, have been implicated in the PKA regulation of the exchanger. NHERF1 is reported to be necessary for conferring cAMP-mediated inhibition of NHE3 when co-expressed in the NHE-deficient PS120 cells (148-150). However, this latter finding is controversial, since in independent studies NHE3 expressing PS120 cells seem to exhibit forskolin-induced inhibition of transport activity without exogenous NHERF ((151),

Orlowski and Wakabayashi unpublished). Nevertheless, NHERFs, containing two PDZ domains, and being able to bind not only NHE3 and other membrane transporters, but ezrin as well, might serve as multifunctional adaptor proteins involved in diverse aspects of cellular signaling (149;152;153).

Studies by the Grinstein and Orlowski laboratories revealed, that a substantial portion of NHE3 in CHO cells is intracellularly located (154). The exchanger is endocytosed via clathrin-coated vesicles (155), and continuously cycles between the plasma membrane and the endosomal vesicles in a phosphatidylinositol 3' kinase (PI3K)-dependent manner (156). The inhibition of NHE3 transport activity by drugs, such as cytochalasinB, latrunculinB, and jasplakinolide, proves the importance of actin cytoskeleton in the optimal activity of the transporter (157). CytochalasinB and latrunculinB disrupts the actin filaments by independent mode of actions, while jasplakinolide actually stabilizes filamentous actin (158-160), implying that a dynamic actin cytoskeleton is a prerequisite of NHE3 function. Considering that the cytoskeleton is known to be involved in endo- and exocytosis (161), and the acute regulation of some membrane transporters (e.g. aquaporin2) (162;163) involve recruitment of the proteins to and from the plasma membrane, it is straightforward to hypothesize that NHE3 transport activity is regulated by altering the dynamics of its trafficking process. In accordance, Donowitz *et al.* (164) demonstrated that in intact ileum and Caco-2 cells, acute regulation of NHE3 by PKC and epidermal growth factor involves vesicular trafficking, changing the amount of transporter on the plasma membrane. Surprisingly, in CHO-derived AP1 cells, while NHE3 activity is inhibited by drugs interfering with the normal organization of the actin cytoskeleton, there is no simultaneous change in the number of transporters

present in the plasma membrane demonstrated by surface-labelling of extracellularly tagged NHE3 (157). Therefore, the cytoskeleton in AP1 cells must influence the intrinsic activity of the transporter, changing its half-maximal $[H^+]_i$ activation value.

Na^+/H^+ exchange is a major cell volume regulatory mechanism (165). Osmotic cell shrinkage leads to NHE activation in a variety of cell types, leading to increased Na^+ uptake followed by osmotically driven water influx. Interestingly, NHE1 and NHE3 are differentially responsive to hyperosmolar stress. In a heterologous expression system, NHE1 was activated, while NHE3 was inhibited in shrunken cells (166). It is likely that in native cells the regulatory volume increase attributed to Na^+/H^+ exchange is mediated by NHE1. The mechanism of the osmotic activation of NHE1 is poorly understood, but it appears to be phosphorylation-independent (167), and probably involves the interaction of cytoskeletal elements (168).

1.4.6 Organellar NHEs

Recently further members of the Na^+/H^+ exchanger family, NHE6 and NHE7, sharing a 70% overall amino acid identity, have been identified (89;90).

By tissue Northern blot analyses, NHE6 appears to be ubiquitously expressed. Within the cell, it is localized to mitochondria, and it mediates the benzamil-sensitive exchange of matrix Na^+ for intermembrane H^+ . It is primarily responsible for establishing the Na^+ gradient utilized by the mitochondrial Na^+/Ca^{2+} exchanger in mitochondrial Ca^{2+} homeostasis. Furthermore, it might have a role in mitochondrial volume regulation. ((89), Numata and Orlowski unpublished)

NHE7 mRNA is ubiquitously expressed in all tissues examined, with the highest expression levels observed in secretory organs. Its predominant intracellular localization was reported to be the late Golgi/*trans*-Golgi network. It functions as a non-selective cation/H⁺ exchanger, and likely plays a role in the cation/volume homeostasis of this organelle. (90)

1.4.7 NHEs in brain

According to the earliest Northern blots of the NHE isoforms, NHE1 is the most abundantly expressed isoform in brain. NHE2 and NHE4 mRNA is also present, though at much lower levels. NHE3 message in brain is barely detectable after long exposure of the Northern autoradiogram (129;132) suggesting a very low expression level.

Using *in situ* hybridization, Ma *et al.* (169) detected all four isoforms in rat brain in an age- and region-specific manner. They concluded that NHE1 is ubiquitous, and the most abundant in hippocampus and cerebellum. The expression pattern of NHE2 and NHE4, both found in cerebral cortex and brainstem-diencephalon, is similar, while NHE3 is only found in cerebellar Purkinje cells. Another *in situ* hybridization analysis found high expression of NHE4 in the cavi ammoni fields of rat hippocampus. (109)

The scope of Northern analysis and *in situ* hybridization is limited in terms of actual physiology of a protein. Also, as reported earlier in the case of NHE2 and NHE4, the use of long cDNA probes can lead to cross reactivity even under high stringency hybridization (127). In order to identify the specific isoforms responsible for the described NHE activities in CNS (see 1.3), isoform specific polyclonal and monoclonal antibodies were used in both western blot analyses and immunohistochemistry. Haddad

et al. identified NHE1, NHE2, NHE4, but not NHE3 in western blots of segregated rat brain (170). In contrast, Wiemann *et al.* described NHE3 immunoreactivity in ventrolateral neurones of the medulla oblongata (171). Yet another study using a monoclonal antibody could not detect NHE4 protein in rat brain (134).

Clearly, there is more work needed in precisely describing distribution of NHEs in brain, and in analyzing the subcellular localization of the respective isoforms.

1.4.8 Initial identification of NHE5

In a quest for other NHE isoforms, Klanke *et al.* (172) used a ³²P-labelled rat NHE2cDNA probe to screen a human genomic library at low stringency. The nucleotide sequence of the identified positive clone contained two putative exons separated by a 2.2-kb intron, yielding 154 codons in open reading frame. Comparison of the deduced amino acid sequence to the corresponding sequences of the four, at that time known NHE isoforms (NHE1-4) made it apparent, that the gene was a new member of the NHE family, termed NHE5, exhibiting 59-73% identity to NHE1 and NHE3 respectively. Subsequent physical and genetic mapping studies localized the gene to chromosomal subbands 16q22.1, and Northern blot analysis demonstrated that NHE5 transcripts were expressed in brain, spleen, and testis and at trace levels in skeletal muscle (172).

1.5 Rationale and Objectives

NHEs are transmembrane proteins that mediate the electroneutral exchange of Na^+ and H^+ across the plasma membrane and thereby regulate intracellular pH and volume homeostasis. Despite the essential nature of the above functions, it is possible to select for cells that are devoid of NHE activity. NHE-deficient cells are viable provided that the culture medium contains HCO_3^- and its pH is adequately buffered at the neutral range (173). To avoid the problem of the coexistence of multiple isoforms in individual cell types in the functional analyses of NHEs, the transporters can be expressed and analyzed in such an NHE-deficient cell line.

The focus of my thesis was to determine the basic functional and some of the regulatory properties of the human brain Na^+/H^+ exchanger isoform 5 (NHE5). In order to describe its pharmacological and biochemical characteristics in respect of the other isoforms, NHE5 was stably transfected into the NHE-deficient Chinese hamster ovary cell AP1 (Chapter 1). AP1 cells proved to be a particularly useful tool in the analyses of both basic functional and regulatory features of various NHE isoforms (103;104;112;166;174). The common cellular background of this heterologous expression system allows a more direct comparison of the particular attributes of individual NHEs. However, in case of NHE5, the most cell type-specific isoform presumably expressed solely in neurons (175;176), CHO may not serve as a perfect model system for identifying regulatory pathways. Consequently, in describing the regulation of NHE5 activity, another approach was taken. We tried to identify native

interacting proteins of the transporter using the yeast two-hybrid assay (177) screening a human brain cDNA library. For the assay, the cytoplasmic tail of NHE5 was used as bait, since this is the part of the exchangers on which diverse intracellular signaling pathways converge (178-180). Chapter 2 and 3 presents two of the candidate interactants recognized by the yeast two-hybrid assay and the functional consequence of their association with NHE5 in the heterologous AP1 expression system.

*Preamble to Chapter1*¹

To begin a systematic analysis of the functional characteristics and physiological roles of NHE5, we have cloned and functionally expressed a cDNA encoding the complete amino acid sequence of human NHE5. The full-length cDNA sequence was eventually cloned from a human brain cDNA library, as earlier attempts at isolating the cDNA from spleen or testis libraries yielded incorrectly spliced transcripts. In parallel experiments by Attaphitaya *et al.* (175), high levels of rat NHE5 mRNA in Northern blot analysis was only detected in brain tissue, strengthening the conclusion that functional expression of NHE5 mRNA may be restricted to brain.

The composite nucleotide sequence of human NHE5 (Fig. P.1) contains a 2688-nucleotide open reading frame, which encodes a protein of 896 amino acids with a molecular mass of ~99 kilodaltons. Hydropathy analysis (181) showed that NHE5 has the same membrane topology as the other plasma membrane Na⁺/H⁺ exchangers, with multiple membrane spanning domains in the *N*-terminal half of the protein and an extensive cytoplasmic domain in the *C*-terminal half (Fig. P.2). Pairwise comparisons of the conserved transmembrane domain (amino acids 41–543 of NHE5) with the corresponding regions of NHE1–4 (TABLE P.1) demonstrated that it is most closely related to NHE3. The overall amino acid similarity between NHE5 and NHE3 (Fig. P.2), with all gaps in the alignment considered a mismatch, is 48% (64% in the *N*-terminal

¹ This section is an abridged summary of the papers by Baird *et al.* (176) and Attaphitaya *et al.* (175), that were the first reports on the attributes of the Na⁺/H⁺ exchanger isoform NHE5. The reconstruction, stable transfection and functional assay of human NHE5 was carried out by E.Z. Szabó.

membrane spanning region and 31% in the C-terminal cytoplasmic region). Human NHE5 is 95% identical to the 898-amino acid rat NHE5 (175).

To reconstruct the complete human NHE5 cDNA lacking intron sequences, six contiguous overlapping regions that spanned the coding region were amplified by PCR using the isolated cDNAs and RACE products as templates. Adjacent fragments were joined by PCR until the coding region was reassembled into a single cDNA fragment containing unique *Kpn*I and *Xba*I restriction endonuclease sites at the 5' and 3' ends, respectively. By using PCR mutagenesis, an influenza virus hemagglutinin epitope YPYDVPDYAS was inserted at the C-terminal end to allow for immunological detection of the protein, and a more optimal translation initiation sequence (182) was engineered at the 5' end of the cDNA (CCCCGCCACCATGC, with ATG as the initiation methionine codon; C in the +4 position was retained because using the more optimal G would have altered an amino acid). The entire PCR product was sequenced to confirm the fidelity of the coding region. The modified human pNHE5_{HA} cDNA was inserted into a mammalian expression vector (pCMV) under the control of the enhancer/promoter region of the immediate early gene of human cytomegalovirus (103).

To determine whether NHE5 is a functional Na⁺/H⁺ exchanger, NHE-deficient Chinese hamster ovary cells (AP1) were transfected with pNHE5_{HA} by the calcium phosphate-DNA co-precipitation method (183), and stable transfectants were selected for by repeated NH₄Cl-induced acid loads (103).

NHE5 activity in clonal cell lines was assayed by measuring the initial rates of $^{22}\text{Na}^+$ influx upon acute intracellular acidification by the NH_4^+ prepulse technique (103). Intracellular H^+ -dependent Na^+ influx activity in the parental AP1 cells was very low and could not be inhibited by the addition of 1 mM amiloride, a concentration that inhibits even the relatively amiloride-resistant NHE3. In contrast, $^{22}\text{Na}^+$ influx activity in cells expressing NHE5 was very high relative to background levels (~25-fold) and was fully inhibited by adding 1 mM amiloride (Fig. P.3).

To examine the distribution of NHE5 in human brain, a multiple tissue Northern blot containing RNA from a number of anatomical structures was hybridized with an NHE5 probe (176). A 4.2-kb NHE5 mRNA was identified in several parts of the brain, including the caudate nucleus, hippocampus, hypothalamus, thalamus, subthalamic nucleus and amygdala, but was notably absent in the corpus callosum, which consists primarily of axons and glial cells (Fig. P.4). Taken together with the data of Attaphitaya *et al.* (175) demonstrating specific *in situ* hybridization signal of NHE5 in dentate gyrus localized to a region containing neuronal cell bodies, these results suggest that NHE5 is a neuron-specific isoform, *i.e.* the most highly cell-type specific isoform of the NHE family.

The following chapter describes the pharmacological and biochemical properties of human NHE5 in the heterologous expression system, the NHE-deficient CHO cell line AP1.

[illegible]

NHE5	MLRAAL-----SLLALPLA-----GAAEPTQKPESPGEPFPGLELFRWQWHEVEAPYLVALWILVASLAKIVFH	65
NHE3	MWHPALGPGWKPLALAVAVTSLRGVGRGIEEEP-----NSGGSFQIVTFKWHHVQDPYIIALWILVASLAKIVFH	70
NHE5	LSRKVTSVLPESCLLILLGLVGLGGIVLAVAKKAQYQLEPGTFFLFLPPIVLDSGYFMPESRLFFDNLGAILTYAVVGT	143
NHE3	LSHKVTSVVPESALLIVLGLVGLGGIVWAADHIASFTLTPTLFFFYLLPPIVLDAGYFMPNRLFFGNLGTILLYAVIGT	148
NHE5	LWNAFTTGAALWGLQQAGLVAPRVQAGLLDFLLFGSLISAVDFVAVLAVFEEVHVNETLFIIVFGESLLNDAVTVVLY	221
NHE3	IWNAATTGLSLYGVFLSGLMGELKI-GLLDFLLFGSLIAAVDPVAVLAVFEEVHVNEVLFIIVFGESLLNDAVTVVLY	225
NHE5	KVCNSFVEMGSANVOATDYLGKVASLFVVSLGGAAVGLVFAFLLALTTRFTKRVRIIEPLLVLFLAYAAYLTAEMASL	299
NHE3	NVFESFVTLGGDAVTGVDVKGIVSFFVSLGGTLVGVIFAFLLSLVTRFTKRVRIIEPGFVFVISYLSYLTSEMSL	303
NHE5	SAILAVTMCGLGCKKYVEANISHKSRTTVKYTMKTLASCAETVIFMLLGISAVDSSKWAWDSGLVLGTLIFILFFRAL	377
NHE3	SAILAITFCGICCKKYVKANISEQSATTVRVYTMKMLASGAETIIFMFLGISAVDPVIWNTAFVLLTLVVISYRAI	381
NHE5	GVVLQTVVLNQFRLVPLDKIDQVMSYGGVLRGAVAFALVILLDRTKVPAKDYFVATTIVVFFTVVQGLTIKPLVKW	455
NHE3	GVVLQTVWILNRYRMVQLETIDQVMSYGGVLRGAVAYALVLLDEKKVKEKNLFVSTTLIVVFFTVVFOGLTIKPLVQW	459
NHE5	LKVKRSEHHKPTLNQELHEHTFDHILAAVEDVVGHHGYHYWRDRWEQFDKKYLSQLLMRRSAYRIRDQIWDVYYRLNI	533
NHE3	LKVKRSEQREPKNLNEKLHGRAFDHILSAIEDISGQIGHNYLRDKWSNFDKFLSKVLMRRSAQKSRDRILNVFHEMLN	537
NHE5	RD AISFVDQGGHVSSTGLTLPS-----MPSRNSVAETSVTNLLRESGSGACLDLQVIDTV-RSGRDREDAVMH	601
NHE3	KDAISYVAEGERRGSLAFIRSPSTDMNVNDFSTPRPSTVEASVSFLRENVSAVCLDMQSLEQRRRSIRDTEDMVTH	615
NHE5	HLLCGGLYKPRRRYKASCSRHFISEDAQERQDKEVFQNMKRRLESFKSTKHNICFTK--SKPRPRKTGRKKDGVAN	677
NHE3	HTLQOYLYKPRQYKHLYSRHELTPEDEKQDKEIFHRTMRKRRLESFKSAKLGINQNKAAKLYKRERAQKRNRSSIP	693
NHE5	AEATNGKHRGLGFQDTAAVILTVESEEEEEESDSETEKEDDEGIIIFVARATSEVLQEGKVSGLVCPSPRIIPPSP	755
NHE3	NGKLPMENLAHNFTIKEKDLELSEPEE-----ATNYEEISGGIEFLASVTKDVASDSGAGIDNVFSPDEDLDPSI	764
NHE5	TCAEKELPWKSGQGD LAVYVSSETTKIVPDMQTGWNQSISSLESASPPCNPQAPILTCLPPHPRGTEEPQVPLHLPS	833
NHE3	LSRVP--PWLSP-GETVVP SQRARV-----QIP-NSPS	793
NHE5	DPRSSFAFPPLAKAGRSRSESSADLPQQQLQPLMGHKDHTLSPGTATSHWCIOFNRSRL	896
NHE3	NFRRLTPFRLSN-KSVDS--FLQADGP EEQ-LQPASP--ESTHM	831

Fig. P.2. Amino acid similarity comparison. The amino acid sequences of human NHE5 is compared with rat NHE3. Asterisks indicate sequence identity. Potential transmembrane domains are *underlined*. The positions of exon boundaries in the human *NHE5* and rat *nhe3* genes are indicated by *arrowheads*. (Baird, *JBC* (1999) 274:4377-4382)

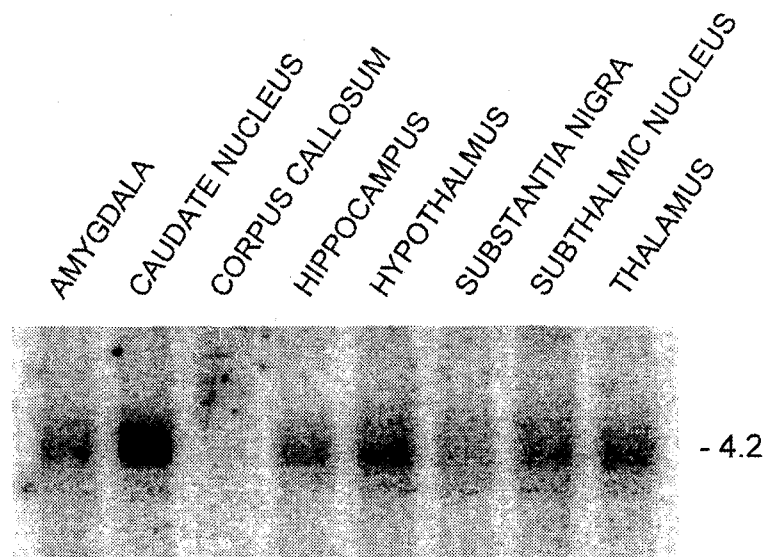
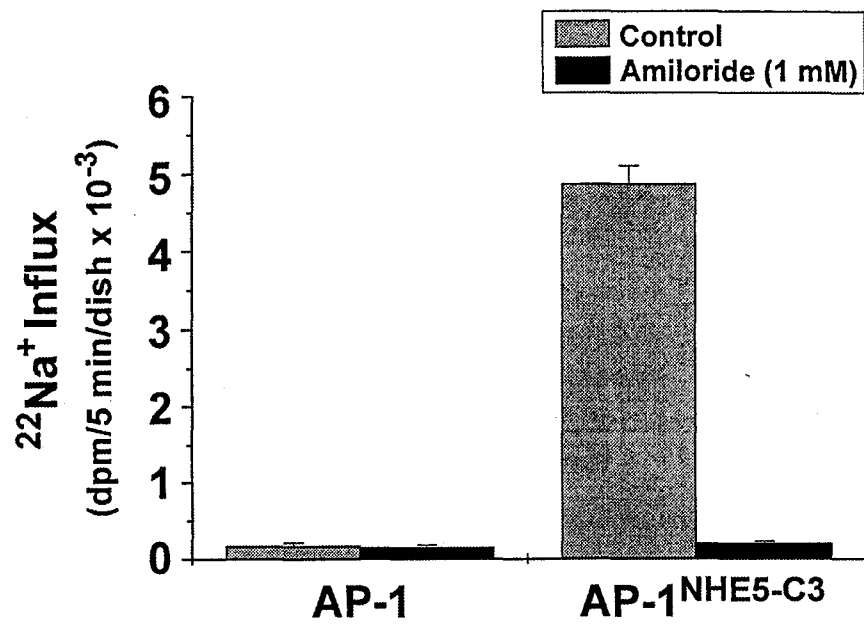


TABLE P.1.

Percentage amino acid identity in pairwise comparisons of NHE isoforms 1-5.

	NHE2	NHE3	NHE4	NHE5
NHE1	62	49	52	50
NHE2		52	71	52
NHE3			46	67
NHE4				46

Amino acids 47-543 of human NHE5 were compared with the corresponding regions of NHE1-4. The extreme *N*-terminal and the more *C*-terminal regions, which do not align well and exhibit only limited similarity among the five isoforms, were not included in this comparison. (Baird, *JBC* (1999) 274:4377-4382)

CHAPTER 1

Kinetic and Pharmacological Properties of Human Brain Na⁺/H⁺ Exchanger Isoform 5 Stably Expressed in Chinese Hamster Ovary Cells¹

Előd Z. Szabó, Masayuki Numata, Gary E. Shull, and John Orłowski

¹ The text and figures of this chapter were published in the *Journal of Biological Chemistry* (2000) 275: 6302–6307.

The recently cloned Na^+/H^+ exchanger Isoform 5 (NHE5) is predominantly expressed in brain, yet little is known about its functional properties. To facilitate its characterization, a full-length cDNA encoding human NHE5 was stably transfected into NHE-deficient Chinese hamster ovary AP1 cells. Pharmacological analyses revealed that H^+ -activated $^{22}\text{Na}^+$ influx mediated by NHE5 was inhibited by several classes of drugs (amiloride compounds, (3-methylsulfonyl-4-piperidinobenzoyl) guanidine methane-sulfonate, cimetidine and harmaline) at half-maximal concentrations that were intermediate to those determined for the high-affinity NHE1 and the low-affinity NHE3 isoforms, but closer to the latter. Kinetic analyses showed that the extracellular Na^+ dependence of NHE5 activity followed a simple hyperbolic relationship with an apparent affinity constant (K_{Na}) of 18.6 ± 1.6 mM. By contrast to other NHE isoforms, NHE5 also exhibited a first-order dependence on the intracellular H^+ concentration, achieving half-maximal activation at $\text{pH } 6.43 \pm 0.08$. Extracellular monovalent cations, such as H^+ and Li^+ , but not K^+ , acted as effective competitive inhibitors of $^{22}\text{Na}^+$ influx by NHE5. In addition, the transport activity of NHE5 was highly dependent on cellular ATP levels. Overall, these functional features distinguish NHE5 from other family members and closely resemble those of an amiloride-resistant NHE isoform identified in hippocampal neurons.

INTRODUCTION

Transient oscillations in the extra- and intracellular pH (pH_o and pH_i , respectively) environments of neurons and other cell types of the nervous system can profoundly modulate neuronal membrane excitability by inhibiting various ligand receptor-mediated currents (184;185), voltage-gated cation channels (186-189) and gap junction coupling (190), as well as by activating a depolarizing inward Na^+ current (ASIC3) (191). Thus, precise control of the neuronal pH milieu is an important biological process and may fulfill a regulatory role in brain function (see reviews (192;193)).

The ion transporters responsible for pH_i regulation in the nervous system are not as well characterized as in peripheral cell types, and this is particularly true for neurons which are often difficult to isolate and/or maintain in culture in a differentiated state. Despite this limitation, accumulating evidence indicates that the acid-base transport systems in brain are heterogeneous, but comparable to other organ systems. In cultured fetal or freshly-isolated neonatal pyramidal CA1 neurons from rat hippocampus, restoration of steady-state pH_i following intracellular acidification involves two principal ion carriers: a Na^+ -dependent $\text{HCO}_3^-/\text{Cl}^-$ exchanger and a novel amiloride-resistant Na^+/H^+ exchanger (NHE) (38;194;195). Later in development, acutely-dissociated hippocampal CA1 neurons from adult rats exhibit an acidifying mechanism mediated by a Na^+ -independent $\text{Cl}^-/\text{HCO}_3^-$ exchanger, most likely the AE3 isoform (196). Na^+/H^+ and Na^+ -independent $\text{Cl}^-/\text{HCO}_3^-$ exchangers also make distinct contributions to pH_i regulation in neurons of the medulla oblongata (197), superior cervical ganglion sympathetic neurons (198), cerebellar Purkinje cells (199), as well as brain synaptosomes (200). By

contrast, pH_i regulation in primary cultures of rat astrocytes is more intricate and involves the three major acid-base transport systems mentioned above (39;201), as well as a fourth pH -regulating mechanism, $\text{Na}^+/\text{HCO}_3^-$ cotransport (39;202). Moreover, rat astrocytes express multiple NHE isoforms (203), which further adds to their pH -regulatory complexity.

More detailed examination of NHE mRNA expression in rat brain revealed that NHE1 is the most abundant and widely dispersed isoform, whereas other family members (*i.e.*, NHE2-4) show a more restricted distribution (169). The importance of NHE1 in neuronal function is convincingly demonstrated by spontaneous (126) or targeted (125) null mutations in mice, which develop ataxia and epileptic-like seizures by two weeks of age and show significant mortality (67%) prior to weaning. These changes are associated with selective loss of neurons in the cerebellum and brainstem (126). By contrast, mice with targeted disruptions of the *Nhe2* and *Nhe3* loci do not display obvious neurological symptoms (131;133); hence their particular roles in nervous system function are less apparent.

In addition to NHE1-4, recent molecular cloning and tissue distribution studies in human (176) and rat (175) have identified a fifth NHE isoform that is distinguished by its predominant expression in discrete regions of the brain, including dentate gyrus, cerebral cortex and hippocampus. Moreover, it shares high sequence similarity to the amiloride-resistant NHE3 isoform which, in brain, is detected only in cerebellar Purkinje cells (169). Based on these observations, it is reasonable to postulate that NHE5, rather than NHE3, is a likely candidate for the amiloride-resistant form of the Na^+/H^+ exchanger reported in hippocampal neurons (195) and possibly other cell types of the nervous

system (201). However, its intrinsic biochemical and pharmacological properties have yet to be defined in detail. To facilitate its characterization without the complicating presence of other NHE isoforms, we stably expressed the human NHE5 cDNA in mutagenized Chinese hamster ovary cells (AP1) devoid of endogenous NHE activity. The results reveal that the functional properties of NHE5 closely resemble those of an amiloride-resistant NHE isoform identified in hippocampal neurons.

EXPERIMENTAL PROCEDURES

Materials

Carrier-free $^{22}\text{NaCl}$ (range of specific activity, 900-950 mCi/mg; concentration, ~10 mCi/ml) was obtained from NEN Life Science Products (Mandel Scientific, Guelph, Ontario). Amiloride, 5-(*N*-ethyl-*N*-isopropyl)amiloride (EIPA), 5-(*N,N*-hexamethylene)-amiloride (HMA), cimetidine, clonidine, harmaline, ouabain, bumetanide, antimycin A, 2-deoxy-*D*-glucose, 2-(*N*-morpholino)ethanesulfonic acid (MES), and 3-(*N*-morpholino)propanesulfonic acid (MOPS) were purchased from Sigma. (3-methanesulfonyl-4-piperidinobenzoyl) guanidine methanesulfonate (HOE694) was kindly provided by Dr. Hans-J. Lang (Hoechst Marion Roussel, AG). Nigericin was purchased from Molecular Probes Inc. (Eugene, OR). α -Minimal essential medium, fetal bovine serum, penicillin/streptomycin, and trypsin-EDTA were from Life Technologies (Burlington, ON). All other chemicals and reagents used in these experiments were from British Drug House Inc. (St. Laurent, Québec) or Fisher Scientific, and were of the highest grade available.

Construction and Stable Expression of Human NHE5

A full-length cDNA encoding human NHE5 was used in this study as previously described (176), except that it did not contain a C-terminal influenza virus hemagglutinin epitope tag in order to preserve the native structure of the protein. The human NHE5 cDNA was inserted into a mammalian expression vector under the control of the enhancer/promoter region from the immediate early gene of human cytomegalovirus (CMV) as previously described (176) and called pNHE5. The pNHE5 plasmid was

stably transfected into NHE-deficient Chinese hamster ovary AP1 cells (204) using the calcium phosphate-DNA co-precipitation method (183) and acid-selection (103;205). Several clonal cell lines were screened for their level of NHE5 expression by measuring H^+ -activated $^{22}Na^+$ influx. For these studies, the cell clone AP1/NHE5^{C6}, which had the highest level of NHE5 activity, was used between passages 2 and 10. The cells were maintained in complete α -minimal essential medium supplemented with 10% fetal bovine serum, 100 units/ml penicillin, 100 μ g/ml streptomycin and 25 mM $NaHCO_3$, pH 7.4, and incubated in an humidified atmosphere of 95% air, 5% CO_2 at 37 °C.

$^{22}Na^+$ Influx Measurements

The cells were grown to confluence in 24-well plates. Prior to $^{22}Na^+$ influx measurements, the cells were acidified intracellularly using the NH_4Cl prepulse technique as previously described (103). The assays were initiated by incubating the cell monolayers in isotonic choline chloride solution (125 mM choline chloride, 1 mM $MgCl_2$, 2 mM $CaCl_2$, 5 mM glucose, 20 mM HEPES-Tris, pH 7.4) containing 1 mM ouabain and carrier-free $^{22}Na^+$ (1 μ Ci/ml) in the absence or presence of the NHE-specific inhibitor EIPA (0.1 mM). The lack of K^+ and the presence of ouabain minimized transport of Na^+ catalyzed by the $Na^+-K^+-2Cl^-$ cotransporter and the $Na^+,K^+-ATPase$. In experiments where the assay buffer contained extracellular K^+ , the medium was further supplemented with 0.1 mM bumetanide to block the $Na^+-K^+-2Cl^-$ cotransporter. The influx of $^{22}Na^+$ was terminated by rapidly washing the cells 3 times with four volumes of ice-cold NaCl stop solution (130 mM NaCl, 1 mM $MgCl_2$, 2 mM $CaCl_2$, 20 mM HEPES-NaOH, pH 7.4). To extract the radiolabel, the monolayers were solubilized with 0.25 ml of 0.5 N NaOH, the

wells were washed with 0.25 ml of 0.5 N HCl. Both the NaOH cell extract and the HCl wash solution were combined in 5 ml scintillation fluid, and transferred to scintillation vials. The radioactivity was assayed by liquid scintillation spectroscopy. Protein content was determined using the Bio-Rad *DC* protein assay kit according to the manufacturer's protocol. Under the conditions of NH_4Cl acid load, the uptake of $^{22}\text{Na}^+$ at low Na^+ concentrations was linear over a 10 min period at 22 °C. Therefore, a time course of 5 min was chosen for most experiments with the following exceptions.

In experiments examining the kinetics of NHE activity as a function of the extracellular Na^+ concentration, the influx of $^{22}\text{Na}^+$ was linear for only 2 min at 100 mM NaCl. Consequently, an uptake time of 1 min was chosen for these studies. For studies designed to examine the activity of Na^+/H^+ exchanger as a function of the intracellular H^+ (H^+_i) concentration, the intracellular pH (pH_i) was set over the range of 5.8 to 7.4 by using the K^+ -nigericin method (206).

Measurements of $^{22}\text{Na}^+$ influx specific to the NHE were determined as the difference between the initial rates of H^+_i -activated $^{22}\text{Na}^+$ influx in the absence and presence of 0.1 mM EIPA, and expressed as EIPA-inhibitable $^{22}\text{Na}^+$ influx.

ATP Depletion

Depletion of cellular ATP was carried out as previously described (166). Briefly, cells were incubated for 10 min in ATP-depleting medium containing 100 mM potassium glutamate, 30 mM KCl, 10 mM NaCl, 1 mM MgCl_2 , 10 mM HEPES (pH 7.4), 5 mM deoxyglucose and 1 $\mu\text{g}/\text{ml}$ antimycin A. This high K^+ , low Na^+ and nominally Ca^{2+} -free medium was used to prevent Na^+ and/or Ca^{2+} loading of the cells upon inhibition of the

Na⁺/K⁺ or Ca²⁺ pumps. Substitution of most of the Cl⁻ by glutamate⁻ was intended to minimize cell swelling. Control cells were incubated in this same solution devoid of deoxyglucose and antimycin A and instead contained 5 mM glucose.

Data Analysis

All experiments represent the average of two to four experiments, each performed in quadruplicate. The data are presented as the mean \pm S.D.

RESULTS

Pharmacological Properties of Human NHE5

The Na^+/H^+ exchanger isoforms characterized to date (*i.e.*, NHE1-4) display a wide range of sensitivities to different classes of pharmacological inhibitors, including amiloride and its analogues (*e.g.*, EIPA and HMA), benzoyl guanidinium compounds (*e.g.*, HOE694 and HOE642 (cariporide)), cimetidine, clonidine, and harmaline (103;104;109;110;112;114). Many of these compounds have been shown to mediate their effects by competing with extracellular Na^+ at the same, or a closely associated, binding site(s) (reviewed in Ref. (107)). To define the sensitivity of human NHE5 to these antagonists, the rate of H^+ -activated $^{22}\text{Na}^+$ influx was measured as a function of the drug concentration in a clonal isolate of NHE5-transfected AP1 cells (*i.e.*, AP1/NHE5^{C6}). As illustrated in Fig. 1.1 and summarized in TABLE 1.1, the order of potency of these compounds was $\text{HMA} \approx \text{EIPA} > \text{HOE694} > \text{amiloride} > \text{cimetidine} > \text{harmaline}$ with apparent half-maximal inhibition ($K_{0.5}$) values of (in μM) 0.37, 0.42, 9.1, 21, 230, and 900, respectively. These values are intermediate between those of NHE1 and NHE3, but closer to the latter. By contrast, clonidine had little, if any, effect on NHE5 activity even though it is an effective inhibitor of other NHE isoforms (103;104).

Kinetic Properties of Human NHE5

To determine the extracellular Na^+ (Na^+_{o}) affinity of NHE5, initial rates of H^+ -activated $^{22}\text{Na}^+$ influx were measured as a function of the Na^+_{o} concentration. The rate of $^{22}\text{Na}^+$ influx was saturable and conformed to simple Michaelis-Menten kinetics (Fig. 1.2A). Transformation of the data according to the Eadie-Hofstee algorithm (V versus

$V/[S]$) yielded a linear relationship (Fig. 1.2B), consistent with the presence of a single Na^+ binding site at the extracellular surface. Calculation of the value of the negative slope gave an apparent affinity constant for Na^+_o (K_{Na}) of 18.6 ± 1.6 mM.

Transport activity was also measured as a function of the H^+_i concentration. This was determined by measuring the rate of $^{22}\text{Na}^+$ influx in cells where the pH_i was clamped over the range of pH 6.0 to 7.4 using the K^+ -nigericin method. The pH_i sensitivity of NHE5 is presented in Fig. 1.3A as a percentage of EIPA-inhibitable $^{22}\text{Na}^+$ influx determined at pH_i 6.0. Transformation of the data according to the Eadie-Hofstee algorithm also revealed a straight line (Fig. 1.3B), suggestive of a single internal H^+ binding site. Calculation of the negative slope gave a half-maximal H^+_i activation value of $\text{pK} = 6.43 \pm 0.08$. This activity profile is in contrast to that observed for other NHE isoforms in several cell types which show a greater than first-order dependence on intracellular protons (107;108;207).

Influence of Other Extracellular Cations on Transport Activity of Human NHE5

Extracellular monovalent cations, including H^+_o , Li^+_o and $\text{NH}_4^+_o$, have generally been shown to decrease H^+_i -activated $^{22}\text{Na}^+$ influx by endogenous (107) and transfected exchangers (*i.e.*, NHE1, NHE2 and NHE3) (103;104) in a competitive manner, although in some cases mixed-type inhibition is observed (208). Moreover, these exchangers are capable of transporting both Li^+ and NH_4^+ , but the rates of translocation are usually slower than that for Na^+ and H^+ . By contrast, external K^+ selectively inhibits NHE1, but only at high, non-physiological concentrations, and does not appear to be translocated (103). Thus, it was of interest to determine whether the rate of Na^+ transport by NHE5 is

also differentially sensitive to the presence of other extracellular monovalent cations (*i.e.*, H^+_o , Li^+_o , and K^+_o).

External protons decreased H^+_i -activated $^{22}Na^+$ influx into NHE5-transfected cells in a concentration-dependent manner (Fig. 1.4A), with apparent half-maximal activity reached at pH_o 8.13 ± 0.15 . This reduction is associated with the gradual decrease in the transmembrane H^+ gradient (ΔpH), but could also partly reflect H^+_o competition for the Na^+_o binding site. To test this latter possibility, the Na^+_o concentration was adjusted to 1 and 10 mM and the initial rates of influx of $^{22}Na^+$ were measured as a function of the H^+_o concentration. Transformation of the data using the Dixon algorithm ($1/V$ versus $[H^+]_o$) resulted in straight lines (Fig. 1.4B), with the slope of the line decreasing in the presence of higher Na^+_o levels. Determination of the intercept of the lines yielded an inhibitory constant (K_i) for H^+_o of approximately 17 nM. These data indicate that the effectiveness of H^+_o to reduce the influx of $^{22}Na^+$ by NHE5 is influenced by the Na^+_o concentration, which is consistent with the notion that H^+_o effectively compete with Na^+_o at a single site.

Similarly, Li^+_o was also a potent and competitive inhibitor of H^+_i -activated $^{22}Na^+$ influx by NHE5 (Fig. 1.5). The apparent half-maximal inhibition was achieved at a concentration of $318 \pm 47 \mu M$ (Fig. 1.5A), which is an order of magnitude lower than that reported for other isoforms (103;104). To characterize the nature of this inhibition in greater detail, the initial rates of 1 mM and 10 mM $^{22}Na^+$ influx were measured as a function of the Li^+_o concentration. Analysis of the data by Dixon plot (Fig. 1.5B) yielded straight lines, with the slope of the line decreasing in the presence of higher Na^+_o levels. This suggested that Li^+_o also interacted in a competitive manner with an apparent $K_i \approx 0.63$ mM. In contrast to H^+_o and Li^+_o , increasing concentrations of K^+_o (1 to 100 mM) had

only a minor inhibitory effect on the initial $^{22}\text{Na}^+$ transport rates of NHE5 (Fig. 1.6). A summary of these data are presented in TABLE 1.2.

ATP Dependence

The transport activity of plasma membrane Na^+/H^+ exchangers is driven by the relative concentration gradients of the respective cations and is not dependent on direct hydrolysis of ATP *per se*. Nevertheless, cellular depletion of this nucleotide has been found to dramatically reduce the activities of known NHEs (166;209) by a mechanism that is not well understood. Thus, it was of interest to determine whether NHE5 was similarly sensitive to ATP. Under the conditions used (10 min incubation with deoxyglucose and antimycin A to block glycolysis and oxidative phosphorylation, respectively), ATP is rapidly depleted by >90% without compromising the integrity of the plasma membrane or adherence of the cells to the culture dishes (166). As shown in Fig. 1.7, NHE5 activity was completely abolished over the pH_i range studied (pH 5.8 and 7.4).

DISCUSSION

Recent studies by us (176) and Melvin and colleagues (175) demonstrated that heterologous expression of the cloned brain cDNAs for human and rat NHE5, respectively, were capable of mediating the exchange of extracellular Na^+ for intracellular H^+ ; activity that could be blocked by high concentrations of amiloride or its analogue EIPA. These data established that NHE5 functions as a plasma membrane Na^+/H^+ exchanger. The present study extends these initial observations by defining the principal biochemical and pharmacological properties of NHE5 in greater detail; thereby providing a functional basis for its identification in native tissues and cell types.

The pharmacological data show that NHE5 has an intermediate affinity for most classes of NHE-inhibitory drugs (amiloride-based compounds, HOE694, cimetidine and harmaline) when compared to other NHE isoforms under comparable experimental conditions, *i.e.*, $\text{NHE1} > \text{NHE2} > \text{NHE5} > \text{NHE3}$. By contrast, NHE5 activity is completely insensitive to clonidine within the concentration range tested, whereas other isoforms including NHE3 are effectively inhibited in the sub-millimolar range (103;104). NHE4 also has an apparent low affinity for many of these antagonists, but its activity in transfected fibroblasts can only be detected under specialized conditions (*i.e.*, prolonged intracellular acidification and exposure to hyperosmolar medium (109) or treatment with 4,4'-diisothiocyanostilbene-2,2'-disulfonic acid (DIDS) (210)). Hence, it is unclear whether these characteristics reflect the actual properties of NHE4 in native tissues, although recent indirect evidence indicates that this may be the case in rat renal cortical tubules (211). Overall, the drug profiles of NHE5 most closely resemble those of NHE3. This result agrees with earlier predictions based on their high amino acid similarity (~

67% identity) in the N-terminal membrane-spanning domain; a region previously found to confer drug sensitivity (112;121).

The low sensitivity of NHE5 to inhibition by several drugs and its prominent expression in discrete regions of the brain, including hippocampus, is consistent with our initial postulate that NHE5 is a likely candidate for the amiloride-resistant form of the Na^+/H^+ exchanger reported in hippocampal neurons by Raley-Susman *et al.* (195). However, in the latter study, NHE activity was unaffected by 1 mM amiloride and 50 μM HMA, but inhibited by 100 μM harmaline. Conversely, NHE5 expressed in AP-1 cells is fully inhibited by amiloride and HMA, but relatively unaffected by harmaline, at the same concentrations. These apparent discrepancies in drug sensitivities are most likely due to the different conditions used to measure transport activity in the two studies. In hippocampal neurons, NHE activity was measured as the rate of pH_i recovery (using the pH-sensitive fluorescent dye BCECF) following intracellular acidification in the presence of a saturating concentration (135 mM) of Na^+_o , which competes with amiloride and its analogues for binding. By contrast, in our study, NHE5 activity was measured as acid-activated $^{22}\text{Na}^+$ influx using trace levels of Na^+_o , thereby allowing the drugs to bind with higher affinity and closer to their true K_i . With respect to harmaline, this compound has been found by others to greatly interfere with the fluorescence signal of BCECF (38;194), thereby complicating interpretation of rates of pH change in its presence, whereas this is not a factor in radioisotope flux measurements.

In addition to pharmacological agents, a number of monovalent cations such as H^+ , Li^+ , NH_4^+ (reviewed in Ref. (107)), and in some cases K^+ (103), have been shown to compete with Na^+ for binding to the extracellular site of the NHEs. Similarly, the present

study demonstrates that H^+_o and Li^+_o can competitively block the H^+_i -activated influx of $^{22}Na^+$ by NHE5. By comparison to other exchangers, the affinity of H^+_o for NHE5 ($K_i \approx 17$ nM) is an order of a magnitude higher than that for NHE1 and NHE3, but similar to that for NHE2 ($K_i \approx 10$ nM). Likewise, extracellular Li^+ is also a severalfold more potent competitor ($K_i \approx 0.63$ mM) of Na^+ influx by NHE5 when compared to other isoforms (104). Although speculative, this raises the possibility that Li^+ modulation of brain NHE5 activity, possibly by influencing pH_i , may be a contributing factor in the complex pharmacodynamics of LiCl treatment (therapeutic concentration ≈ 1 mM) of bipolar affective disorder (212). Unlike Li^+_o and H^+_o , K^+_o had a minimal effect on $^{22}Na^+$ influx by NHE5 and is similar to that found for NHE2 and NHE3. Conversely, K^+_o at high concentrations (*i.e.*, 100 mM) acted as a modest competitive inhibitor of Na^+ transport by NHE1 (103). Though not demonstrated in this study, Li^+ and NH_4^+ can also be translocated across the membrane in exchange for Na^+ or H^+ , but usually at a slower rate (107). On the other hand, external K^+ does not appear to be transported by most NHEs (103;107). However, Chambrey and colleagues (210) have recently reported that mouse LAP1 fibroblast cells stably expressing rat NHE4 are capable of mediating K^+ -dependent pH_i recovery upon treatment with DIDS; an effect that was not observed in untransfected cells. Again, whether this is an intrinsic property of NHE4 *in vivo* is uncertain.

The cation dependence of NHE5 activity was also assessed. The steady state velocities of most NHE isoforms (*i.e.*, NHE1, NHE2 and NHE3) show a saturating, first-order dependence on the Na^+_o concentration, indicative of a single binding site (103;104). Similarly, the Na^+_o -dependent velocity of NHE5 follows a rectangular hyperbola, consistent with simple, saturating Michaelis-Menten kinetics. The value for half-

maximal velocity ($K_{Na} = 18.6$ mM) was within the range of K_{Na} values (3 to 50 mM) reported for other NHEs in different cell types and vesicle preparations (103;104;107;209). It is noteworthy that this value is close to that reported for the amiloride-resistant NHE present in rat hippocampal neurons (*i.e.*, ~ 23 mM) (195). An exception to this pattern is NHE4 which manifests either a sigmoidal (109) or hyperbolic (210) dependence on the Na^+_o concentration depending on whether it is expressed in hypertonically-exposed PS120 fibroblasts or DIDS-treated LAP1 cells, respectively. The underlying basis for this kinetic difference is unknown.

The steady state velocity of NHE5 also shows an apparent first-order dependence on the intracellular proton concentration, as was reported for the amiloride-resistant NHE in hippocampal neurons (195). However, this characteristic is in marked contrast to that described for the majority of other plasma membrane NHEs which exhibit a greater than first-order dependence on the H^+_i concentration (107;108;200;213). This is suggestive of a second class of H^+ binding site, in addition to the transport site, with positive cooperative binding characteristics. This property was first described for the renal apical membrane NHE (*i.e.*, NHE3) by Aronson and colleagues (107;108) who proposed that this apparent allosteric H^+_i activation could be explained most simply by assuming the presence of one or more ionizable groups that, upon protonation, alter the conformation of the protein and enhance the rate of cation transport. However, in renal mesangial cells, the biphasic H^+_i -dependence of NHE activity was not strictly a function of pH_i , as it could be linearized within the physiological pH range upon hormonal stimulation (214). These observations suggest that the allosteric regulation by H^+_i may not necessarily reflect protonation of certain ionizable residues of the transporter, but instead may result

from effects on cell-specific regulatory factors that modulate NHE activity in a pH- and/or hormone-sensitive manner. Nevertheless, the roles of direct protonation of NHE and of an ancillary regulator are not mutually exclusive and may in fact be complementary.

In intact cells, plasma membrane NHEs require physiological levels (*i.e.*, millimolar) of ATP for optimal function. Acute cellular depletion of this nucleotide drastically inhibits NHE activity in native (215-217) and NHE-transfected (166;209;218) cells. Most notably, the activity of NHE3 is almost completely suppressed upon ATP depletion, even in the presence of a large transmembrane H^+ gradient, whereas the activities of NHE1 and NHE2 are only partially reduced (166). With respect to the latter isoforms, kinetic analyses indicate that this inhibition is mainly accounted for by reductions in their affinities for H^+ (166;218). However, the more drastic reduction of NHE3 activity, as well as that of NHE5, suggests a more complex mechanism; possibly reflecting alterations in both pH sensitivity and maximum velocity.

The molecular mechanisms underlying ATP regulation of the NHE isoforms remain obscure. Earlier studies of NHE1 showed that its state of phosphorylation is unaltered during acute ATP depletion (219). Hence, changes in direct phosphorylation of the exchanger are unlikely to account for the effects of ATP. Functional analyses of C-terminal truncation mutants of NHE1 indicated that the region encompassing amino acids 516-595 was sufficient to confer sensitivity to ATP (220). More recent investigations have suggested that the ATP dependence of NHE1 involves two distinct mechanisms: one that requires hydrolysis of ATP and likely involves an energy-dependent event, and a second process that does not require the hydrolysis of the γ -phosphate of ATP but may

involve its binding to an as yet unidentified ancillary factor that activates the exchanger (221;222). Whether these mechanisms also apply to other isoforms, including NHE5, is unknown.

In summary, we have demonstrated that NHE5 has pharmacological and biochemical properties that readily distinguish it from other NHE isoforms characterized to date. Moreover, its features resemble those of an amiloride-resistant NHE isoform identified in cultured hippocampal neurons. The regulatory properties of NHE5 and its physiological role(s) in neuronal cell function remain to be elucidated.

Preamble to Chapter2 and Chapter3

Following the initial characterisation of NHE5, we wanted to clarify the exchanger's basic regulatory properties.

Previous studies using the NHE-deficient cellular background, AP1 cells, demonstrated that NHE isoforms are differentially regulated by serine/threonine kinases. In this heterologous system, NHE1 is activated, whereas NHE3 is inhibited by both the PKA and PKC signalling pathways, and hyperosmolarity as well (166;223).

Even though Attaphitaya *et al.* (151) could demonstrate that NHE5 has very similar regulatory properties to NHE3 in the related system PS120 cells, we were unable to reproduce this regulatory data in AP1 cells. Unlike NHE3, NHE5 is not downregulated by the PKA and PKC pathways, and hyperosmolarity does not seem to inhibit its activity in AP1 cells.

To delineate the *in vivo* regulation of NHE5, we adopted a different approach. Using the yeast two-hybrid system and a human brain cDNA library we tried to identify interacting proteins of NHE5. This approach has the additional advantage of identifying native interactant proteins that might not be present or might not be able to operate in a heterologous expression system. Chapter 2 and 3 presents our studies on two of the candidate interactants recognized by the yeast two-hybrid assay.

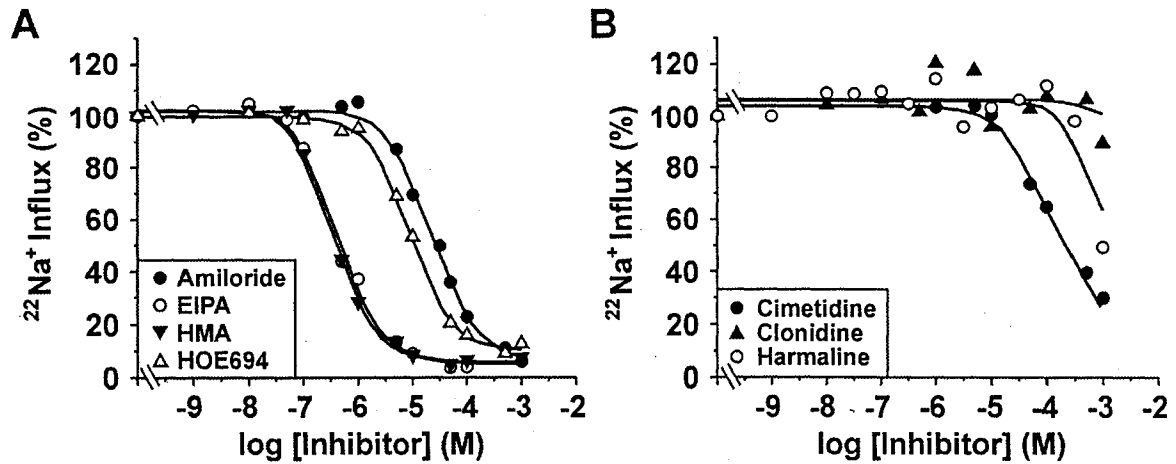


Fig. 1.1. Concentration-response profiles for inhibition of human NHE5 activity by various pharmacological agents. AP-1 cells expressing human NHE5 (AP1/NHE5^{C6}) were grown to confluence in 24-well plates. Prior to $^{22}\text{Na}^+$ influx measurements, the cells were loaded with H^+ using the NH_4Cl prepulse technique. Initial rates of H^+ -activated $^{22}\text{Na}^+$ influx were measured in the (A) presence of increasing concentrations (10^{-9} to 10^{-3} M) of amiloride (closed circle), EIPA (open circle), HMA (closed triangle), and HOE694 (open triangle) and in the (B) presence of increasing concentrations (10^{-9} to 10^{-3} M) of cimetidine (closed circle), clonidine (closed triangle), and harmaline (open circle) as detailed under *Experimental Procedures*. Data were normalized as a percentage of the maximal rate of H^+ -activated $^{22}\text{Na}^+$ influx in the absence of inhibitor. Values represent the average of two to four experiments, each performed in quadruplicate.

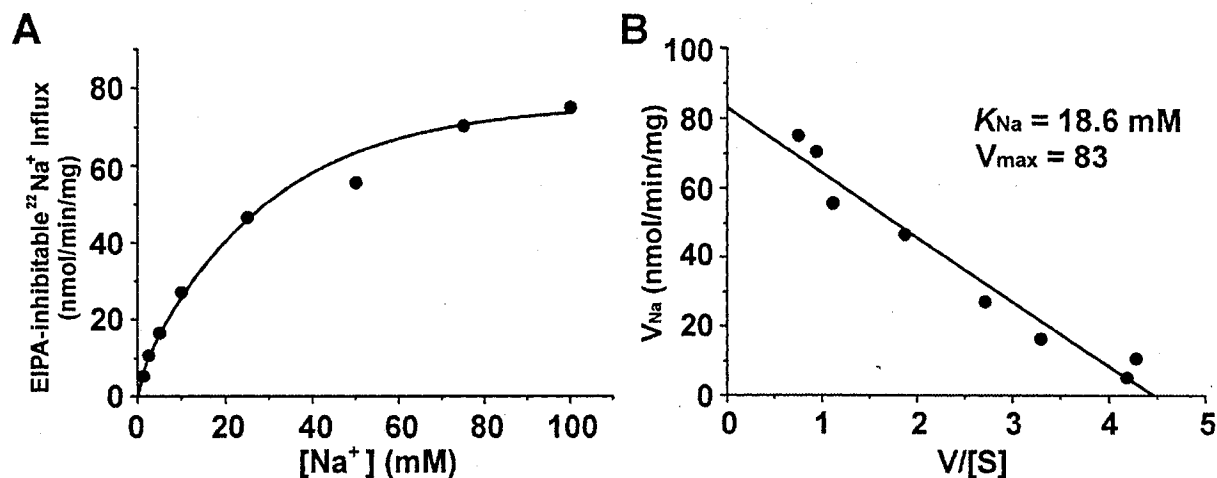


Fig. 1.2. Transport activity of human NHE5 as a function of the extracellular Na^+ concentration. AP1/NHE5^{C6} cells were acid loaded using the NH_4Cl prepulse technique. *A*, initial rates of H^+ -activated $^{22}\text{Na}^+$ influx were measured at increasing concentrations of extracellular Na^+ . Isoosmolarity was maintained by adjusting the choline chloride concentration. Background $^{22}\text{Na}^+$ uptake that was not inhibitable by 0.1 mM EIPA was subtracted from the total influx. Na^+/H^+ exchanger activity is expressed as EIPA-inhibitable $^{22}\text{Na}^+$ influx (nmol/min/mg protein). *B*, the apparent affinity constant (K_{Na}) for Na^+_o was calculated from the linear transformation of the data according to the algorithm of Eadie-Hofstee. Values represent the average of three experiments, each performed in quadruplicate.

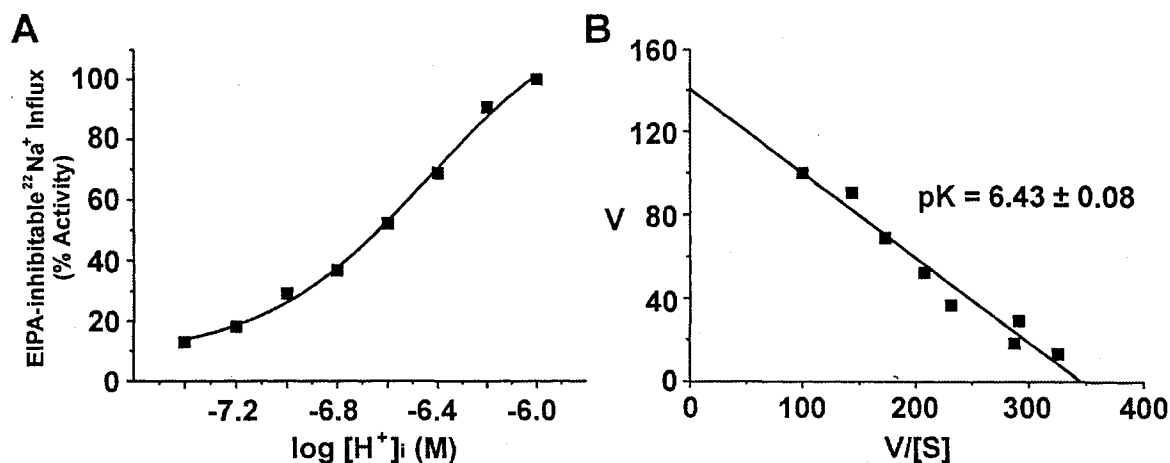


Fig. 1.3. Transport activity of human NHE5 as a function of the intracellular H^+ concentration. *A*, the initial rates of EIPA-inhibitable $^{22}\text{Na}^+$ influx by AP1/NHE5^{C6} cells were determined at increasing concentrations of intracellular H^+ (pH_i 7.4 to 6.0). The pH_i was clamped at different concentrations using the K^+ -nigericin method as described under *Experimental Procedures*. Data were normalized as a percentage of the maximal rate of EIPA-inhibitable $^{22}\text{Na}^+$ influx at pH_i 6.0. *B*, the apparent affinity constant (pK) for H^+ was calculated from the linear transformation of the data according to the algorithm of Eadie-Hofstee. Values represent the average of three experiments, each performed in quadruplicate.

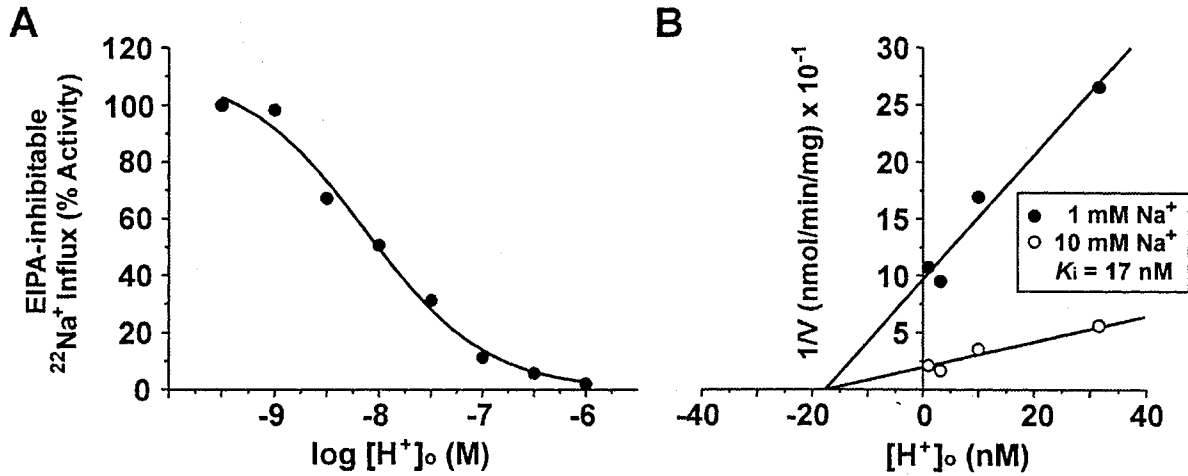


Fig. 1.4. Influence of extracellular H^+ on EIPA-inhibitable $^{22}\text{Na}^+$ influx in AP-1 cells expressing human NHE5. AP1/NHE5^{C6} cells were preloaded with H^+ using the NH_4Cl prepulse technique. Initial rates of EIPA-inhibitable $^{22}\text{Na}^+$ influx were measured as a function of increasing extracellular H^+ (pH_o 6.0-9.5). *A*, the $^{22}\text{Na}^+$ influx medium containing carrier-free $^{22}\text{NaCl}$ (1 $\mu\text{Ci}/\text{ml}$) was buffered with 30 mM MES-Tris (pH 6.0-6.5), 30 mM MOPS-Tris (pH 7.0), 30 mM HEPES-Tris (pH 7.5-9.5). Data were normalized as a percentage of the maximal rate of EIPA-inhibitable $^{22}\text{Na}^+$ influx at pH_o 9.5. *B*, the initial rates of transport as a function of pH_o were measured in the presence of different extracellular Na^+ concentrations (1 and 10 mM), and the data were plotted according to the Dixon algorithm ($1/V$ versus $[\text{H}^+]_o$). Values represent the average of at least two experiments, each performed in quadruplicate.

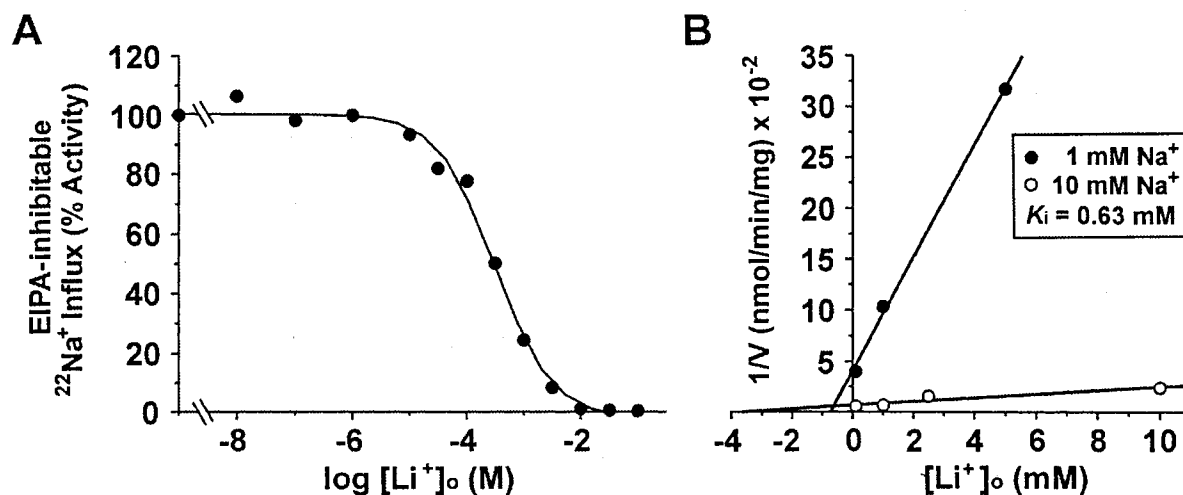


Fig. 1.5. **Influence of extracellular Li^+ on EIPA-inhibitable $^{22}\text{Na}^+$ influx in AP-1 cells expressing human NHE5.** AP1/NHE5^{C6} cells were preloaded with H^+ using the NH_4Cl prepulse technique. A, initial rates of amiloride-inhibitable $^{22}\text{Na}^+$ influx were measured in the presence of increasing concentrations of Li^+_o (10^{-8} to 10^{-1} M). Isoosmolarity was maintained by adjusting the choline chloride concentration. Data were normalized as a percentage of the maximal rate of EIPA-inhibitable $^{22}\text{Na}^+$ influx in the absence of Li^+_o . B, the initial rates of transport as a function of Li^+_o were measured in the presence of different extracellular Na^+ concentrations (1 and 10 mM), and the data were plotted according to the Dixon algorithm ($1/V$ versus $[\text{Li}^+]_o$). Values represent the average of at least two experiments, each performed in quadruplicate.

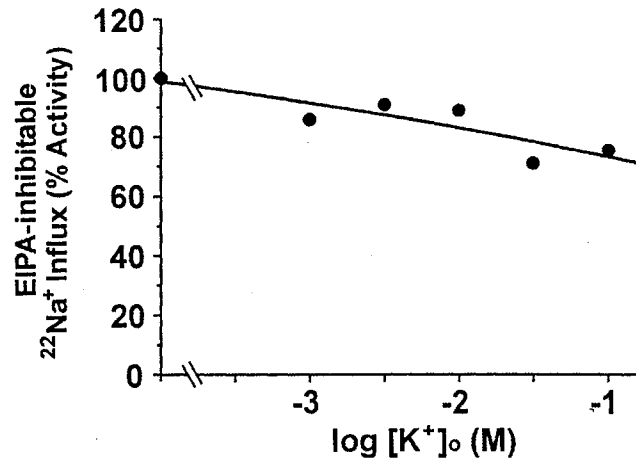


Fig. 1.6. **Influence of extracellular K⁺ on EIPA-inhibitable ²²Na⁺ influx in AP-1 cells expressing human NHE5.** AP1/NHE5^{C6} cells were preloaded with H⁺ using the NH₄Cl prepulse technique. Initial rates of EIPA-inhibitable ²²Na⁺ influx were measured in the presence of increasing concentrations of K⁺_o (10⁻³ to 10⁻¹ M). Isoosmolarity was maintained by adjusting the choline chloride concentration. Data were normalized as a percentage of the maximal rate of EIPA-inhibitable ²²Na⁺ influx in the absence of K⁺_o. Values represent the average of two experiments, each performed in quadruplicate.

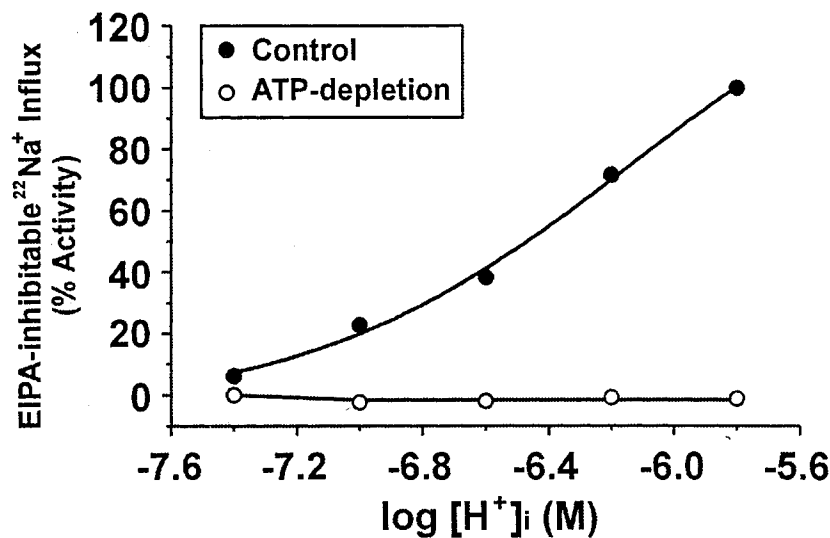


Fig. 1.7. **ATP dependence of the activity of human NHE5.** AP1/NHE5^{C6} cells were grown to confluence in 24-well plates. Prior to ²²Na⁺ influx measurements, the cells were incubated for 10 min in ATP-depleting or control solutions. Following repeated washing, the pH_i was adjusted to different concentrations using the K⁺-nigericin technique. The cells were washed with isotonic choline chloride solution, and then incubated for 4 min at 22 °C in *N*-methyl-D-glucammonium⁺-balanced salt solutions specific for each pH_i (pH-clamp solutions). All solutions contained 2 mM NaCl, 1 mM MgCl₂, 1 mM CaCl₂, 10 mM HEPES, pH 7.4, varying concentrations of K⁺, and the K⁺/H⁺ exchange ionophore nigericin (10 μM). The osmolality of the individual solutions was adjusted by *N*-methyl-D-glucammonium chloride. Since at equilibrium $[K^+]_i/[K^+]_o = [H^+]_i/[H^+]_o$, under these conditions the pH_i is determined by the imposed [K⁺] gradient, and the extracellular pH (pH_o = 7.4), and can be calculated assuming K⁺_i = 140 mM. ²²Na⁺ influx measurements were initiated in the same K⁺-nigericin solutions supplemented with ²²Na⁺ (1 μCi/ml) and 1 mM ouabain in the absence or presence of 0.1 mM EIPA. ²²Na⁺ influx was linear with time for at least 10 min under these experimental conditions. Data were normalized as a percentage of EIPA-inhibitable ²²Na⁺ influx at pH_i 5.8. Values represent the average of two experiments, each performed in quadruplicate.

TABLE 1.1

Comparison of the inhibition constants of rat NHE1, rat NHE3 and human NHE5 isoforms for various pharmacological agents

Inhibitor	Inhibition Constants ($K_{0.5}$)		
	NHE1 ^a	NHE3 ^a	NHE5
	<i>M</i>		
Amiloride compounds			
Amiloride	$1.6 \pm 0.1 \times 10^{-6}$	$1.0 \pm 0.1 \times 10^{-4}$	$2.1 \pm 0.2 \times 10^{-5}$
EIPA	$1.5 \pm 0.2 \times 10^{-8}$	$2.4 \pm 0.2 \times 10^{-6}$	$4.2 \pm 0.5 \times 10^{-7}$
HMA	$1.3 \pm 0.1 \times 10^{-8}$	$2.4 \pm 0.4 \times 10^{-6}$	$3.7 \pm 0.3 \times 10^{-7}$
Nonamiloride compounds			
HOE694	$8.5 \pm 0.2 \times 10^{-8}$	$6.4 \pm 0.3 \times 10^{-4}$	$9.1 \pm 0.6 \times 10^{-6}$
Cimetidine	$2.6 \pm 0.2 \times 10^{-5}$	$6.2 \pm 0.4 \times 10^{-3}$	$2.3 \pm 0.4 \times 10^{-4}$
Harmaline	$1.4 \pm 0.2 \times 10^{-4}$	$1.0 \pm 0.1 \times 10^{-3}$	$9.4 \pm 0.8 \times 10^{-4}$
Clonidine	$2.1 \pm 0.2 \times 10^{-4}$	$6.2 \pm 0.5 \times 10^{-4}$	None

^a $K_{0.5}$ values for NHE1 and NHE3 were obtained from Refs. 103 and 112, except those for HMA which were determined in this study. Values are presented as the mean \pm S.D.

TABLE 1.2

Comparison of the apparent affinity constants of rat NHE1, NHE3, and human NHE5 isoforms for various intra- and extracellular monovalent cations

Cation	Apparent Affinity Constants ($K_{0.5}$)		
	NHE1	NHE3	NHE5
Na^+_o (mM)	10.0 ± 1.4	4.7 ± 0.6	18.6 ± 1.6
H^+_i (pK)	6.75 ± 0.05	6.45 ± 0.08	6.43 ± 0.08
H^+_o (pK)	7.0 ± 0.1	7.0 ± 0.1	8.13 ± 0.15
Li^+_o (mM)	3.4 ± 0.3	2.6 ± 0.6	0.32 ± 0.04
K^+_o (mM)	19.5 ± 1.3	none	slight inhibition

^a $K_{0.5}$ values for NHE1 and NHE3 were obtained from Ref. 103.

Values are presented as the mean \pm S.D.

CHAPTER 2

AMP-activated Protein Kinase Regulates Brain-specific Na⁺/H⁺ Exchanger Isoform 5¹

Masayuki Numata*, Elöd Z. Szabó*, Pietro Iannuzzi, and
John Orłowski

¹ This manuscript is in preparation for submission to the *Journal of Biological Chemistry*.

* These authors contributed equally.

Na⁺/H⁺ exchanger isoform 5 (NHE5) is a brain specific isoform involved in intracellular pH homeostasis and volume regulation. To find novel interacting proteins that are involved in NHE5 regulation, we carried out a yeast two-hybrid screening. A clone encoding the AMP-activated protein kinase (AMPK) α 2 subunit was further analyzed in this study. AMPK is a serine/threonine kinase that is activated by elevated ratios of [AMP]/[ATP], regulating various biological processes in response to hypoxia or exercise. By both GST pull-down and co-immunoprecipitation experiments, the interaction with NHE5 was confirmed. Upon co-transfection of myc-tagged AMPK α 2 subunit with HA-tagged NHE5, AMPK α 2 exhibited co-localization with NHE5 showing patchy pattern on the plasma membrane by double-labeling immunofluorescence microscopy. *In vitro* phosphorylation demonstrated two independent domains in the NHE5 C-terminus, G543-I654 and G789-L896, that are capable of being phosphorylated by purified AMPK. The presence of AMP further enhanced the level of phosphorylation by two-fold. Interestingly, these phosphorylation sites coincided with the AMPK α 2 subunit interacting domains. Activation of endogenous AMPK by 5-aminoimidazole-4-carboxamide riboside (AICAR), a membrane permeable AMP analogue, as well as heterologous expression of the full-length and constitutive active form of α 2 subunit increased the transporter activity measured by ²²Na⁺ influx over 1.5-fold. Conversely, overexpression of a dominant negative α 2 construct suppressed the transporter activity up to 50%. We propose a model wherein elevated AMPK activity in response to the increase in cellular [AMP]/[ATP] caused

by stress such as hypoxia, regulates intracellular pH and volume through direct phosphorylation of NHE5.

INTRODUCTION

Na^+/H^+ exchangers (NHEs) are electroneutral transporters that exchange Na^+ for H^+ across the plasma membrane and play an important role in intracellular pH homeostasis and volume regulation. To date, seven isoforms have been cloned from mammals. NHE1-5 are functional in the plasma membrane and classified as plasma membrane type (91), while NHE6 and 7 predominantly reside in organellar membranes (89;90). NHEs share similar structural properties with a relatively conserved *N*-terminal transmembrane domain responsible for Na^+ and H^+ translocation, and a more diverse *C*-terminal cytosolic tail that is crucial for isoform specific regulation by phosphorylation-dependent and independent mechanisms (reviewed in (91)).

Intracellular pH (pH_i) changes can influence a number of processes within the nervous system such as neuronal excitability and synaptic transmission. Multiple Na^+/H^+ exchanger (NHE) isoforms are known to contribute to central nervous system pH regulation. The importance of NHE1, the most abundant and widely expressed isoform, in neuronal function was demonstrated by spontaneous null mutations in mice, which develop ataxia and epileptic-like seizures by 2 weeks of age and show significant mortality (67%) prior to weaning (126). Meanwhile, the fact that both *nhe1* spontaneous mutant and knockout mice (125) survived until 2 weeks of postnatal age with normal brain development suggests that a different isoform has complementary or even more important roles in maintaining brain function during this critical developmental stage. In favour of this hypothesis, a brain specific isoform, NHE5, was isolated from human (176) and rat (175) recently. The amino acid sequences from these two species share as much as 95% identity, suggesting some evolutionarily conserved biological function of this

molecule. This isoform is unique in being relatively insensitive to amiloride and its derivatives, and having a first-order dependence on the intracellular H^+ concentration (224).

Compared to other isoforms, only limited amount of knowledge is available on the regulation mechanism of NHE5 (151). To better understand the regulation of NHE5 by protein-protein interactions, we screened a human brain yeast two-hybrid cDNA library. One clone turned out to be AMPK $\alpha 2$, the catalytic subunit of the heterotrimeric AMP-activated protein kinase (AMPK) complex. In this paper, we show that AMPK interacts with the C-terminal tail of NHE5 both *in vitro* and *in vivo* and overexpression of NHE5 causes redistribution of AMPK $\alpha 2$ from the nucleus/cytosol to the plasma membrane showing patchy appearance co-localizing with NHE5 by dual-labeling confocal immunofluorescence microscopy. *In vitro* phosphorylation experiments demonstrated that the NHE5 C-terminus is phosphorylated by AMPK. Activation of AMPK by AICAR, a membrane-permeable AMP analogue, or overexpression of a constitutive active form of AMPK $\alpha 2$ increased transporter activity. Conversely, overexpression of dominant negative constructs decreased the transporter activity. Taken together, these results suggest that AMPK regulate NHE5 by direct association and phosphorylation. This may account for a novel mechanism of NHE regulation in response to metabolic stress.

EXPERIMENTAL PROCEDURES

Materials

α -Minimal essential medium, fetal bovine serum, penicillin/streptomycin, and trypsin-EDTA were from Life Technologies (Burlington, ON). Amiloride and AICAR were from Sigma. Radioactive materials were purchased through PerkinElmer Canada. All other chemicals and reagents, unless otherwise indicated, were from Fisher Scientific or Sigma, and were of the highest grade available.

Yeast Two Hybrid Screening

The human NHE5 cDNA corresponding to G543-L896 (C-terminus) was amplified by PCR using two oligos (Forward: 5'-ATG GCC ATG GCC ATT GGC CAC GTC TTG TCT TCC-3', Reverse: 5'-TAG CCC GGG CTA CAG CCG GCT GCC TCT GTT G-3') and subcloned into the *Nco*I and *Xma*I sites of the pAS2-1 vector (NHE5B/pAS2-1 (Clontech, Palo Alto, CA) in-frame with the *GAL4* 1-147 DNA binding domain. *S. cerevisiae* strain AH109 (*MATa*, *trp1-901*, *leu2-3, 112*, *ura3-52*, *his3-200*, *gal4 Δ* , *gal80 Δ* , *LYS2::GAL1_{UAS}-GAL1_{TATA}-HIS3*, *GAL2_{UAS}-GAL2_{TATA}-ADE2*, *ura3::MEL1_{UAS}-MEL1_{TATA}-lacZ*) was co-transformed with NHE5B/pAS2-1 carrying the *Trp* gene and the *GAL4* DNA binding domain, and a human brain cDNA library cloned into the pACT2 vector (Clontech), carrying the *LEU2* gene and the *GAL4*-(768-881) activation domain using a modified lithium acetate method (225). Over 2×10^6 clones were screened in four separate experiments on the synthetic complete (SC) media containing 0.67% bacto-yeast nitrogen base without amino acids (DIFCO laboratories, Detroit, MI), 2% glucose, 1.5% bacto-agar and 0.2% -Leu-Trp-His-Ade drop-out mix and subjected to β -galactosidase

filter assay. For the β -galactosidase filter assay, a replica was taken from each plate onto filter paper (VWR Scientific Products, West Chester, PA), frozen rapidly in liquid nitrogen and incubated with 0.35 mg/ml 5-bromo-4-chloro-3-indolyl- β -D-galactopyranoside (X-gal) in the buffer containing 60 mM Na_2HPO_4 , 40 mM NaH_2PO_4 , 10 mM KCl, 1 mM MgSO_4 (pH 7.0) at room temperature for up to 4 h. The resulting Leu^+ , Trp^+ , His^+ , Ade^+ , LacZ^+ colonies were streaked on SC-Leu-Trp-His-Ade plates two additional times and single colonies were inoculated into liquid SC-Leu media supplemented with Trp, His, and Ade for 3-4 days culture to release the NHE5B/pAS2-1 plasmid. Library-derived cDNA clones in pACT2 coding for putative NHE5 interacting proteins were rescued from yeast cells and directly transformed into DH5 α cells. The identities of the clones were determined by DNA sequencing by Sanger method and compared against the National Cancer Center for Biotechnology Information database using the BLAST search program.

The four rounds of screening yielded about 300 clones satisfying both nutritional and color selection schemes (His^+ , Ade^+ , LacZ^+). All clones were sequenced, and clones that were in-frame with the GAL4 activation domain were further analyzed after excluding well-known false positive clones, such as transferrin, ribosomal proteins and mitochondrial proteins. Nine of the remaining clones, including AMPK α 2 and arrestin3, were confirmed by mating assay using the MAT α strain Y187 (Clontech) and the MATa strain AH109.

Cloning of AMPK α 2 and Construction of Plasmids encoding Epitope-tagged Proteins

One cDNA clone identified by the yeast two-hybrid screen encoded AMPK $\alpha 2$ lacking the first 6 amino acids. To isolate the full-length cDNA, PCR was carried out with the following set of oligos. Forward: 5'-CCC AAG CTT GCC ACC ATG GCT GAG AAG CAG AAG CAC GAC GGG CGG GTG AAG ATC GGA C- 3', and reverse: 5'-CGG AAT TCT TAA CGG GCT AAA GTA GTA CTA ATC AGA CTG G- 3'. The amplified fragment was subcloned into the mammalian expression vector pCMV under the control of the enhancer/promoter region of the immediate early gene of human cytomegalovirus at the *HindIII* and *EcoRI* sites, and the sequence was verified subsequently.

To allow for immunological detection of the proteins, we created epitope-tagged versions of NHE5 and AMPK $\alpha 2$. AMPK $\alpha 2$ -myc was constructed by PCR using the sense oligo from the above reaction and an antisense oligo containing the coding sequence for the myc epitope in frame and an *XbaI* site (5'-GCT CTA GAC TAG TTC AGG TCC TCC TCG CTA ATT AGC TTC TGT TCA ACG GGC TAA AGT AGT AAT CAG ACT GG- 3'). The amplified fragment was subcloned into pCMV at the *HindIII* and *XbaI* sites, and the sequence was verified. For NHE5, first, a unique *NotI* restriction endonuclease site was introduced in the coding region within the first predicted extracellular loop of the protein altering two amino acid residues at positions 36 and 37 from Leu-Phe to Arg-Gly (³⁴LELFR to ³⁴LERGR). A *NotI-NotI* DNA fragment encoding a triple HA epitope (*NotI* sites underlined; rgrifYPYDVPDYAg YPYDVPDYAgYPYDVPDYAaqcg) was then inserted into the *NotI* site (tag inserted between amino acids Glu³⁵ and Arg³⁸) and the modified cDNA/protein was called NHE5-36HA3. The construct was subcloned into the mammalian expression vector pCMV, and

the cDNA was sequenced to confirm the presence of the mutation and to ensure that other random mutations were not introduced. A stable transfectant of NHE5-36HA3 based on the AP1 cell line (AP1/NHE5-36HA3) was created by acid selection (103). In control experiments, the mutation had no obvious effect on the functional properties of NHE5.

Glutathione S-transferase (GST) Pull-down

For producing GST fusion proteins, different regions of the AMPK $\alpha 2$ and NHE5 cDNAs were amplified by PCR, excised with *Bam*HI and *Eco*RI and inserted into the same restriction sites of the pGEX-2T bacterial expression vector (Amersham Pharmacia Biotech) in frame with the amino-terminal GST tag. Transformed BL21 *E. coli* cells derived from single colonies were inoculated in 5 ml 2YT + Amp (100 μ g/ml) media overnight and protein expression was induced by further incubation in 50 ml of the same media containing 0.4 mM isopropyl-1-thio- β -D-galactopyranoside (IPTG) at 30°C for 3h. *E. coli* cells were collected by centrifugation, resuspended in 1 ml lysis buffer containing 0.5% NP40, 1mM EDTA, 0.1 mg/ml lysozyme and proteinase inhibitor cocktails (Roche Diagnostics, Laval, Quebec Canada) in PBS, incubated on ice for 15 min and sonicated 4 times for 30 sec on ice. Cell debris were removed by centrifugation at 16,000 g for 20 min and the GST fusion proteins were purified by incubation with reduced form glutathione (GSH) sepharose beads (Amersham Pharmacia Biotech) at 4°C for 2 h. For producing an *in vitro* translated protein of the C-terminus of NHE5, cDNA corresponding to this region (G491-L896) was amplified by PCR using the following primer set (Forward: 5'-CCC AAG CTT GCC ACC ATG GGC TAC CAC TAC TGG AGG GAC-3', Reverse: 5'-CCC TCT AGA CTA CAG CCG GCT GCC TCT GTT G-3') and the

HindIII-XbaI excised fragment was ligated into the pCMV vector. For mapping the binding domains of NHE5, full-length AMPK $\alpha 2$ cDNA in the same vector was used for *in vitro* translation. The T7 promoter in the vector enabled *in vitro* transcription-translation coupling reaction using rabbit reticulocyte lysates (Promega, Madison, WI). Following four washes in the lysis buffer without lysozyme, the beads were incubated with ^{35}S -labeled *in vitro* translated protein generated by the TnT reticulocyte lysate system (Promega, Madison, WI). After overnight incubation at 4 °C the beads were washed six times in the same buffer. ^{35}S -labeled *in vitro* translated protein bound to the GST fusion protein was detected by SDS-PAGE followed by autoradiography.

Co-immunoprecipitation

Cell lysates of the stable cell line AP1/NHE5-36HA3 were prepared in PBS containing 0.5% NP40, 1mM EDTA and proteinase inhibitor cocktail. Five hundred μl of cell lysates containing approximately 250 μg of protein were precleaned by incubation with protein G-conjugated sepharose beads (Amersham Pharmacia Biotech) and incubated with 1.5 μl anti-HA monoclonal antibody (HA.11 clone 16B12 (5-7 mg/ml) (Covance, Richmond, CA)) at 4°C for 2 h, followed by overnight incubation with 20 μl protein G sepharose beads. The beads were washed with lysis buffer for 5 times and the NHE5 – AMPK interaction was detected by Western blot with a monoclonal antibody to the $\beta 1$ subunit of AMPK (Transduction Laboratories, Lexington, KY). Cell lysates from untransfected AP1 cells were used as control.

Immunofluorescence Microscopy

0.5 µg of each NHE5-36HA3 and AMPK α 2-myc were simultaneously transfected into CHO cells grown on glass cover slips by Lipofectamine reagent (Gibco BRL, Burlington, Ontario, Canada) and intracellular localization of these proteins were analyzed 16-24 h after transfection. Cells were fixed with 2% paraformaldehyde in PBS for 20 min and blocked in 5% non-fat skim milk and 0.1% Triton X100 in PBS (PBS-TX) for 15 min. Following incubation with 5-7 µg/ml anti-HA mouse monoclonal antibody and rabbit polyclonal anti-myc antibody for 1 h, cells were incubated with 1.75 µg/ml Cy3-conjugated anti mouse IgG (Jackson Laboratories) and 1.5 µg/ml Oregon-green conjugated anti rabbit IgG (Molecular Probes, Eugene, OR) for 1 h. All antibodies were diluted in PBS-TX. After extensive washes with PBS-TX, cover slips were mounted on glass slides and the fluorescence signals were analyzed by confocal microscopy.

In Vitro Phosphorylation Assay

GST-NHE5 fusion proteins were purified by GSH sepharose beads and phosphorylation assay was performed by incubation with AMP-activated protein kinase purified from rat liver (Upstate Biotechnology, Lake Placid, NY) as described previously with some modifications (226). In short, about 20 µg GST fusion proteins on the GSH sepharose solid support was incubated with 10 mU AMPK in a final volume of 25 µl containing 40 mM HEPES (pH 7.0), 300 µM AMP, 80 mM NaCl, 5 mM MgCl₂, 0.8 mM EDTA, 0.4 mM dithiothreitol and 10 µCi [γ -³²P]-ATP (NEN Life Science Products, Boston, MA). After incubation at 30°C for 7 min, beads were sedimented by quick centrifugation and washed six times with PBS containing 0.5% NP40 and 1 mM EDTA. GST fusion proteins were eluted in SDS sample buffer containing 50 mM Tris-Cl (pH 6.8), 2% SDS,

0.1% bromophenol blue and 10% glycerol and resolved by SDS-PAGE. The gel was stained with Coomassie blue, dried and exposed to X-ray film (Kodak, Rochester, NY).

²²Na⁺ Influx Assay

Either AP1, the NHE-deficient CHO cell line, or AP1/NHE5, the parental cell line stably expressing human NHE5 cDNA (224), was used for this study. Cells were plated in 24-well polystyrene tissue culture dishes (Corning Incorporated, Corning, NY) and, for the AP1 cells, were transiently co-transfected with NHE5 and different AMPK α 2 constructs by the Lipofectamine reagent. The ²²Na⁺ influx assay was conducted as described previously (103) except that acid challenging prior to influx assay was omitted. In short, confluent monolayers of cells were washed with isotonic choline chloride solution (125 mM choline chloride, 1 mM MgCl₂, 2 mM CaCl₂, 20 mM HEPES-Tris, pH 7.4) and incubated with 1 μ Ci/ml ²²Na⁺ (PerkinElmer Canada) in the same solution containing 1 mM ouabain at room temperature for 5 min. The assay was terminated by rapidly washing the cells three times with 4 volumes of ice-cold NaCl stop solution (130 mM NaCl, 1 mM MgCl₂, 2 mM CaCl₂, 20 mM HEPES-NaOH, pH 7.4). Cell monolayers were subsequently solubilized by 0.25 ml of 0.5 M NaOH followed by neutralization with the same volume of 0.5 M HCl. Radioactivity was assayed by liquid scintillation spectroscopy. All experiments represent the average of two to five experiments, each performed in quadruplicate. The data are presented as the mean \pm S.D.

RESULTS AND DISCUSSION

Identification of the $\alpha 2$ Subunit of AMPK as an NHE5 Interacting Protein

To gain insight into the function and regulation of the brain specific Na^+/H^+ exchanger isoform NHE5, the C-terminal cytosolic tail of NHE5 was used as bait to screen a human brain cDNA library using the yeast two-hybrid system. The positive clone encoding $\alpha 2$ subunit of AMPK was further analyzed in this study. AMPK is a serine/threonine kinase that is activated by elevated $[\text{AMP}]/[\text{ATP}]$ ratio and the upstream kinase AMPKK. It is composed of a catalytic subunit (α) and two regulatory subunits (β and γ). To date, two α ($\alpha 1$ and $\alpha 2$) and β ($\beta 1$ and $\beta 2$) and three γ ($\gamma 1$ -3) isoforms have been identified with different tissue expressions and intracellular localizations (227-233). The N-terminus half of the $\alpha 2$ subunit (amino acid residues 1-312) is a catalytic domain and the latter half (residues 313-552) is a regulatory domain that serves as the binding site for the β and γ subunits.

To further substantiate the association of NHE5 and AMPK $\alpha 2$, we assessed the interaction by GST pull-down assay. Since the original clone was missing the first six amino acid residues at the N-terminus, the full-length cDNA was obtained by PCR. For GST pull-down, different parts of AMPK $\alpha 2$ cDNA were isolated and inserted into pGEX-2T to make in-frame GST-AMPK bacterial expression constructs. ^{35}S -labeled in vitro translated protein representing the C-terminus of NHE5 was incubated with GST fusion proteins derived from different parts of AMPK $\alpha 2$ in order to determine the responsible binding domains. As shown in Fig. 2.1A, in vitro translated NHE5 protein bound to S313-R421 with the highest affinity, followed by M1-G98 and A422-R552. To

define more precise binding sites in the segment encompassing S313-R421, smaller GST-AMPK $\alpha 2$ fusion proteins were analyzed. The predominant binding domain was mapped to reside between 386 and 421 (Fig. 2.1B). The weak binding at the *N*-terminal catalytic domain (residues 1-98) may reflect interaction associated with phosphorylation of NHE5.

To determine the binding domain within NHE5, we generated GST fusion proteins corresponding to three different sections of the NHE5 cytosolic tail, G543-I654, G689-G789 and G789-L896. The *in vitro* translated full-length AMPK $\alpha 2$ labelled with ^{35}S -methionine exhibited significant binding to two independent regions, G543-I654 and G789-L896 (Fig. 2.2). We were unable to analyze the binding capability of the section between I654 and G689 because GST fusion proteins containing this area were unable to be expressed even under milder induction conditions, most likely due to the toxicity of the proteins. Our attempt to map between G543 and I654, and G789 and L896 by GST pull-down and yeast two-hybrid gave unsatisfactory results showing similar signals in all the small sections within these areas (data not shown). Since two independent assays showed similar results, we postulate that relatively widely distributed binding sites within the NHE5 *C*-terminus and/or multiple binding sites are required for the interaction.

In Vivo Interaction between NHE5 and AMPK

To examine the relevance of the association between NHE5 and AMPK *in vivo*, we transfected NHE5-36HA3 into AP1 cells, the CHO mutants devoid of endogenous NHE activity, and a stable cell line (AP1/NHE5-36HA3) was established by acid selection as described previously (103). Cell lysates isolated from these cells as well as control AP1 cells were immunoprecipitated with an anti-HA antibody and the presence of

endogenous AMPK complex was probed with an anti AMPK β 1 antibody by Western blot analysis. AMPK was detected only in the immunocomplex isolated from AP1/NHE5-36HA3 cells, but not in the untransfected AP1 cells (Fig. 2.3). When CHO cells were transiently transfected with myc-tagged α 2 subunit and HA-tagged NHE5, immunoprecipitated with an anti-HA antibody and probed with anti-myc antibody for Western blot, we were able to detect the specifically associated myc-tagged AMPK α 2 subunit (data not shown). Thus, NHE5 showed *in vivo* association with both β 1 and α 2 subunit, suggesting that NHE5 forms a protein complex comprised of the α and β subunits and presumably γ subunit, making the AMPK enzyme complex in close proximity to the site of action on NHE5.

To further evaluate the physiological relevance of the interaction, we next investigated the intracellular localization of NHE5 and AMPK. CHO cells grown on glass cover slips were transiently transfected with AMPK α 2-myc and NHE5-36HA3 and their localization *in situ* was analyzed by confocal immunofluorescence microscopy after double staining with an anti-myc polyclonal and an anti-HA monoclonal antibody. As reported previously (234), the majority of AMPK α 2-myc signal was observed in the nucleus and cytosol in cells transfected with AMPK α 2 alone (Fig. 2.4D). In sharp contrast, co-transfection of AMPK α 2 with NHE5 caused pronounced redistribution of AMPK α 2 to the plasma membrane with patchy appearances, which co-localized with the NHE5 signal (Figs. 2.4A-C). These results, taken together, suggest that the interaction between AMPK α 2 and NHE5 is taking place *in vivo* and may have an important biological role.

NHE5 Can Be Phosphorylated by AMPK

To understand the physiological consequences of the binding of AMPK to NHE5, we examined whether NHE5 can be a substrate for AMPK. GST-NHE5 fusion proteins used for the GST pull-down experiments were incubated with purified AMPK enzyme (Upstate Biotechnology) in the presence of [γ - 32 P]-ATP, resolved in SDS-PAGE and analyzed by autoradiography. GST fusion proteins corresponding to G543-I654 and G789-L896 (C-terminus) of NHE5, the same domains binding to AMPK α 2 (Fig. 2.2), were strongly phosphorylated by AMPK (Fig. 2.5). The intensity of the phosphorylation signals, measured by a FluorChem digital imaging system (Alpha Innotech Corporation, San Leandro, CA), were enhanced over two-fold by inclusion of 0.3 mM AMP, demonstrating the unique aspect of the phosphorylation reaction by AMPK. No detectable phosphorylation was observed in the GST fusion protein comprising G689-G789 or GST alone, further supporting the specificity of the reaction. It is of note that these sections in NHE5 have several consensus recognition sequences for AMPK established from synthetic peptide studies (ϕ (X β)XX S/T XXX ϕ , where ϕ is a hydrophobic and β is a basic residue) (235) such as ⁵⁷¹LLRESGSGACL⁵⁸¹ and ⁸³⁰LPSDPRSSFAF⁸⁴⁰. As revealed by more recent studies, the substrate specificity of AMPK is considerably variable (236), and it is possible that there are more recognition sites in NHE5 in addition to these “conventional” ones.

AMPK Augments Transporter Activity by NHE5

To examine the physiological relevance of phosphorylation by AMPK, we treated AP1/NHE5 cells, the NHE-deficient CHO cell line AP1 stably transfected with NHE5

(224), with AICAR, a membrane permeable AMP analogue, and measured the NHE activity by $^{22}\text{Na}^+$ influx assay. AICAR treatment increased the amiloride-inhibitable $^{22}\text{Na}^+$ influx of AP1/NHE5 cells up to 2.5-fold in a dose- (Fig. 2.6A) and time-dependent (Fig. 2.6B) manner. The treatment had no effect on the $^{22}\text{Na}^+$ uptake of AP1 cells, which lack endogenous plasma membrane-type NHE activity (data not shown).

To further establish the importance of AMPK on NHE5 regulation, we next heterologously co-expressed NHE5 and constitutive-active or dominant negative AMPK $\alpha 2$ in AP1 cells and studied their effects on NHE5 activity. While heterologous expression of the constitutive active mutant (amino acid residues 1-312) AMPK $\alpha 2$ exhibited around 50% increase in the NHE5 activity, expression of dominant negative constructs (residues 313-552 and 395-552) showed 30-50% decrease (Fig. 2.7). Unexpectedly, heterologous expression of full-length $\alpha 2$ subunit also showed 30-50% elevation of NHE5 activity, which is almost as significant an effect as observed in the constitutive active mutant (residues 1-312) expressing cells. To achieve maximum enzymatic activity as well as protein expression level, concomitant expression of all the three subunits (α , β and γ) are needed (237). Although the precise reason why transfection of full-length $\alpha 2$ subunit alone elevated Na^+ influx by NHE5 is not known, it is possible that the binding of NHE5 to $\alpha 2$ subunit mimicked the effect of assembling into the complete triplet complex. Alternatively, limited amount of β and γ subunits may have been enough for the upregulation.

Possible Role of AMPK in pH Regulation in Brain

AMPK was originally identified as a metabolic sensor that phosphorylates and attenuates metabolic enzymes such as acetyl-CoA carboxylase and HMG-CoA reductase by direct phosphorylation in response to elevated [AMP]/[ATP] ratio to preserve intracellular ATP (238). AMPK is known to inhibit the Cl⁻ conductance of cystic fibrosis transmembrane conductance regulator (CFTR) by direct binding and phosphorylation (239). Our study is the second report showing AMPK is directly involved in the regulation of a membrane protein by direct phosphorylation.

Brain has a high metabolic rate and glucose consumption, where sensing and responding to metabolic change is particularly important. Recent studies implicated that neurons and activated astrocytes have high levels of AMPK expression (240). Our finding that NHE5 is activated by phosphorylation by AMPK suggests a role of AMPK in pH and volume regulation in the brain under metabolic stress and hypoxia.

A major source of intracellular protons, in addition to metabolic CO₂ production, is the reaction $\text{ATP} \leftrightarrow \text{ADP} + \text{P}_i + \text{H}^+$ ((8) and analyzed in detail in by Hochachka and Mommsen in (9)). The H⁺ production by this reaction becomes especially relevant during anoxia, when H⁺ is not consumed by oxidative phosphorylation. The ATP hydrolysis reaction establishes a direct connection between the energy status of the cell (the [ADP]/[ATP] ratio) and the intracellular pH. AMPK detects changes in the [AMP]/[ATP] ratio, which varies according to the square of the [ADP]/[ATP] ratio (241), consequently AMPK is a sensitive indirect pH_i detector. During prolonged anoxia, the only way to maintain ATP production is by glycolysis. Phosphofructokinase 1 (PFK-1) is a major control point of glycolysis catalyzing the irreversible phosphorylation of fructose 6-P to fructose 1,6-bis-P. PFK-1 is regulated by not only substrates of the

reaction and allosteric modifiers (ATP, AMP, fructose 6-P, fructose 2,6-bis-P), but also by pH_i . Remarkably, only 0.1 pH unit change can completely shut PFK-1 down or maximally activate it (63). Prolonged anaerobic conditions will inevitably lead to pH_i decrease, which, unless corrected, will inhibit PFK-1 and thereby halt glycolysis. The activation of NHE5 by AMPK at critically ATP-dependent and pH-sensitive cellular locations might be such a correcting mechanism.

It has recently been reported by Salt *et al.* that in pancreatic β cells such as INS-1 and HIT-T15 cells, AMPK activity is elevated over 5-fold upon glucose depletion (242), supporting the idea that mammalian AMPK can be activated in response to glucose deprivation, similar to the yeast homologue SNF1. Remarkably, our preliminary experiments showed that glucose removal from the media increased NHE5 activity to 1.5-fold in NHE deficient CHO cells (data not shown). We are currently working to determine the direct relationship between glucose deprivation, increased AMPK activity and NHE5 activity in our experimental system.

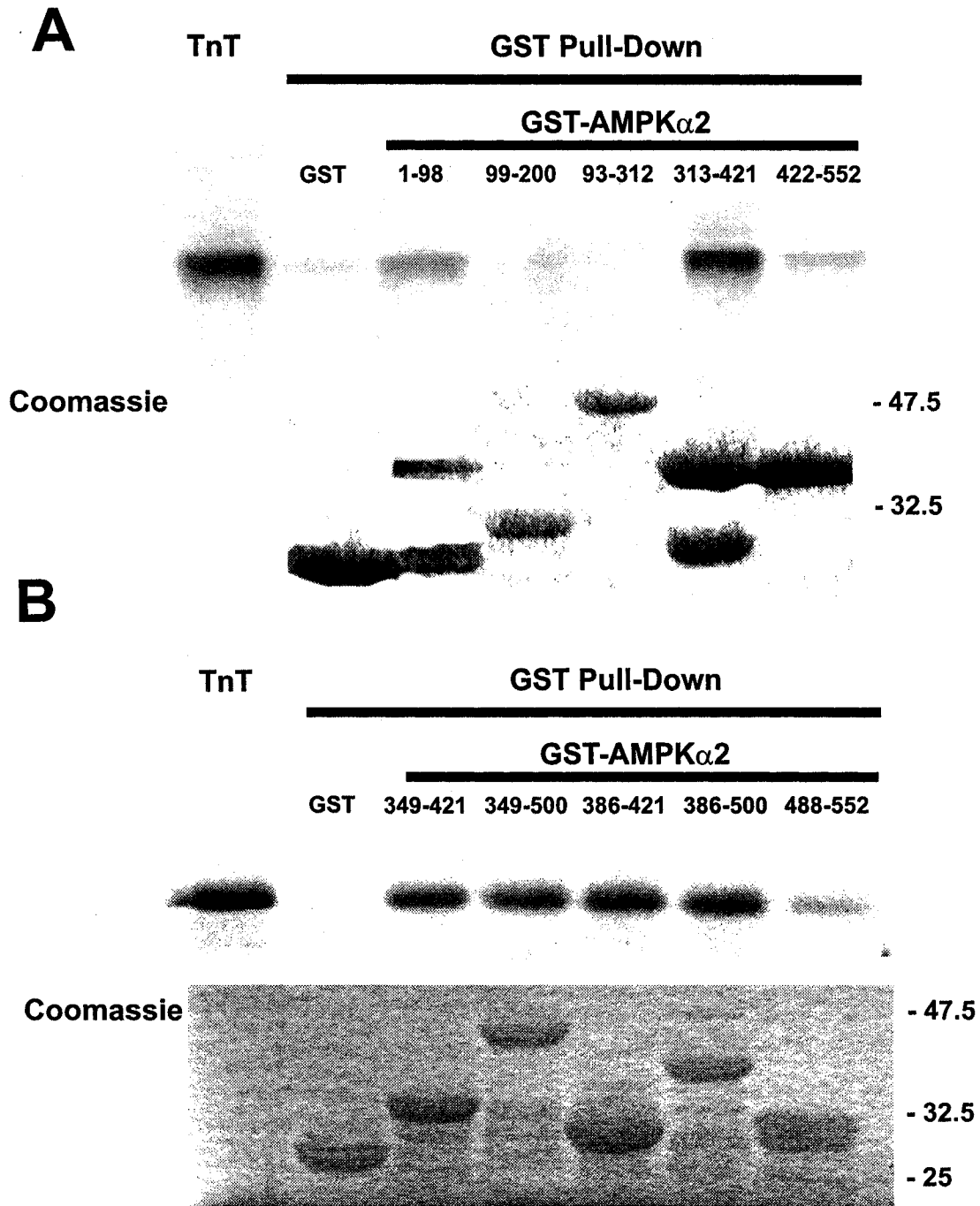


Fig. 2.1. The C-terminal tail of NHE5 binds to AMPK α 2. 35 S-labeled *in vitro* translated NHE5 C-terminus protein (G491-L896) was subjected to GST pull-down assay using the indicated GST-AMPK α 2 constructs. Samples were separated by SDS-PAGE, and analyzed by autoradiography. NHE5 was pulled down by GST-(M1-G98)AMPK α 2, and GST-(A313-R421)AMPK α 2 (A). Further mapping (B) with smaller fragments encompassing region S313-R421. Coomassie stained gels are shown to demonstrate equal loading of GST fusion proteins. Gels are representative of three replicate experiments.

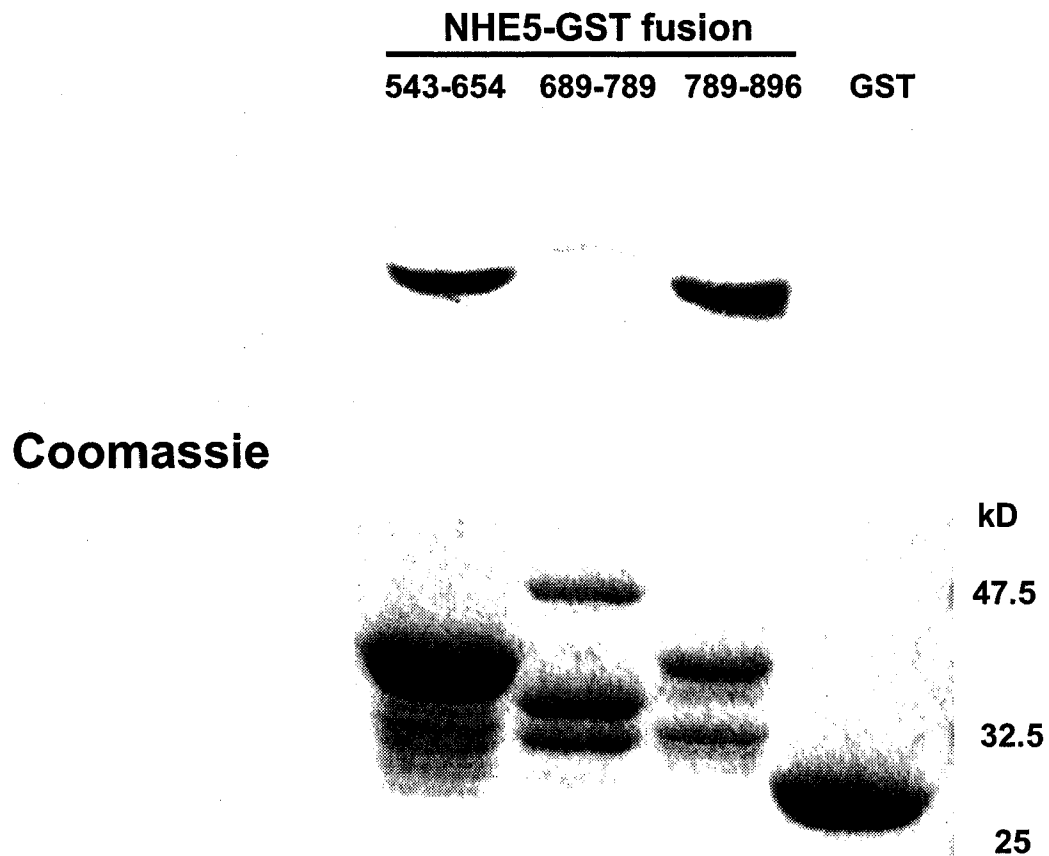


Fig. 2.2. Two independent parts of the C-terminus of NHE5 bind to AMPK α 2. ^{35}S -labeled *in vitro* translated full-length AMPK α 2 protein was subjected to GST pull-down assay using the indicated GST-NHE5 constructs. Samples were separated by SDS-PAGE, and analyzed by autoradiography. AMPK α 2 was pulled down by GST-(G543-I654)NHE5 and GST-(G789-L896)NHE5. The Coomassie stain is shown to demonstrate equal loading of GST fusion proteins. Results are representative of three replicate experiments.

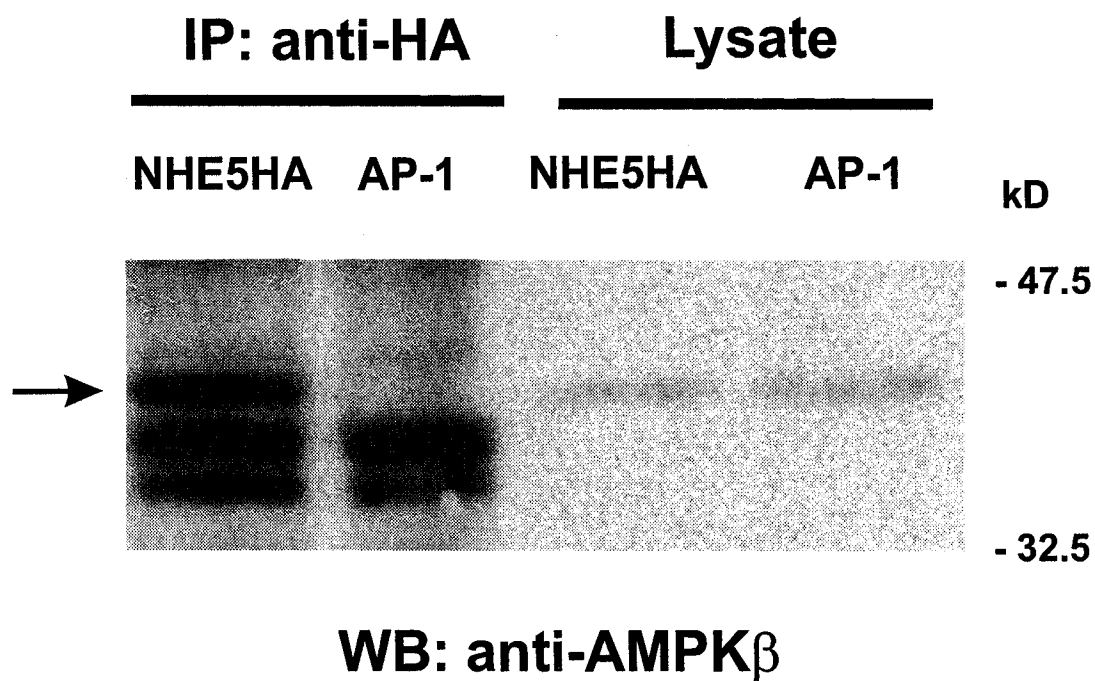


Fig. 2.3. *In vivo* interaction between NHE5 and AMPK. Cell lysates isolated from AP1/NHE5-36HA3 cells or untransfected AP1 cells were immunoprecipitated with an anti-HA antibody and immunoprecipitates were analyzed by western blot probed with an anti AMPK β 1 antibody. 38 kD band was detected only from the AP1/NHE5-36HA3 cells. Results shown are representative of three replicate experiments.

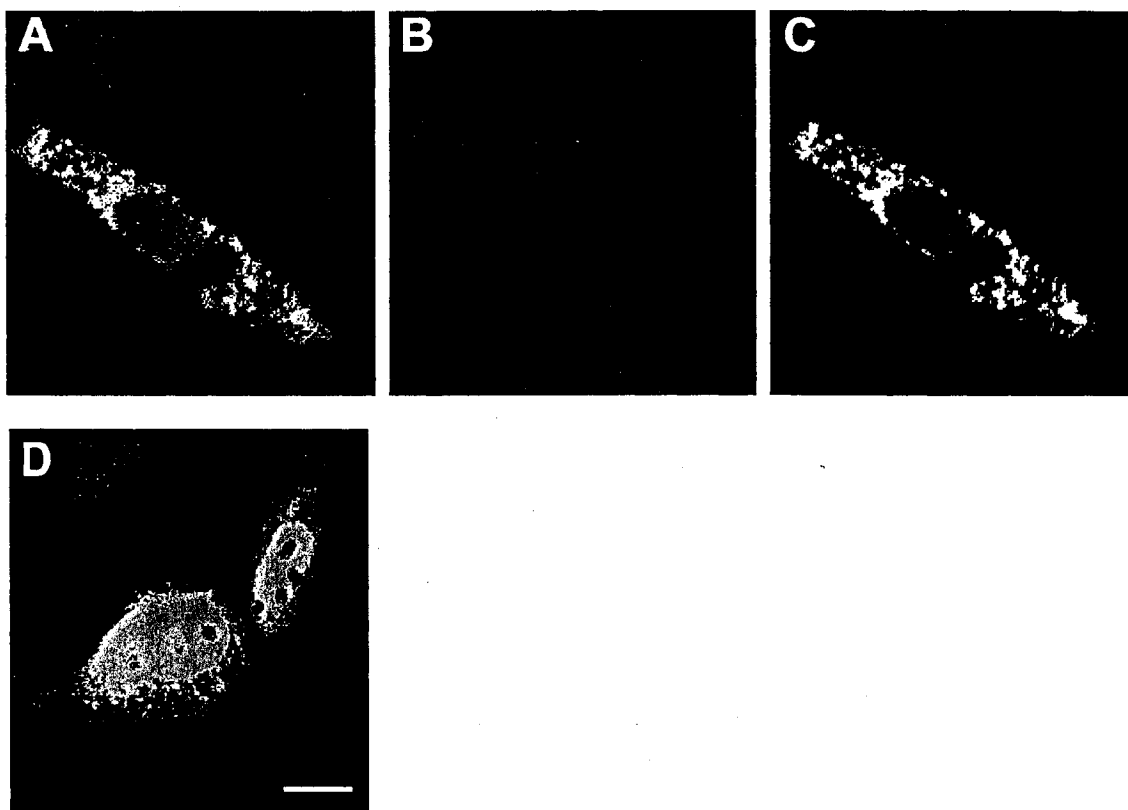
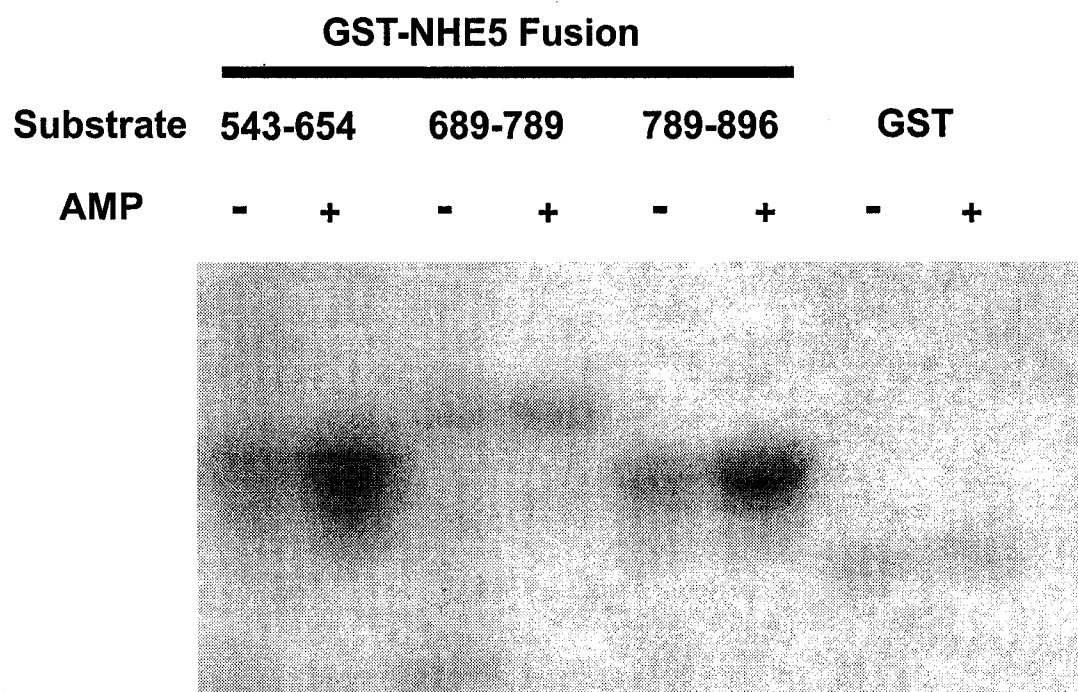


Fig. 2.4. Immunofluorescent confocal microscopy showing NHE5 co-localizing with AMPK α 2 on the plasma membrane. HA-tagged NHE5 and myc-tagged AMPK α 2 were transiently transfected into CHO cells and visualized by cy3 (red) (A) and Oregon Green (green) (B) conjugated secondary antibodies respectively. Note that AMPK α 2-myc alone shows predominantly nuclear and cytosolic localization (D). The scale bar corresponds to 10 μ m.



Coomassie

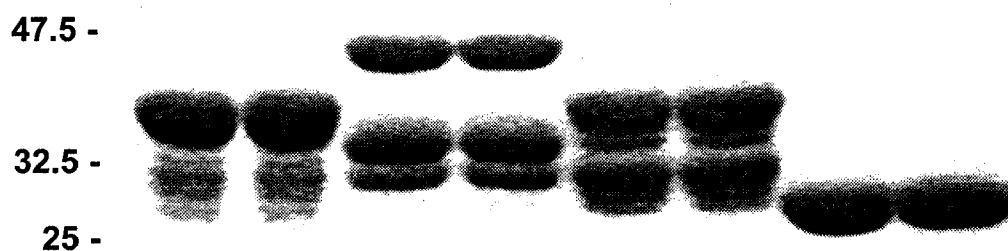


Fig. 2.5. NHE5 can be phosphorylated by AMPK. GST-NHE5 fusion proteins were incubated with AMPK in the presence or absence of 0.3 mM AMP, subjected to 12.5% SDS-PAGE and analyzed by autoradiography. G543-I654 and G789-L896 were specifically phosphorylated by AMPK, and the signal was enhanced in the presence of AMP. The Coomassie stain is shown to demonstrate equal loading of proteins. Results are representative of three replicate experiments.

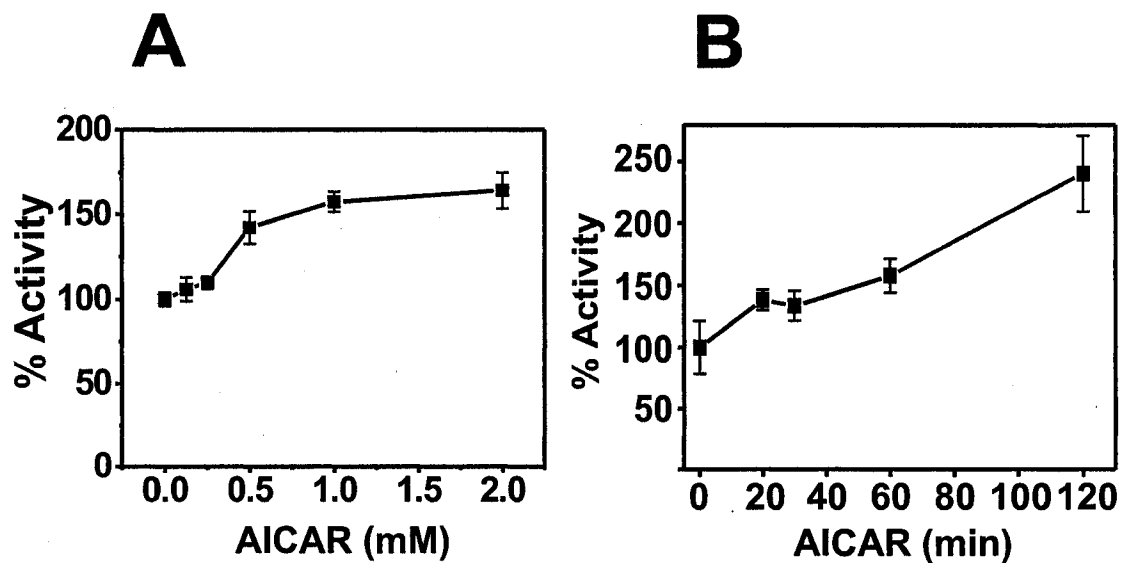


Fig. 2.6. **Activation of endogenous AMPK by AICAR.** AICAR treatment increases transporter activity in dose- and time-dependent manners. AP1/NHE5 cells were pretreated with AICAR (0-2.0 mM) for 60 min (A) or 1.0 mM for 0-120 min (B) and $^{22}\text{Na}^+$ influx was measured as described in *Experimental Procedures*. All the experiments were conducted in quadruplicate and repeated at least three times.

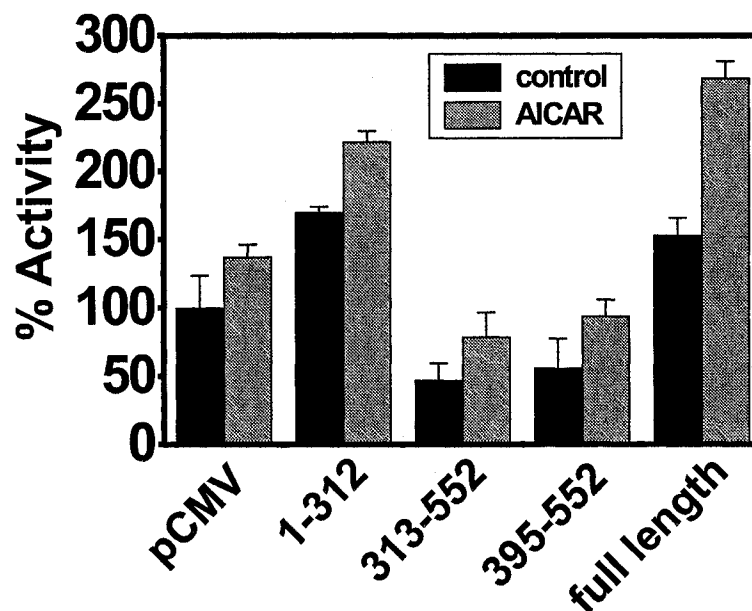


Fig. 2.7. Effects of constitutive active and dominant negative AMPK $\alpha 2$ on NHE5 activity. NHE5 and either AMPK $\alpha 2$ or pCMV (control) were transiently transfected into NHE-deficient AP1 cells. 36 hrs after transfection, $^{22}\text{Na}^+$ influx was measured as described in *Experimental Procedures*. In each experiment, $^{22}\text{Na}^+$ influx experiment was duplicated and half of them were conducted in the presence of 1.0 mM amiloride to obtain the background. After the backgrounds were subtracted, the relative values to the control (transfected with NHE5 and pCMV) were calculated. All the experiments were conducted in quadruplicate and repeated at least three times.

CHAPTER 3

*Arrestin3 Binds and Regulates Brain-specific Na⁺/H⁺ Exchanger Isoform 5*¹

Elöd Z. Szabó*, Masayuki Numata*, Pietro Iannuzzi, and
John Orlowski

¹ This manuscript is in preparation for submission to the *Journal of Biological Chemistry*.

* These authors contributed equally.

NHE5 is a brain specific Na^+/H^+ exchanger isoform, the function of which is yet unclear. Using the yeast two-hybrid system, we have identified arrestin3 as a putative NHE5 interacting protein. Arrestins were previously shown to associate with and regulate transmembrane proteins of only the G protein-coupled receptor family. We demonstrate that NHE5 binds arrestin3 both *in vitro*, in GST pull-down assays, and *in vivo*, as confirmed by co-immunoprecipitation. Furthermore, the binding is phosphorylation-dependent, and the kinase most likely responsible for the phosphorylation is casein kinase II. When co-expressed with NHE5 in CHO cells, the intracellular distribution of arrestin3 changes, showing co-localization with the exchanger under confocal immunofluorescence microscopy. Functionally, co-expression of arrestin3 with NHE5 seems to attenuate the basal activity of the transporter. Our data reveals new aspects of both arrestin function and NHE5 regulation.

INTRODUCTION

Na^+/H^+ exchangers (NHEs) are transmembrane proteins that mediate the electroneutral exchange of Na^+ and H^+ across membranes. There are seven mammalian isoforms identified to date, of which NHE1-5 are plasma membrane type (reviewed in (88;91)), while NHE6 and NHE7 are organellar exchangers (89;90). They all share a similar structure of a relatively conserved *N*-terminal transmembrane domain with 12 membrane-spanning regions, and a more disparate *C*-terminal cytoplasmic tail. NHE1, NHE6 and NHE7 are ubiquitous, probably performing 'housekeeping' functions of pH and volume homeostasis of cells and intracellular organelles. In contrast, NHE2-5 are more restricted in their pattern of expression, and play a role in specialized functions such as Na^+ and HCO_3^- absorption and reabsorption in the gastrointestinal tract and the kidney.

NHE5 is the most cell type-specific isoform, believed to be functionally expressed in brain only (175;176;224). Apart from the recent work by Attaphitaya *et al.* (151) showing that NHE5 is attenuated by both PKA and PKC little is known about the regulation and function of this isoform. In the current study, we applied the yeast two-hybrid system to screen for novel interacting proteins of NHE5 yielding an insight to the cellular physiology of the transporter. One of the interactants identified was arrestin3.

Arrestins form a family of regulatory proteins with four identified members in mammals: the two visual arrestins (rod and cone) and two non-visual arrestins (β -arrestins). Visual arrestins are expressed in the retina, whereas β -arrestin1 (arrestin2) and β -arrestin2 (arrestin3) are ubiquitously expressed outside the retina, although in various proportions in different tissues (243). β -arrestins play a dual role in the signal

transduction of numerous G-protein coupled receptors (GPCRs). First, they are responsible for the agonist-induced desensitization of GPCRs, by rapidly binding to GPCR Kinase (GRK) phosphorylated receptors and sterically interdicting activation of the G-protein. Second, they target the receptors to clathrin-coated pits for internalization by directly binding to both clathrin and the adaptor protein AP-2 (for recent reviews see (243-245)). Either lysosomal degradation or dephosphorylation and subsequent resensitization of the receptor follow internalization of a GPCR. β -arrestins bind a number of other proteins too, namely, members of the mitogen-activated protein kinase (MAPK) cascades such as ERK, JNK3 and Src (246-248). These interactions define a new role for β -arrestins as scaffolds linking activated GPCRs to MAPK cascades (reviewed in (245;249)).

In this paper we present the novel finding that a transmembrane protein other than the heptahelical GPCRs can directly interact with arrestin3. NHE5 binds to arrestin 3 both *in vitro* and *in vivo*, as demonstrated by GST pull-down assays, co-immunoprecipitation and confocal immunofluorescence microscopy. Furthermore, this binding is phosphorylation-dependent, and influences the activity of the transporter.

EXPERIMENTAL PROCEDURES

Materials

α -Minimal essential medium, fetal bovine serum, penicillin/streptomycin, and trypsin-EDTA were from Life Technologies (Burlington, ON). Radioactive materials were purchased through PerkinElmer Canada. All other drugs and reagents, unless otherwise indicated, were from Fisher Scientific or Sigma, and were of the highest grade available.

Yeast Two-Hybrid Screening

The screening described in Chapter 2 presented the clone B1-7 forming the basis of this study. Clone B1-7 comprises the C-terminal half of arrestin3, amino acid residues H211-C409. The full-length cDNA of arrestin3 was cloned from a human bone marrow mRNA library as described below.

Construction of Plasmids

Plasmids were constructed according to the QuikChange™ site-directed mutagenesis protocol (Stratagene) using specific pairs of oligos with the desired mutations.

pCMV/NHE5- Δ AC, is the wild-type NHE5 cDNA missing amino acids 700-720, a highly negatively charged region (acidic cluster). Oligos used were 5'-GCT GCT GTG ATA TTA ACC GTG GGG ATC ATC TTT GTG GCT CGT GCC-3' (sense) and 5'-GGC ACG AGC CAC AAA GAT GAT CCC CAC GGT TAA TAT CAC AGC AGC-3' (antisense). In pCMV/NHE5-ST \rightarrow AA and pCMV/NHE5-ST \rightarrow DD all serines and threonines within the acidic cluster region, five in total, were replaced by either alanines or aspartates. Oligos used were 5'-GCT GAG GAG GAG GAG GAG GAG GCC GAC

GCT GCA GAG GCA GAG AAG GAG GAC GAT GAG GGG-3' (sense), 5'-TGC CTC TGC AGC GTC GGC CTC CTC CTC CTC CTC AGC CTC CAC GGT TAA TAT CAC AGC-3' (antisense), and 5'-GAT GAG GAG GAG GAG GAG GAG GAC GAC GAT GAT GAG GAT GAG AAG GAG GAC GAT GAG GGG-3' (sense), 5'-ATC CTC CAT CAT CGT CGT CCT CCT CCT CTC CTC CTC ATC CTC CAC GGT TAA TAT CAC AGC-3' (antisense) for ST→AA and ST→DD respectively. All constructs were verified by sequencing.

Cloning of Full-length cDNAs

Full-length arrestin3 and arrestin2 cDNAs were cloned from a human bone marrow mRNA library by RT PCR using random hexamer primers followed by combined PCR using two sets of specific oligos corresponding to the 5' and 3' ends, as well as the middle region of the published sequences (GeneBank accession numbers NM_004041 and NM_004313 for arrestin2 and arrestin3 respectively). For proof reading amplification, Pfu-turbo (Stratagene) or Vent polymerase (NEB) was used in all PCR reactions.

To isolate the full-length cDNA encoding arrestin3, 0.5 µg of human bone marrow mRNA (Clontech) was heat denatured at 65°C for 10 min in the presence of random hexamer primers (Promega) and incubated with reverse transcriptase (Gibco) at 42°C for 1h. The reaction mix was diluted 1/200 with distilled water and 2.5 µl was subjected to PCR with the following set of oligos. Sense: 5'-CCC AAG CTT GCC ACC ATG GGG GAG AAA CCC GGG ACC AGG GTC-3' (-ATG/*Hind*III, oligo A) and reverse: 5'-GAC GTG GAC ATT TAC ATT GAG GGG CTC CC-3' (ending at codon

corresponding to H211). The C-terminus of the clone in pACT2/B1-7 was amplified by a separate PCR reaction using the following oligos, forward: 5'-TAC CAT GGG GAG CCC CTC AAT GTA AAT GTC-3' (starting at codon corresponding to Y210) and antisense: 5'-GCT CTA GAG GTT CAG ATC CTC CTC GGA GAT GAG CTT CTG CTG GAA TTC GCA GAG TTG ATC-3' (3'-myc/*Xba*I, oligo **B**). The antisense oligo contains the coding sequence for the myc epitope in frame and an *Xba*I site, while the sense oligo contains a *Hind*III site for subcloning purpose. The gel-purified N-terminal 677 bp fragment and the C-terminal 648 bp fragment, overlapping 24 bp, were combined and subjected to a second round of PCR in the absence of primers for the first cycle, followed by another 24 cycles in the presence of oligos **A** and **B**. The obtained 1290 bp PCR fragment was subcloned into the *Hind*III and *Xba*I sites of the pCMV vector and the sequence of the clone was verified. For arrestin2, essentially the same procedure was followed.

Stable Transfection and Cell Culture

The NHE-deficient CHO cell line, AP1, was transfected by the calcium phosphate-DNA co-precipitation method (183), and stable NHE5 transfectants, both wild-type and mutants, were selected for by the NH₄Cl-induced acid challenge technique as described previously (103;205). Single clones were subsequently isolated and the expression levels were monitored by Western blot and ²²Na⁺ influx assay. The clone with the highest expression level was used for further analysis. Cells were maintained in complete α -minimal essential medium (α -MEM) supplemented with 10% fetal bovine serum, and

25mM NaHCO₃, pH 7.4, and incubated in an humidified atmosphere of 95% air and 5% CO₂ at 37°C.

Glutathione S-transferase (GST) Pull-down

For producing GST fusion proteins, different parts of arrestin3 and NHE5 cDNAs were amplified by PCR, excised with *Bam*HI and *Eco*RI and inserted into the same restriction sites of pGEX-2T bacterial expression vector (Amersham Pharmacia Biotech) in frame with the amino-terminal GST coding sequence. After sequence confirmation, plasmids were transformed into BL21 *E.coli* cells for protein expression. Overnight culture of clonal BL21 cells grown in 5ml 2YT + Amp (100 µg/ml) was diluted in 1:10 and protein expression was induced by further incubation in the 50 ml media containing 0.4mM isopropyl-1-thio-β-D-galactopyranoside (IPTG) at 30°C for 3h. Cells were collected by centrifugation, resuspended in 1ml PBS buffer containing 0.5% NP40, 1mM EDTA, 0.1 mg/ml lysozyme and proteinase inhibitor cocktail (Roche Diagnostics, Laval, QC, Canada), incubated on ice for 15 min, and sonicated 4 times for 20 sec on ice. Cell debris were removed by centrifugation at 16,000g for 20 min at 4°C, and the GST fusion proteins were purified by incubation with GSH sepharose beads (Amersham Pharmacia Biotech) for 2-3 h at 4°C. The expression constructs, pCMV/NHE5-G491ATG, described earlier (Chapter 2), and pCMV/arrestin3, were *in vitro* translated and ³⁵S-labelled by the TnT reticulocyte lysate system (Promega, Madison, WI) according to the manufacturer's protocol.

Following three washes in 0.5% NP40 buffer (0.5% NP40, 1 mM EDTA, and proteinase inhibitor cocktail in PBS), the purified GST fusion proteins, in 200 µl buffer,

were incubated with the *in vitro* translated proteins, 2-3 µl of TnT reaction mixture, overnight at 4°C. In some cases, the GST fusion proteins were incubated with purified CK1 or CK2 (NEB) in the presence of non-radioactive 0.2 mM ATP prior to the inclusion of the ³⁵S-labeled TnT product to evaluate the effect of the CK1 and CK2 phosphorylation on the interaction between NHE5 and arrestins. After six extensive washes with 0.5% NP40 buffer, proteins were eluted in SDS sample buffer containing 50 mM Tris-Cl (pH 6.8), 2% SDS, 0.1% bromophenol blue and 10% glycerol, and separated in an 10 or 12% SDS-PAGE. The gels were dried and the signal was detected by autoradiography.

Co-immunoprecipitation

CHO cells were transiently co-transfected with NHE5-36HA3 and either arrestin3-myc or arrestin2-myc using the Lipofectamine reagent and protocol supplied by the manufacturer (Gibco BRL, Burlington, Ontario, Canada). Cell lysates were prepared 24 hrs after transfection by incubation in 0.5% NP40 buffer on ice. Five hundred µl of cell lysates containing approximately 250 µg of protein were precleaned by incubation with protein-A conjugated agarose beads (Amersham Pharmacia Biotech) and incubated with 3 µl rabbit polyclonal anti-myc antibody, A-14 (Santa Cruz Biotechnology, Santa Cruz, CA), at 4°C for 2 h, followed by incubation with 20 µl protein A-conjugated agarose beads overnight. After washing the beads in the buffer four times, immunocomplexes were eluted in SDS sample buffer, separated in 8 or 10% SDS-PAGE, and transferred onto PVDF membranes. Blots were blocked with 5% nonfat skim-milk in PBS containing 0.1% Tween-20 (PBS-T), and exposed to the primary antibody, mouse monoclonal anti-

HA, HA.11 (Covance, Richmond, CA) at 1:5000 dilution. After treatment with an HRP-conjugated anti-mouse IgG (Jackson Laboratory, 1/10,000 dilution), the immunoreactive bands were visualized by the enhanced chemiluminescence kit (Amersham Pharmacia Biotech).

To further verify the *in vivo* interaction, cell lysates prepared from the stable cell line AP1/NHE5-36HA3 transiently transfected with arrestin3-myc, were immunoprecipitated with the monoclonal anti-HA antibody at 1:5000 dilution, and co-precipitated arrestin3-myc was detected by Western blot probed with HRP-conjugated anti-myc monoclonal antibody, 9E10-HRP (Roche Diagnostics, Laval, QC, Canada) at 1:20000 dilution.

Immunofluorescence Microscopy

CHO cells grown on glass coverslips were transiently transfected with 0.5 µg of arrestin3-myc and either NHE5-36HA3 or NHE1HA cDNA by Lipofectamine. At 24 hrs posttransfection, the cells were fixed in 2% paraformaldehyde/PBS for 20 min and blocked in 5% non-fat skim milk in 0.1% Triton X100/PBS (PBS-TX) for 15 min. Cell monolayers were incubated with 6 µg/ml anti-HA mouse monoclonal antibody, HA.11 (Covance, Richmond, CA), and 1.0 µg/ml anti-myc rabbit polyclonal antibody, A-14 (Santa Cruz Biotechnology, Santa Cruz, CA), for 1 h. Following washes in PBS-TX, cells were incubated with 1.75 µg/ml Cy3-conjugated anti mouse IgG (Jackson Laboratories) and 1.5 µg/ml Oregon-green conjugated anti rabbit IgG (Molecular Probes, Eugene, OR) for 1 h. All antibodies were diluted in PBS-TX. After extensive washes

with PBS-TX, cover slips were mounted on slide glasses and fluorescence signal was analyzed using a confocal microscope.

In Vitro Phosphorylation Assay

GST-NHE5 fusion proteins were purified by GSH sepharose beads and phosphorylation assay was performed by incubation with casein kinase I or II (CK1, CK2) (NEB).

Briefly, about 20 µg GST fusion protein on the GSH sepharose solid support was incubated with 100U of CK2 or 400U of CK1, 0.2mM ATP and 1 µCi [γ -³²P]-ATP (PerkinElmer Canada) in the supplied buffer in a final volume of 25 µl. After incubation at 30°C for 15 min, the reactions were stopped on ice, the beads were quickly washed with ice-cold 0.5% NP40 washing buffer for six times, and the phosphorylated GST fusion proteins were separated in 12% SDS-PAGE. The gel was stained with Coomassie blue, de-stained in 25% methanol, 10% acetic acid, fixed in 7% methanol, 7% acetic acid, 1% glycerol, and dried. The phosphorylation signal was detected by autoradiography. Equal loading of samples was determined by Coomassie staining.

In Vivo Phosphorylation

Stably transfected cells, AP1/NHE5-36HA3 and AP1/NHE5-36HA3 Δ AC, were grown to near confluence in 10-cm dishes. After 30 min phosphate-free chasing, cells were labelled *in vivo* for 2 h at 37°C in phosphate-free α -MEM containing 0.25 mCi/ml [³²P]orthophosphate. Following extensive washes, cells were processed for immunoprecipitation by monoclonal anti-HA antibody as above. Briefly, cell lysates were prepared in 0.5% NP40 buffer, immunoprecipitated by monoclonal anti-HA

antibody, separated by 10% SDS-PAGE, transferred onto PVDF membranes, and analyzed by autoradiography. The membrane was subsequently probed with the anti-HA antibody for equal loading.

²²Na⁺ Influx Assay

Either AP1, the NHE-deficient Chinese hamster ovary fibroblast cell line, or AP1/NHE5, the parental cell line stably expressing human NHE5 cDNA, was used for this study. Cells were plated in 12-well (co-transfection, NHE5:arrestin3-myc, ratio of DNA 1:2) or 24-well (single transfection, arrestin3-myc) polystyrene tissue culture dishes (Corning Incorporated, Corning, NY), and were transiently co-transfected with either pCMV/arrestin3-myc or pCMV, and NHE5 cDNA when the AP1 cell line was used, by the Lipofectamine reagent. In particular, transfection was performed at 50% confluence, using 9 µg of DNA, and 15 µl Lipofectamine per plate (12- or 24-well). Transfection efficiency reached 40-60 % of total number of cells, and was monitored by western blots and immunofluorescence microscopy performed on glass coverslips plated and treated in parallel. The protein content in each transfected sample set was measured to ensure that equal numbers of cells were analyzed. The ²²Na⁺ uptake assay was performed at 24 hrs after transfection. Briefly, wells were quickly washed with isotonic choline chloride solution (125 mM choline chloride, 1 mM MgCl₂, 2 mM CaCl₂, 20 mM HEPES-Tris, pH 7.4) and incubated with 1 µCi/ml ²²Na⁺ (PerkinElmer Canada) in the same solution containing 1mM ouabain at room temperature for 5 min. The ²²Na⁺ influx was terminated by rapidly washing the cells three times with 4 volumes of ice-cold NaCl stop solution (130 mM NaCl, 1 mM MgCl₂, 2 mM CaCl₂, 20 mM HEPES-NaOH, pH 7.4).

Cell monolayers were subsequently solubilized by 0.25 ml (in 24-well plates) or 0.5 ml (in 12-well plates) of 0.5 M NaOH followed by neutralization with the same volume of 0.5 M HCl. Radioactivity was assayed by liquid scintillation spectroscopy. Each experiment was performed in quadruplicate (24-well) or hexuplicate (12-well). The data are presented as the mean \pm S.D.

RESULTS AND DISCUSSION

The yeast two-hybrid system identifies arrestin3 as an interacting protein of NHE5

Although the biochemical and pharmacological properties of NHE5 have been described (224), not much is known about the cellular distribution and function of this brain specific NHE isoform. In the current study, we employed the yeast two-hybrid assay to identify interacting proteins of NHE5 in order to further define its role in cellular physiology. We screened over 2×10^6 clones in a human brain cDNA library using the C-terminal cytoplasmic tail of NHE5 as bait. One of the candidate interactants (clone B1-7) was the regulatory protein arrestin3 (Fig. 3.1).

β -arrestins (arrestin2 and arrestin3), are non-visual arrestins that play an essential role in the signal transduction of G-protein coupled receptors (GPCRs). Upon activation, GPCRs are phosphorylated by members of the G-protein coupled receptor kinase (GRK) family, providing the phosphoserine/threonine residues required for arrestin binding. The interaction is not only regulated by GRK phosphorylation, but also by agonist-induced conformational change, so that arrestins bind with the highest affinity to the agonist-activated and phosphorylated GPCRs ((250) and reviewed in (244;245)). The binding will sterically inhibit further G protein activation leading to activity-induced desensitization of the receptors. Arrestins are also capable of binding to the heavy chain of clathrin and the β_2 -adaptin unit of the AP-2 heterotetrameric complex initiating internalization by targeting GPCRs to clathrin-coated pits (251;252). Depending on the specific GPCR, internalization is either followed by degradation of the receptor in lysosomes or resensitization by recycling to the cell surface (253-258).

In vivo interaction between NHE5 and arrestin3

The yeast two-hybrid system, due to its extreme sensitivity, is well known for producing false positive results. Therefore, we sought to confirm our previous binding data by further experiments.

First, we wanted to see, whether NHE5 and arrestin3 co-localize in mammalian cells too. To this end, the intracellular localization of arrestin3 in respect to NHE5 was analyzed in CHO cells by confocal immunofluorescence microscopy. Cells were transiently transfected with arrestin3-myc and NHE5-36HA3, fixed at 24 hrs posttransfection, and stained with anti-myc polyclonal and anti-HA monoclonal antibody. As shown in Fig. 3.2ABC, when arrestin3 is co-expressed with NHE5, they co-localize at patchy appearances on the plasma membrane and within the cell. Arrestin3 in the absence of GPCR stimulation is a ubiquitous cytoplasmic protein (258;259). In accordance, arrestin3 single transfection showed ubiquitous cytosolic expression in CHO cells (Fig. 3.2G). To exclude the possibility that overexpression of a membrane protein caused artificial mislocalization or aggregation of arrestin3 we investigated the effect of NHE1 expression on the intracellular localization of arrestin3. As presented in Fig. 3E, arrestin3 showed cytosolic localization, similar to the pattern of single arrestin3 transfection, when co-expressed with NHE1. Together, these results suggest that overexpression of NHE5 specifically caused redistribution of arrestin3.

Second, to confirm the morphological data, immunoprecipitation was performed from CHO cells transiently transfected with both NHE5-36HA3 and arrestin3-myc using a rabbit polyclonal anti-myc antibody. The presence of NHE5 in the immunoprecipitate was analysed by Western blot probed with monoclonal anti-HA antibody. As shown in

Fig. 3.3A, NHE5 was precipitated by the anti-myc antibody along with arrestin3 only in transfected CHO cells, and not in the untransfected control. We were also able to precipitate arrestin3 by the anti-HA antibody along with NHE5 from the stable cell line AP1/NHE5-36HA3 transfected with arrestin3-myc (Fig. 3.3B). Since arrestin3 migrates close to the IgG heavy chain in an SDS-PAGE, the presence of the band representing arrestin3 could only be shown unambiguously by using an HRP-conjugated monoclonal anti-myc antibody (9E10-HRP).

Recently, Szász *et al.* conducting similar experiments to our own suggested that NHE5 may reside in recycling endosomes. The epitope-tagged NHE5 (NHE5-36HA3) upon heterologous expression in CHO cells co-localized with the recycling endosome marker transferrin receptor (K. Szász and J. Orlowski personal communication). Thus, the patchy intracellular appearance in our experiments (Fig. 3.2ABC) may reflect NHE5 and arrestin3 in recycling endosomes.

As discussed above, a principal function of β -arrestins is to target agonist-activated GPCRs to clathrin-coated pits for subsequent internalization. It is conceivable, that the association of arrestin3 with NHE5 might lead to internalization of the protein complex. In agreement, our preliminary co-immunoprecipitation experiments suggest that NHE5 is interacting with clathrin/adaptin complexes (data not shown). We are currently characterising the involvement of arrestin3 in NHE5 internalization process using different arrestin3 mutants lacking either the binding site to clathrin/adaptin (260;261) or to NHE5 (see below).

NHE5 binds to arrestin3 in vitro

Arrestins share a similar molecular architecture determined by mutagenesis studies (250) and further substantiated by the solution of the visual arrestin crystal structure (262). They are comprised of three functional and two regulatory domains. The functional domains include: a receptor activation recognition domain (A: amino acid residues 24-180), a secondary receptor binding domain (S: amino acids 180-330), and a phosphate sensor domain (P: amino acid residues 160-182). The regulatory domains are the *N*-terminal R1 (amino acid residues 1-24) and the *C*-terminal R2 domain (amino acid residues 330-409) (Fig. 3.1A).

To confirm the *in vivo* binding results, as well as to map the binding domain with respect to the molecular architecture of arrestin3, we employed a GST pull-down assay. To this end, a number of bacterial expression constructs corresponding to different parts of arrestin3 fused to the GST protein were produced. BL-21 *E. coli* cells were transformed with the pGEX-2T vector based plasmids, and the protein expression was induced by IPTG. To assess the binding capabilities, the harvested GSH sepharose beads-bound GST fusion proteins were incubated with the ³⁵S-labelled *in vitro* translated NHE5 protein. Bound proteins were eluted in SDS sample buffer, subjected to SDS-PAGE, and analyzed by autoradiography .

In the first round of GST pull-down experiments (Fig. 3.4A) the three GST-arrestin3 fusion proteins used were H211-C409 (*C*-terminus), the portion identified by the yeast two-hybrid, and two smaller progressively *N*-terminally truncated segments L291-C409 and D377-C409. Two of these fragments, H211-C409 and L291-C409, specifically bound the *in vitro* translated NHE5 cytoplasmic tail. These results confirm the yeast two-hybrid data (H211-C409) and tentatively narrow the binding domain to

L291-F376. In the following experiments (Fig. 3.4BC) the binding region was further defined and the smallest region binding NHE5 was shown to be L291-E339. A smaller region, L291-R332, covering the C-terminal 30 amino acids of the secondary receptor binding domain (S) did not exhibit significant binding to NHE5. Thus the NHE5 binding site lies partly in the C-terminal regulatory domain (R2) of arrestin3, but is distinct from both the clathrin binding sequence, ³⁷³LIEF³⁷⁶, and the AP-2 binding region (residues 391-400) (244).

Phosphorylation-dependent binding of arrestin3 to NHE5

NHE5 has a highly negatively charged region (residues 700-720) in its cytoplasmic tail unique among the NHE isoforms (Fig. 3.1B). This region, tentatively termed acidic cluster (AC), contains four serines and a threonine that are potential targets of acidophilic Ser/Thr protein kinases. Acidophilic Ser/Thr protein kinases prefer carboxylic residues in the proximity of the phosphorylated serine/threonine residues and are few in number compared to the more numerous group of basophilic and/or proline-directed protein kinases (263). Major members of the acidophilic kinase group are the casein kinases, casein kinase I and II (CK1, CK2) (263;264) their consensus sequences being (D/E)₂₄-XX-S/T and S/T-XX-E/D respectively (263;265;266). Interestingly, although no distinct GRK phosphorylation consensus motifs have been identified, mutagenesis and phosphorylation studies using synthetic peptides have demonstrated that GRKs prefer pairs of acidic amino acids in proximity to phosphorylatable serine/threonine residues (267;268). While the role of GRKs in GPCR desensitization is well-established (reviewed in (243;268)), only recently have casein kinase I α (269) and

casein kinase II (270) been implicated in agonist-dependent GPCR phosphorylation and arrestin-dependent internalization of a GPCR.

In order to examine the possibility that the binding of arrestin3 to NHE5 might depend on the phosphorylation status of the exchanger we did the following experiments. First, we checked whether NHE5 is phosphorylated *in vivo*. To this end, we performed metabolic labelling of cells stably expressing the wild-type (AP1/NHE5-36HA3) or the acidic cluster deletion mutant (AP1/NHE5-36HA3 Δ AC) exchanger with [32 P]orthophosphate, followed by immunoprecipitation with a monoclonal anti-HA antibody. As revealed in Fig. 3.5, there is a clear difference, in the amount of incorporated 32 P between wild-type and Δ AC NHE5. According to the densitometric analysis by a FluorChem digital imaging system (Alpha Innotech Corporation, San Leandro, CA) the mutant band is about 25% less phosphorylated than the wild-type protein suggesting the contribution of the AC region to the phosphorylation status of NHE5 *in vivo*. The imaging software interprets the somewhat smearier band reflecting NHE5 as higher background. The thicker band, on the other hand, might reflect degraded protein, and therefore the 25% value may be an underestimation.

Next, we tested whether NHE5 can be phosphorylated *in vitro*. For this experiment, we used GST fusion proteins of NHE5 encompassing the full cytoplasmic tail but residues 655-686. All GST fusion proteins containing this latter portion of the exchanger were unable to be expressed in BL21 cells as discussed earlier (Chapter 2). As shown in Fig. 3.6, only the middle portion of the cytoplasmic tail, G689-G789, embracing the acidic cluster, was phosphorylated by CK1 or CK2. CK2 seems to

phosphorylate NHE5 more efficiently than CK1 at least *in vitro*, which is in agreement with their respective consensus motifs and the sequence of NHE5.

Finally, we analyzed the ability of the *in vitro* phosphorylated region, G689-G789, to bind full-length arrestin3. As the S/T residues in the acidic cluster region are certainly phosphorylated *in vivo* (Fig. 3.5), we decided to analyze their potential role in facilitating the interaction between NHE5 and arrestin3. To do this, we created mutant NHE5 GST fusion constructs that are either unphosphorylatable (ST→AA) or mimic phosphorylation (ST→DD). In these mutants, either alanines or aspartic acids replaced all five of the serines and threonines within the AC region (Fig. 3.1B). For the experiment, wild-type and mutant GST fusion proteins were subjected to *in vitro* phosphorylation by CK2, followed by a GST pull-down assay using the *in vitro* translated and ³⁵S-labelled full-length arrestin3. As demonstrated in Fig. 3.7, the NHE5 region G689-G789 binds arrestin3 in a phosphorylation-dependent manner. The shorter fragments, G689-G720, essentially the acidic cluster, and the fragment G720-G789 are not sufficient for binding regardless of phosphorylation status. The inability of the ST→DD mutant to promote constitutive binding of arrestin3 brings up the possibility that it is not the phosphorylation-created negative charges, but rather a specific conformation of the protein during the CK2 activity that is important for arrestin3 binding.

The transporter activity of NHE5 is influenced by the expression of arrestin3

In order to investigate the functional relevance of the binding of arrestin3 to NHE5, Na⁺/H⁺ exchanger activity was assessed by ²²Na⁺ influx assay. For this experiment, AP1 cells were transiently co-transfected with arrestin3 and NHE5. The

transfection efficiency was monitored by western blot and immunofluorescence microscopy, and equal numbers of cells were subjected to the assay. Transient co-expression of arrestin3 and NHE5 inhibited the basal activity of the transporter by an average of $35 \pm 9\%$ (mean \pm S.D) (Fig. 3.8). In one out of five experiments there was a significant increase in activity (15%). To examine this effect more thoroughly, we performed the same experiment in the stable cell line AP1/NHE5 transfected with either arrestin3 or pCMV as a negative control. The expression of arrestin3 consistently inhibited the transporter activity under these conditions by an average of $40 \pm 18\%$ (data not shown).

Regardless of the carefully controlled influx experiments we were not able to unequivocally demonstrate a uniform effect of arrestin3 on NHE5 function. It is possible that endogenous members of the GPCR family or the involvement of other signaling pathways might interfere with the interaction of NHE5 and arrestin3. In this context, it is worthwhile to remark the new emerging role of arrestins as adaptors facilitating Src kinase signaling and the activation of mitogen-activated protein kinase (MAPK) cascades such as the ERK (247) and JNK3 (248) cascades. These signaling cascades are involved in cellular proliferation, differentiation, development, and apoptosis (245). By binding to several members of the MAPK cascades, arrestins connect GPCRs to these signaling pathways and may direct the activated kinases to specific intracellular locations. In our system, it is possible that, depending on the expression level, arrestin3 may perturb the function of these MAPK cascades leading to altered cell-cycle, intracellular organellar structures, and trafficking, influencing the function of membrane proteins.

In the current study, we report the novel finding that arrestin3 binds to a non-GPCR membrane protein, the brain specific Na^+/H^+ exchanger isoform NHE5. The interaction is phosphorylation-dependent, and was confirmed both *in vitro* and *in vivo*. Functionally, the association of the transporter and arrestin3 attenuates the basal activity of NHE5.

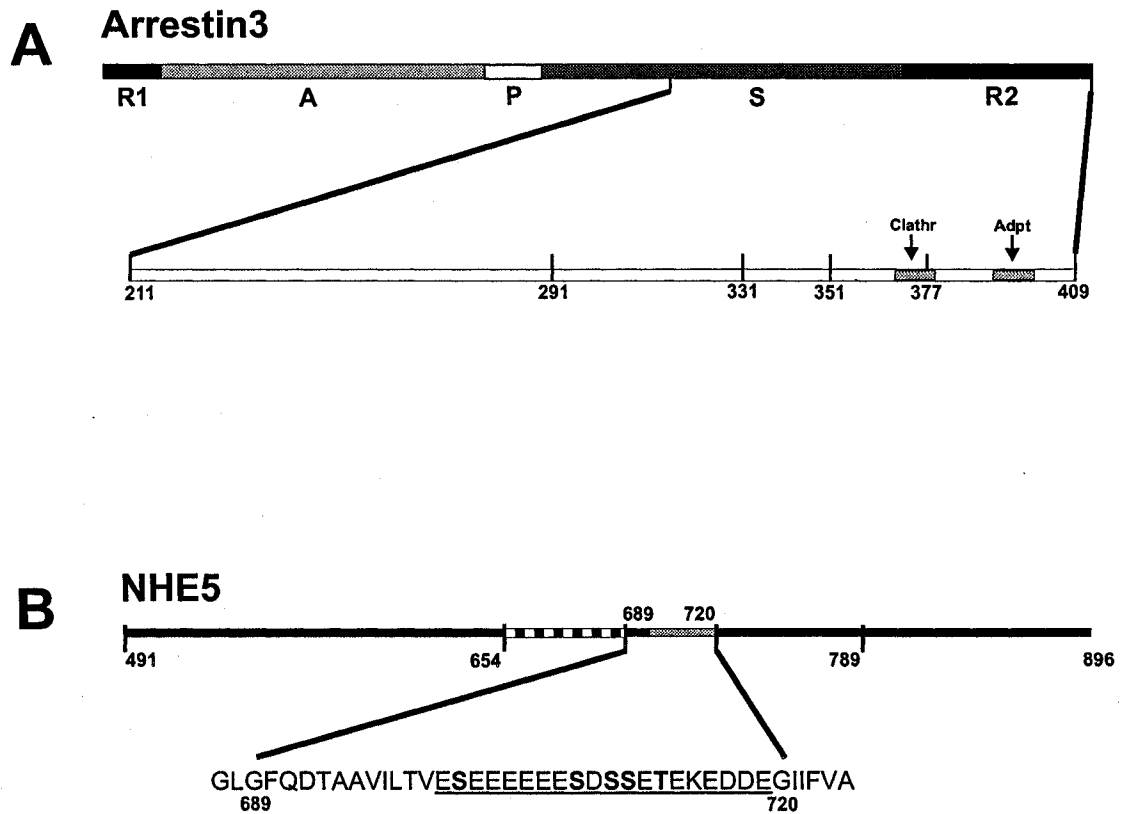


Fig. 3.1. Diagram of arrestin3 and NHE5 cytoplasmic tail. A: Domains of arrestin3 include a receptor activation recognition domain (A: amino acid residues 24-180), a secondary receptor binding domain (S: amino acids 180-330), a phosphate sensor domain (P: amino acid residues 160-182), and the two regulatory domains R1 (amino acid residues 1-24) and R2 (amino acid residues 330-409). The clathrin (Clathr) and the AP-2 binding region (Adpt) in R2 are indicated. B: Cytoplasmic tail of NHE5 (for details see *Results and Discussion*), the acidic cluster region is underlined.

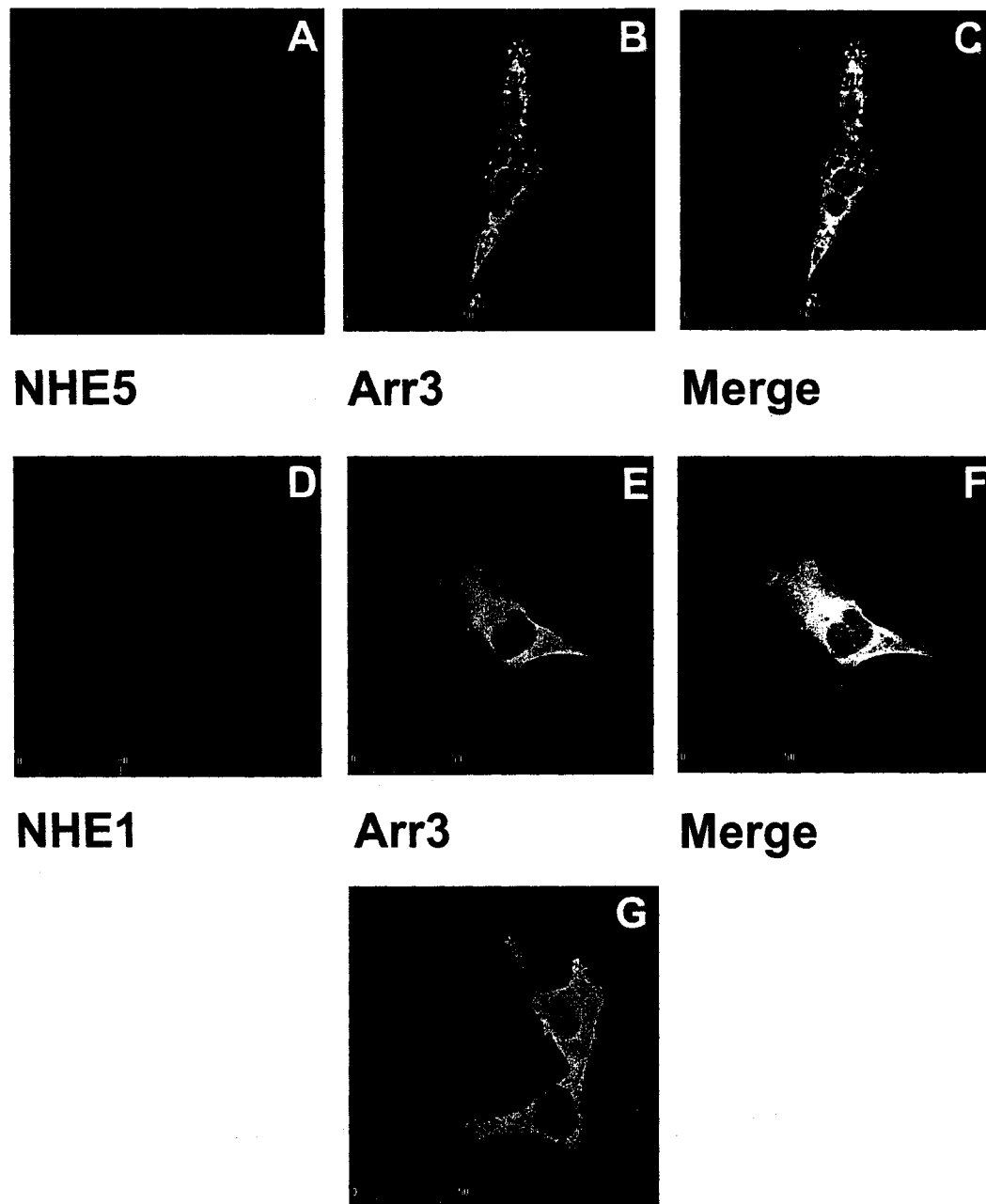
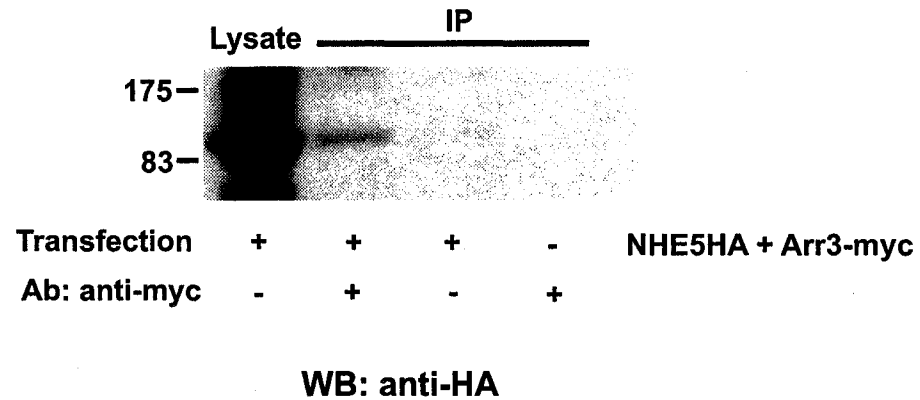
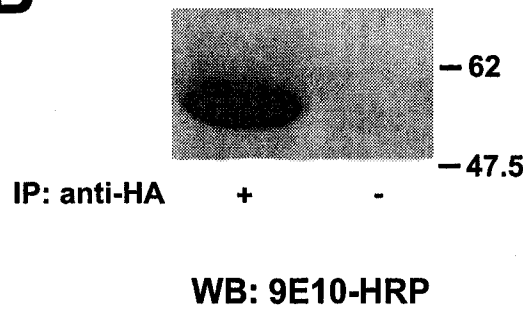


Fig. 3.2. Confocal immunofluorescent microscopy of CHO cells transfected with NHE5 and arrestin3. Arrestin3-myc alone (G) or arrestin3-myc and either NHE5-36HA3 (ABC) or NHE1HA (DEF) were transiently transfected into CHO cells and were visualized by Oregon Green (green, BEG) and cy3 (red, AD) conjugated secondary antibodies respectively. The scale bar corresponds to 50 μ m.

A



B

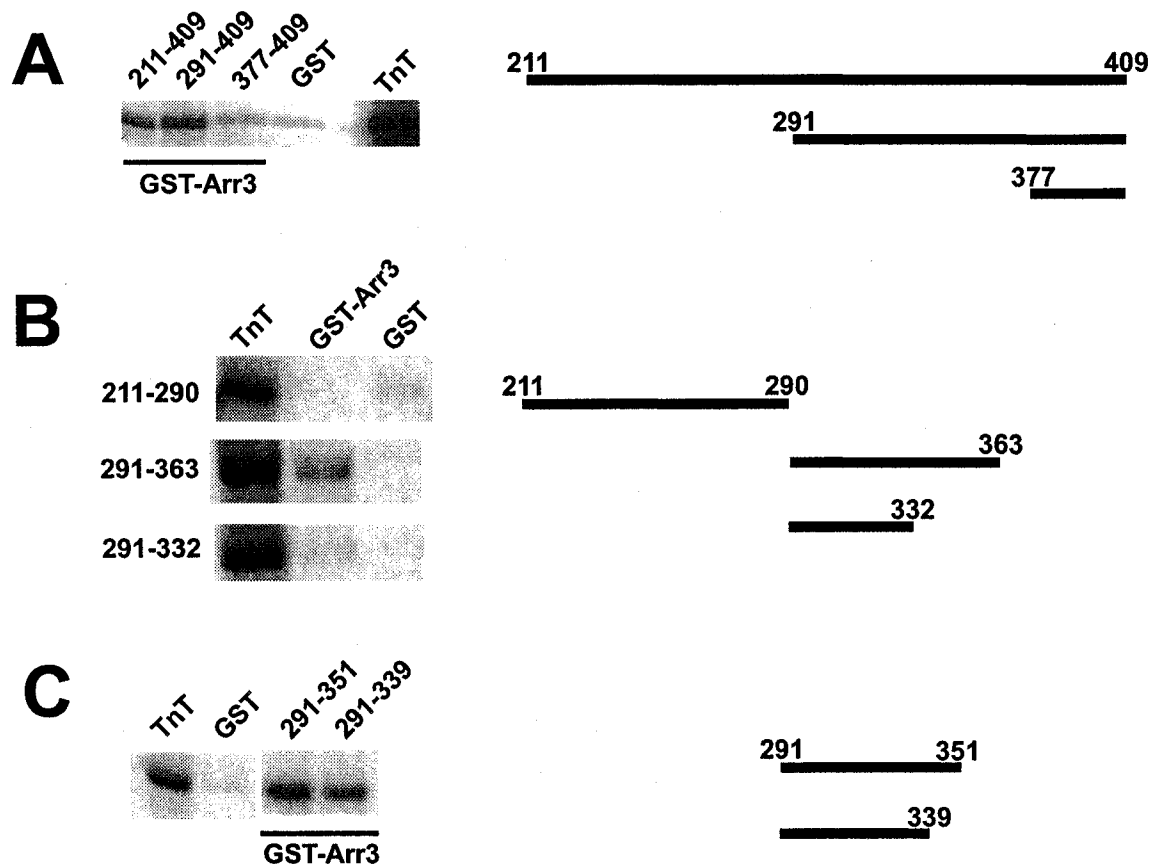


NHE5HA stable cell line transiently transfected with Arr3-myc

Fig. 3.3. In vivo interaction between NHE5 and arrestin3.

A: Cell lysates isolated from untransfected and NHE5-36HA3 and arrestin3-myc co-transfected CHO cells were immunoprecipitated with a polyclonal anti-myc antibody and immunoprecipitates were analyzed by western blot probed with a monoclonal anti-HA antibody.

B: Cell lysates from AP1/NHE5-36HA3 transfected with arrestin3-myc were immunoprecipitated by an anti-HA antibody, immunoprecipitates were analyzed by western blot probed with an HRP-conjugated monoclonal anti-myc antibody. Results shown are representative of three replicate experiments.



TnT: NHE5/G491ATGwt

Fig. 3.4. The cytoplasmic tail of NHE5 binds arrestin3 *in vitro*. ^{35}S -labeled *in vitro* translated NHE5 C-terminus protein (G491-L896) was subjected to GST pull-down assay using the indicated GST-arrestin3 constructs. Samples were separated by SDS-PAGE, and analyzed by autoradiography. NHE5 was pulled down by the minimal domain GST-(L291-E339) of arrestin3. A schematic representation of GST-arrestin3 constructs is shown. All results shown are representative of at least three replicate experiments.

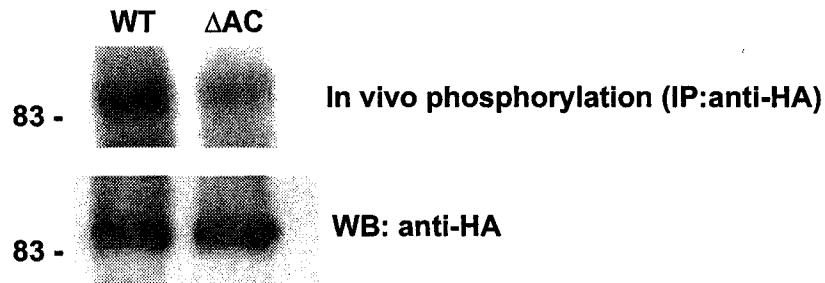


Fig. 3.5. NHE5 is a phosphoprotein *in vivo*.

Stably transfected cells, AP1/NHE5-36HA3 and AP1/NHE5-36HA3ΔAC, were metabolically labelled with [32 P]orthophosphate. Immunoprecipitation was performed by monoclonal anti-HA antibody, the precipitate was separated by SDS-PAGE, transferred onto PVDF membranes, and analyzed by autoradiography. The membrane was subsequently probed with the anti-HA antibody for equal loading.

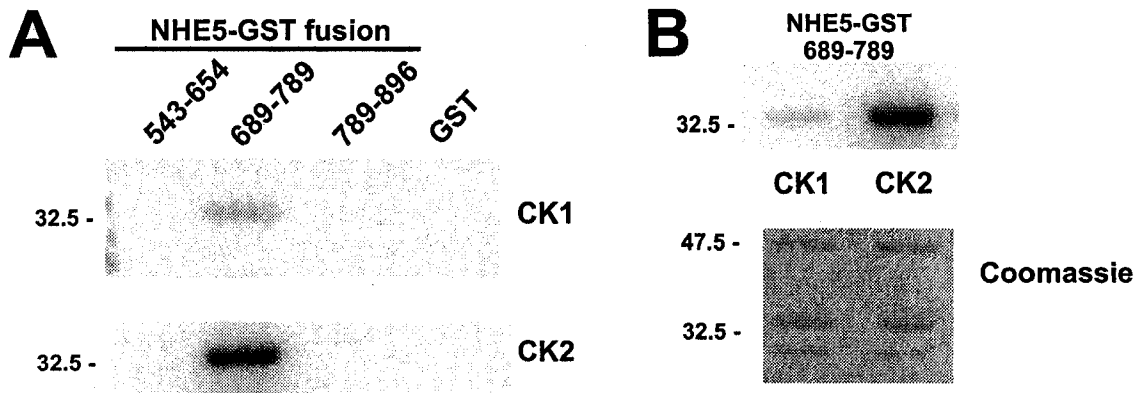
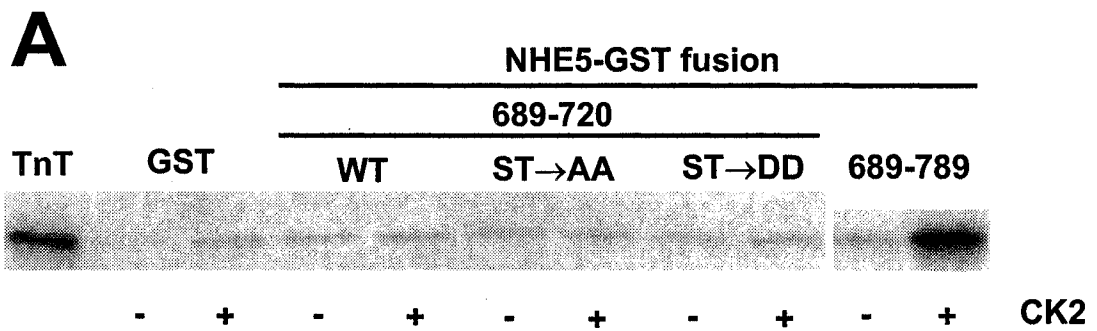
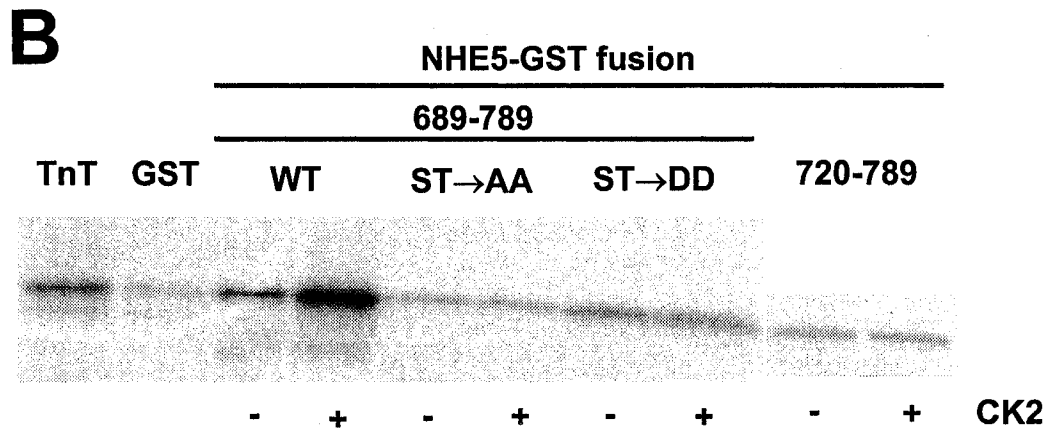


Fig. 3.6. NHE5 can be phosphorylated by Casein Kinase I and II *in vitro*.

GST-NHE5 fusion proteins were *in vitro* phosphorylated by CK1 or CK2 in the presence of [γ - 32 P]-ATP, subjected to 12% SDS-PAGE and analyzed by autoradiography. Equal loading of samples is demonstrated by Coomassie staining. Results shown are representative of three replicate experiments.



TnT: Arr3 full length



TnT: Arr3 full length

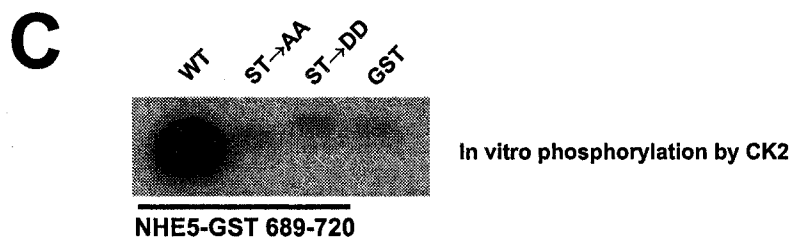


Fig. 3.7. Full-length arrestin3 binds to phosphorylated NHE5.

A and B: GST-NHE5 fusion proteins were *in vitro* phosphorylated by CK2 prior to GST pull-down assay. *In vitro* translated, ^{35}S -labelled full-length arrestin3 was pulled down by the wild-type phosphorylated G689-G789 fragment only.

C: autoradiograph of control phosphorylation experiment conducted in the presence of $[\gamma\text{-}^{32}\text{P}]\text{-ATP}$. Results shown are representative of three replicate experiments.

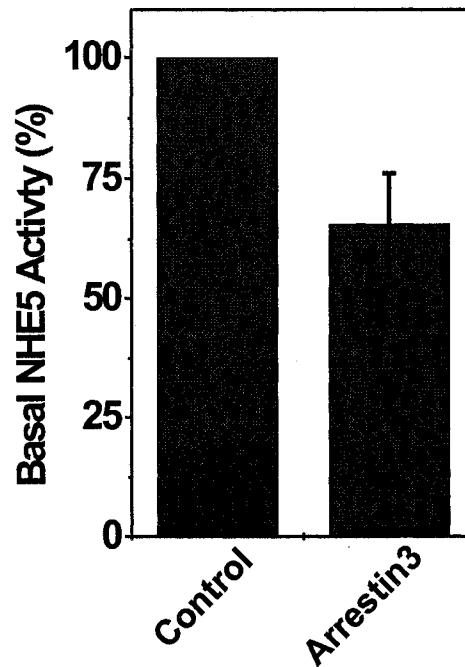


Fig. 3.8. Expression of arrestin3 effects the basal transport activity of NHE5. AP1 cells were co-transfected with pCMV/NHE5 and either pCMV/arrestin3-myc or pCMV as control. 24 hrs after transfection the basal activity of NHE5 was assessed by $^{22}\text{Na}^+$ influx assay. Data were normalized as a percentage of the basal transport activity rate of the exchanger in the absence of 1mM amiloride. Values represent the average of over five independent experiments, each performed in hexuplicate.

GENERAL DISCUSSION AND CONCLUSION

The results of this thesis extend our general knowledge of the Na^+/H^+ exchanger gene family and clarify the biochemical, pharmacological and some of the regulatory properties of NHE5.

NHE5 was cloned from a human brain cDNA library and was reconstructed by standard PCR techniques (176). It proved to be a functional exchanger in the heterologous expression system AP1 cell line. AP1 cells are Chinese hamster ovary cells devoid of Na^+/H^+ exchange activity (103), and therefore, are suitable means for the basic description of NHE characteristics. Data provided in Chapter 1 establish the biochemical and pharmacological characteristics of NHE5.

NHE5 has an intermediate affinity for most classes of NHE-inhibitory drugs compared to other NHE isoforms under similar experimental conditions (TABLE 1.1 in Chapter 1). The only exception is clonidine, an α_2 -adrenergic agonist, to which NHE5, in contrast to NHE1-3, is completely insensitive. This observation may prove very useful in functionally isolating NHE5 activity in further studies in native tissues or primary cell lines. The intermediate drug profiles of NHE5 are somewhat closer to those of NHE3, a fact that could be predicted from their high amino acid similarity, ~67% identity, in the *N*-terminal transmembrane region previously demonstrated to carry the drug sensitivity of the exchangers (112;121).

Although, in terms of its biochemical properties, NHE5 shares many similarities with the other isoforms, it has several distinct characteristics as well. For instance, NHE5, like the other isoforms, is inhibited by the monovalent cations H^+ , Li^+ , but its affinity for both H^+_o and Li^+_o is an order of a magnitude higher than the respective affinities of NHE1 or NHE3 (TABLE 1.2 in Chapter 1). The physiological significance of this observation is unclear, but it is inviting to speculate that NHE5 may play a role in the complex pharmacodynamics of LiCl treatment of bipolar affective disorder. The therapeutic concentration of Li^+ in serum is ~ 1 mM (212). At this level, in a solution containing trace amounts of Na^+ , Li^+ inhibits transport activity more than 50% ($K_{0.5} = 0.32$ mM). However, under physiological conditions, $Na^+_o \approx 145$ mM, the inhibition might not be that significant. In a $^{22}Na^+$ influx assay at this $[Na^+]_o$, the radioactive substrate would be diluted to the extent that $^{22}Na^+$ uptake measurements were impractical. Experiments using the pH-sensitive dye BCECF and ratiometric fluorescent microscopy conducted in physiological extracellular solution supplemented with LiCl could test the validity of this hypothesis.

The apparent affinity constant of NHE5 for both Na^+_o and H^+_i are similar in value to the other isoforms (TABLE 1.2 in Chapter 1). NHE5 has a first-order dependence on the extracellular Na^+ concentration indicating a single extracellular Na^+ binding site. However, unlike the majority of NHEs characterized to date, human NHE5 has a first-order dependence on intracellular H^+ . This first-order dependence seemingly precludes the existence of allosteric modification of NHE5 activity by intracellular pH. However, cooperative activation of NHE5 can still be conferred by auxiliary regulatory factors.

One such factor might be the AMP activated protein kinase (AMPK). AMPK is a ubiquitous heterotrimeric serine/threonine kinase, composed of the catalytic α subunit, and the regulatory subunits β and γ . AMPK is activated during metabolic stress in response to elevated AMP/ATP ratios, and was originally found to phosphorylate a number of key metabolic enzymes (e.g. acetyl-CoA carboxylase, HMG-CoA reductase) thereby inhibiting ATP-consuming anabolic pathways and preserving cellular energy stores (reviewed in (238;241)). Recently, however, it has also been implicated in the regulation of a membrane protein; AMPK directly phosphorylates and inhibits the cystic fibrosis transmembrane conductance regulator (CFTR) (239).

In Chapter 2, we provide evidence that the $\alpha 2$ catalytic subunit of AMPK binds NHE5 cytoplasmic tail both *in vitro* and *in vivo*. Moreover, AMPK phosphorylates NHE5 at distinct sites *in vitro*. Functional studies conducted on the AP1/NHE5 stable cell line revealed that overexpression of a constitutive active mutant AMPK $\alpha 2$ (amino acid residues 1-312) exhibited around 50% increase in the NHE5 activity, while expression of dominant negative constructs (residues 313-552 and 395-552) showed 30-50% decrease in transporter activity. Additionally, the membrane permeable AMP analogue AICAR activates NHE5 in a dose- and time-dependent manner in the AP1/NHE5 cell line. Taken together, these data suggest that AMPK is an *in vivo* regulator of NHE5 function.

Although the relevance of this regulation is not yet clear, it is possible that AMPK serves the function of an allosteric activator. Anoxia for instance, will not only lead to AMP/ATP ratio increase and consequent AMPK activation, but also to pH_i decrease. This inevitably happens because the major determinant of intracellular pH during anaerobic metabolism is the ADP concentration (for detailed analysis see (9)). In fact, the AMP/ATP ratio is a very subtle indicator of pH_i change, since it varies according to the square of ADP/ATP ratio (241). Therefore, even though $[\text{H}^+]_i$ does not allosterically activate NHE5, this still might happen during anoxia through AMPK activity.

In Chapter 3, we demonstrate that arrestin3, a member of the arrestin gene family, is an additional protein that can associate with NHE5. Arrestins play a crucial role in G-protein coupled receptor (GPCR) signal transduction being responsible for agonist-induced desensitization. They bind to agonist-activated and phosphorylated GPCRs and sterically hinder further G-protein association with the receptor. Furthermore, they also initiate internalization by virtue of their clathrin- and adaptin-binding abilities directing GPCRs to clathrin-coated pits (for reviews see (243-245)).

The study presented in Chapter 3 establishes NHE5 as the first non-GPCR membrane protein that arrestin is capable of binding. Arrestin3 binds to the cytoplasmic tail of NHE5 both *in vitro* and *in vivo*. The binding region, L290-E339, is distinct from the clathrin-binding as well as the β_2 -adaptin binding region of arrestin3. Therefore, structurally, it is plausible that arrestin3 directs NHE5 to clathrin-coated pits for internalization. In their most recent work, Szász *et al.* (Szász and Orlowski, paper in

submission) demonstrate that NHE5 is found intracellularly in a distinct set of recycling endosomes. Thus, the patchy intracellular signals, where NHE5 and arrestin3 co-localize in our study, likely correspond to recycling endosomes (Fig. 3.2).

We have shown that, at least *in vitro*, the binding of arrestin3 to NHE5 is phosphorylation-dependent (Fig. 3.7). This is reminiscent of the classical arrestin – GPCR association, whereby arrestin binds to the phosphorylated and agonist-activated GPCR. Whether the binding between arrestin3 and NHE5 is constitutive or regulated by specific signalling, such as the extent of phosphorylation of the exchanger, is yet to be tested. Our confocal microscopy data showing nearly perfect co-localization in all cells expressing both proteins suggests constitutive association. To clarify this issue and to avoid potential problems associated with overexpression of heterologous gene products, the Ecdysone-Inducible Mammalian Expression System (Invitrogen) allowing tightly controlled expression can be used in future studies.

It is important to note that, although the NHE5 binding region (L290-E339) lies partly within the secondary receptor-binding domain (residues 180-330) of arrestin3, this association might not hinder binding of GPCRs, as the large activation-recognition domain (residues 24-180) too supports the GPCR-binding (250). Consequently, it is possible that arrestin might assist the endocytosis of certain GPCRs and NHE5 simultaneously in one protein complex. To test this hypothesis, we established, and are in the process of analyzing a cell line that overexpresses both NHE5 and the prototype

GPCR β_2 -adrenergic receptor (β_2 AR was generously provided by Dr. Ferguson, University of Western Ontario, London, Ontario, Canada).

Experiments conducted on the above cell line (AP1/NHE5/ β_2 AR) should also shed some light on the controversial results of our functional assay. Overexpression of arrestin3 attenuates the basal transport activity of NHE5, but in one out of five experiments, the activity is significantly upregulated. As discussed in Chapter 3, this may be because endogenous GPCRs may interfere in the interaction of NHE5 and arrestin3. Overexpressing β_2 AR will presumably rectify this problem by becoming the dominant GPCR in the system. The regulation of the prototype GPCR β_2 AR by arrestins has been thoroughly described (243;244), and can help in sorting out the functional relevance of NHE5 – arrestin3 interaction.

Arrestins not only assist desensitization, but they are also involved in the resensitization of certain GPCRs (256;271). The prerequisite of resensitization is dephosphorylation of the GRK phosphorylated GPCRs that occurs in endosomes after arrestin dissociation (253;271;272). It seems that the conformational change that triggers arrestin dissociation off and subsequent phosphatase binding to the GPCR is dependent on the presence of acidic intraendosomal pH (273;274). It is possible that NHE5 plays a role in the regulation of the intravesicular pH along with the resident V-type ATPase. If there is such a role of NHE5, it could be analyzed by comparing its putative effect on GPCR resensitization to the effect of the non-functional mutant NHE5D185A. The mutation at D185, an amino acid residue in TM5 conserved throughout all NHE species,

leads to complete loss of transport activity while preserving the structural integrity of the protein (Orlowski unpublished).

Although Szászi *et al.* (Szászi and Orlowski, paper in submission) has provided information on the intracellular localization of NHE5 in a heterologous expression system, its native distribution remains indefinite. In the Chinese hamster ovary cell line AP1/NHE5-36HA3, NHE5 is found in the plasma membrane, as well as in a distinct set of recycling endosomes. These endosomes do not completely overlap with the intracellular residence of the closely related exchanger NHE3 (154). Heterologous expression in the rat pheochromocytoma derived neuronal model cell PC12 is probably more conducive to understanding the *in situ* localization of NHE5. Preliminary experiments reveal an intriguing presence of NHE5 at the tip of and along the dendrites of these neuronal cells (Fig. D.1).

Though there are indirect morphological (175) and biochemical (176) data on the neuron-specificity of NHE5 (Chapter 1), there is no direct evidence as yet to support this claim. In order to prove the neuron-specificity and to gain an insight into the expression level and CNS tissue distribution of NHE5, we are in the process of producing anti NHE5 polyclonal antibodies. These antibodies will also be useful in further biochemical experiments in heterologous expression systems.

Conceivably, the targeted disruption of the *Nhe5* locus could provide tremendous insight into the physiology of NHE5. Given the abundance of pH regulatory mechanisms

and transporters in general (see Introduction) and Na^+/H^+ exchangers in particular, it would be difficult to predict the phenotype of such knockout mice. For instance, regardless of the ubiquitous expression of NHE1, the spontaneous null mutation (126), as well as the targeted disruption of the *Nhe1* allele (125) demonstrates CNS-restricted features. The phenotype include, apart from significant mortality before weaning, ataxia and a novel seizure pattern termed slow-wave epilepsy. These findings imply selective vulnerability of certain CNS areas to defects in pH homeostasis. It is possible that in other CNS locations NHE5 or some other pH regulatory mechanism complements NHE1 function. By the same line of thought, an NHE5 knockout phenotype might present with selective neuronal loss in regions where the exchanger is not functionally redundant.

In agreement with this hypothesis is a recent analysis of a large kindred of autosomal dominant spinocerebellar ataxia type 4 (275). Dominantly inherited spinocerebellar ataxias (SCAs) are a heterogeneous group of neurologic disorders characterized by variable degrees of degeneration of the cerebellum, spinal tracts, and brain stem (276). Patients with SCA4 have an invariant sensory axonal neuropathy in addition to their spinocerebellar ataxia and no defects in eye movements. Linkage analysis in the five-generation pedigree placed *SCA4* to chromosome band 16q22.1 the same band where *Nhe5* is mapped (172).

In conclusion, the present thesis expands the general knowledge of the Na^+/H^+ exchanger gene family by describing the basic characteristics of NHE5, and emphasises novel regulatory paradigms in the NHE field by revealing the regulation of NHE5 by

AMPK and arrestin3. As alluded to in the current section, there is plenty to be done in the emerging areas for completely clarifying the physiology of the Na^+/H^+ exchanger isoform NHE5.

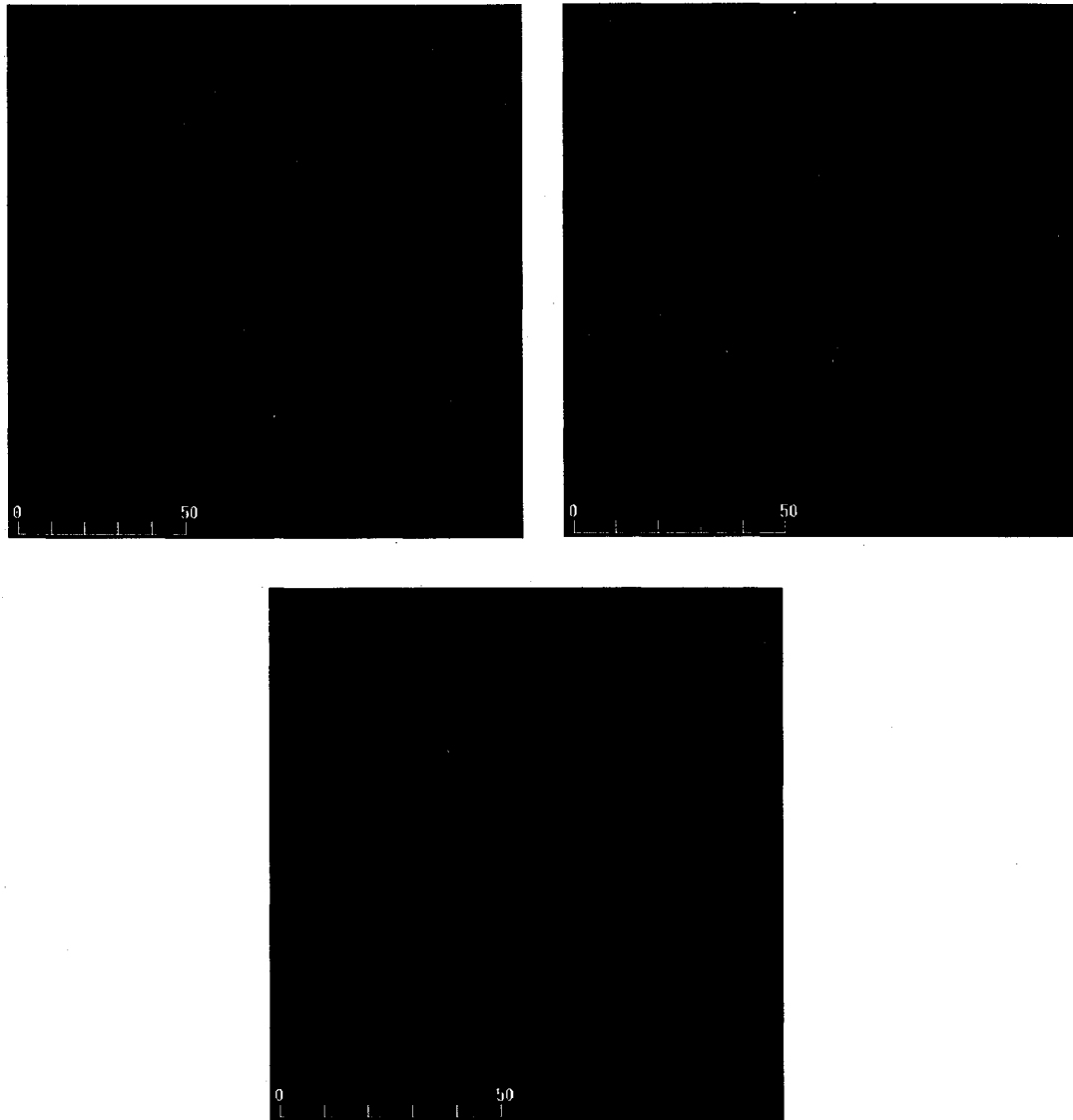


Fig. D.1. Expression of NHE5 in PC12 cells. PC12 cells were transfected with pCMV/NHE5-36HA3 using the Lipofectamine reagent. 48 hrs after transfection cells were fixed and the signal was analyzed by immunocytochemistry using a monoclonal anti-HA antibody (see *Experimental Procedures* in Chapter 3 for details). The scale bar corresponds to 50 μm .

REFERENCE LIST

1. **Antosiewicz, J., J.A. McCammon, and M.K. Gilson.** The determinants of pK_as in proteins. *Biochemistry* - 35: 7819-7833, 1996.
2. **Schulte, U. and B. Fakler.** Gating of inward-rectifier K⁺ channels by intracellular pH. *Eur J Biochem* - 267: 5837-5841, 2000.
3. **Chesler, M.** The regulation and modulation of pH in the nervous system. *Prog Neurobiol* - 34: 401-427, 1990.
4. **Laming, P.R., H. Kimelberg, S. Robinson, A. Salm, N. Hawrylak, C. Muller, B. Roots, and K. Ng.** Neuronal-glial interactions and behaviour. *Neurosci Biobehav Rev* - 24: 295-340, 2000.
5. **Deitmer, J.W. and C.R. Rose.** pH regulation and proton signalling by glial cells. *Prog Neurobiol* - 48: 73-103, 1996.
6. **Atkins PW.** Equilibrium electrochemistry. In: *Physical Chemistry*, edited by Atkins PW. Oxford University Press, 1990,
7. **Roos, A. and W.F. Boron.** Intracellular pH. *Physiol Rev* - 61: 296-434, 1981.
8. **Busa, W.B. and R. Nuccitelli.** Metabolic regulation via intracellular pH. *Am J Physiol* - 246: R409-R438, 1984.
9. **Hochachka, P.W. and T.P. Mommsen.** Protons and anaerobiosis. *Science* - 219: 1391-1397, 1983.
10. **Guyton AC.** Regulation of Acid-Base Balance. In: *Textbook of Medical Physiology*, edited by Guyton AC. W.B. Saunders, 1991,
11. **Soleimani, M. and C.E. Burnham.** Na⁺:HCO₃⁻ cotransporters (NBC): cloning and characterization. *J Membr Biol* - 183: 71-84, 2001.
12. **Alper, S.L.** The band 3-related anion exchanger (AE) gene family. *Annu Rev Physiol* - 53: 549-564, 1991.
13. **Lee, B.S., R.B. Gunn, and R.R. Kopito.** Functional differences among nonerythroid anion exchangers expressed in a transfected human cell line. *J Biol Chem* - 266: 11448-11454, 1991.
14. **Tanner, M.J.** The structure and function of band 3 (AE1): recent developments (review). *Mol Membr Biol* - 14: 155-165, 1997.

15. **Motais, R., B. Fievet, F. Borgese, and F. Garcia-Romeu.** Association of the band 3 protein with a volume-activated, anion and amino acid channel: a molecular approach. *J Exp Biol* - 200 (Pt 2): 361-367, 1997.
16. **Jay, D.G.** Role of band 3 in homeostasis and cell shape. *Cell* - 86: 853-854, 1996.
17. **Peters, L.L., R.A. Shivdasani, S.C. Liu, M. Hanspal, K.M. John, J.M. Gonzalez, C. Brugnara, B. Gwynn, N. Mohandas, S.L. Alper, S.H. Orkin, and S.E. Lux.** Anion exchanger 1 (band 3) is required to prevent erythrocyte membrane surface loss but not to form the membrane skeleton. *Cell* - 86: 917-927, 1996.
18. **Quilty, J.A. and R.A. Reithmeier.** Trafficking and folding defects in hereditary spherocytosis mutants of the human red cell anion exchanger. *Traffic* - 1: 987-998, 2000.
19. **Low, P.S., P. Rathinavelu, and M.L. Harrison.** Regulation of glycolysis via reversible enzyme binding to the membrane protein, band 3. *J Biol Chem* - 268: 14627-14631, 1993.
20. **Kay, M.M.** Isolation of the phagocytosis-inducing IgG-binding antigen on senescent somatic cells. *Nature* - 289: 491-494, 1981.
21. **Kay, M.M., J. Hughes, I. Zagon, and F.B. Lin.** Brain membrane protein band 3 performs the same functions as erythrocyte band 3. *Proc Natl Acad Sci U S A* - 88: 2778-2782, 1991.
22. **Tsuganezawa, H., K. Kobayashi, M. Iyori, T. Araki, A. Koizumi, S. Watanabe, A. Kaneko, T. Fukao, T. Monkawa, T. Yoshida, D.K. Kim, Y. Kanai, H. Endou, M. Hayashi, and T. Saruta.** A new member of the HCO₃⁻ transporter superfamily is an apical anion exchanger of beta-intercalated cells in the kidney. *J Biol Chem* - 276: 8180-8189, 2001.
23. **Soleimani, M., T. Greeley, S. Petrovic, Z. Wang, H. Amlal, P. Kopp, and C.E. Burnham.** Pendrin: an apical Cl⁻/OH⁻/HCO₃⁻ exchanger in the kidney cortex. *Am J Physiol Renal Physiol* - 280: F356-F364, 2001.
24. **Melvin, J.E., K. Park, L. Richardson, P.J. Schultheis, and G.E. Shull.** Mouse down-regulated in adenoma (DRA) is an intestinal Cl⁻/HCO₃⁻ exchanger and is up-regulated in colon of mice lacking the NHE3 Na⁺/H⁺ exchanger. *J Biol Chem* - 274: 22855-22861, 1999.
25. **Chegwidden, W.R. and N.D. Carter.** Introduction to the carbonic anhydrases. *EXS* - 14-28, 2000.
26. **Sterling, D., R.A. Reithmeier, and J.R. Casey.** A transport metabolon. Functional interaction of carbonic anhydrase II and chloride/bicarbonate exchangers. *J Biol Chem* - 276: 47886-47894, 2001.
27. **Miles, E.W., S. Rhee, and D.R. Davies.** The molecular basis of substrate channeling. *J Biol Chem* - 274: 12193-12196, 1999.
28. **Reithmeier, R.A.** A membrane metabolon linking carbonic anhydrase with chloride/bicarbonate anion exchangers. *Blood Cells Mol Dis* - 27: 85-89, 2001.

29. **Velot, C., M.B. Mixon, M. Teige, and P.A. Srere.** Model of a quinary structure between Krebs TCA cycle enzymes: a model for the metabolon. *Biochemistry* - 36: 14271-14276, 1997.
30. **Russell, J.M. and W.F. Boron.** Role of chloride transport in regulation of intracellular pH. *Nature* - 264: 73-74, 1976.
31. **Thomas, R.C.** The role of bicarbonate, chloride and sodium ions in the regulation of intracellular pH in snail neurones. *J Physiol* - 273: 317-338, 1977.
32. **Alpern, R.J.** Cell mechanisms of proximal tubule acidification. *Physiol Rev* - 70: 79-114, 1990.
33. **Liu, S., D. Piwnica-Worms, and M. Lieberman.** Intracellular pH regulation in cultured embryonic chick heart cells. Na(+)-dependent Cl-/HCO₃⁻ exchange. *J Gen Physiol* - 96: 1247-1269, 1990.
34. **Bevensee, M.O., R.A. Weed, and W.F. Boron.** Intracellular pH regulation in cultured astrocytes from rat hippocampus. I. Role Of HCO₃⁻. *J Gen Physiol* - 110: 453-465, 1997.
35. **Faff, L., C. Ohlemeyer, and H. Kettenmann.** Intracellular pH regulation in cultured microglial cells from mouse brain. *J Neurosci Res* - 46: 294-304, 1996.
36. **Mellergard, P., Y.B. Ouyang, and B.K. Siesjo.** Intracellular pH regulation in cultured rat astrocytes in CO₂/HCO₃⁻-containing media. *Exp Brain Res* - 95: 371-380, 1993.
37. **Schlue, W.R. and J.W. Deitmer.** Ionic mechanisms of intracellular pH regulation in the nervous system. *Ciba Found Symp* - 139: 47-69, 1988.
38. **Schwiening, C.J. and W.F. Boron.** Regulation of intracellular pH in pyramidal neurones from the rat hippocampus by Na(+)-dependent Cl(-)-HCO₃⁻ exchange. *J Physiol* - 475: 59-67, 1994.
39. **Shrode, L.D. and R.W. Putnam.** Intracellular pH regulation in primary rat astrocytes and C6 glioma cells. *Glia* - 12: 196-210, 1994.
40. **Romero, M.F. and W.F. Boron.** Electrogenic Na⁺/HCO₃⁻ cotransporters: cloning and physiology. *Annu Rev Physiol* - 61: 699-723, 1999.
41. **Gross, E., K. Hawkins, A. Pushkin, P. Sassani, R. Dukkupati, N. Abuladze, U. Hopfer, and I. Kurtz.** Phosphorylation of Ser(982) in the sodium bicarbonate cotransporter kNBC1 shifts the HCO₃⁻ : Na⁺ stoichiometry from 3 : 1 to 2 : 1 in murine proximal tubule cells. *J Physiol* - 537: 659-665, 2001.
42. **Muller-Berger, S., O. Ducoudret, A. Diakov, and E. Fromter.** The renal Na-HCO₃-cotransporter expressed in *Xenopus laevis* oocytes: change in stoichiometry in response to elevation of cytosolic Ca²⁺ concentration. *Pflugers Arch* - 442: 718-728, 2001.
43. **Gross, E., K. Hawkins, N. Abuladze, A. Pushkin, C.U. Cotton, U. Hopfer, and I. Kurtz.** The stoichiometry of the electrogenic sodium bicarbonate cotransporter NBC1 is cell-type dependent. *J Physiol* - 531: 597-603, 2001.

44. **Grichtchenko, I.I., I. Choi, X. Zhong, P. Bray-Ward, J.M. Russell, and W.F. Boron.** Cloning, characterization, and chromosomal mapping of a human electroneutral Na(+)-driven Cl-HCO₃ exchanger. *J Biol Chem* - 276: 8358-8363, 2001.
45. **Amlal, H., C.E. Burnham, and M. Soleimani.** Characterization of Na⁺/HCO₃⁻ cotransporter isoform NBC-3. *Am J Physiol* - 276: F903-F913, 1999.
46. **Wang, C.Z., H. Yano, K. Nagashima, and S. Seino.** The Na⁺-driven Cl⁻/HCO₃⁻ exchanger. Cloning, tissue distribution, and functional characterization. *J Biol Chem* - 275: 35486-35490, 2000.
47. **Leem, C.H. and R.D. Vaughan-Jones.** Sarcolemmal mechanisms for pHi recovery from alkalosis in the guinea-pig ventricular myocyte. *J Physiol* - 509 (Pt 2): 487-496, 1998.
48. **Forgac, M.** Structure and properties of the vacuolar (H⁺)-ATPases. *J Biol Chem* - 274: 12951-12954, 1999.
49. **van Adelsberg, J. and Q. Al-Awqati.** Regulation of cell pH by Ca²⁺-mediated exocytotic insertion of H⁺-ATPases. *J Cell Biol* - 102: 1638-1645, 1986.
50. **Martinez-Zaguilan, R., R.M. Lynch, G.M. Martinez, and R.J. Gillies.** Vacuolar-type H(+)-ATPases are functionally expressed in plasma membranes of human tumor cells. *Am J Physiol* - 265: C1015-C1029, 1993.
51. **Pappas, C.A. and B.R. Ransom.** A depolarization-stimulated, bafilomycin-inhibitable H⁺ pump in hippocampal astrocytes. *Glia* - 9: 280-291, 1993.
52. **Volk, C., T. Albert, and O.S. Kempster.** A proton-translocating H⁺-ATPase is involved in C6 glial pH regulation. *Biochim Biophys Acta* - 1372: 28-36, 1998.
53. **Swallow, C.J., S. Grinstein, and O.D. Rotstein.** A vacuolar type H(+)-ATPase regulates cytoplasmic pH in murine macrophages. *J Biol Chem* - 265: 7645-7654, 1990.
54. **Nordstrom, T., L.D. Shrode, O.D. Rotstein, R. Romanek, T. Goto, J.N. Heersche, M.F. Manolson, G.F. Brisseau, and S. Grinstein.** Chronic extracellular acidosis induces plasmalemmal vacuolar type H⁺ ATPase activity in osteoclasts. *J Biol Chem* - 272: 6354-6360, 1997.
55. **Wadsworth, S.J. and G.D. van Rossum.** Role of vacuolar adenosine triphosphatase in the regulation of cytosolic pH in hepatocytes. *J Membr Biol* - 142: 21-34, 1994.
56. **DeCoursey, T.E.** Hypothesis: do voltage-gated H(+) channels in alveolar epithelial cells contribute to CO(2) elimination by the lung? *Am J Physiol Cell Physiol* - 278: C1-C10, 2000.
57. **Eder, C. and T.E. DeCoursey.** Voltage-gated proton channels in microglia. *Prog Neurobiol* - 64: 277-305, 2001.

58. **DeCoursey, T.E. and V.V. Cherny.** Common themes and problems of bioenergetics and voltage-gated proton channels. *Biochim Biophys Acta* - 1458: 104-119, 2000.
59. **Thomas, R.C. and R.W. Meech.** Hydrogen ion currents and intracellular pH in depolarized voltage-clamped snail neurones. *Nature* - 299: 826-828, 1982.
60. **Orchard, C.H. and J.C. Kentish.** Effects of changes of pH on the contractile function of cardiac muscle. *Am J Physiol* - 258: C967-C981, 1990.
61. **Shrode, L.D., H. Tapper, and S. Grinstein.** Role of intracellular pH in proliferation, transformation, and apoptosis. *J Bioenerg Biomembr* - 29: 393-399, 1997.
62. **Tominaga, T., T. Ishizaki, S. Narumiya, and D.L. Barber.** p160ROCK mediates RhoA activation of Na-H exchange. *EMBO J* - 17: 4712-4722, 1998.
63. **Trivedi, B. and W.H. Danforth.** Effect of pH on the kinetics of frog muscle phosphofructokinase. *J Biol Chem* - 241: 4110-4112, 1966.
64. **Nicholson, C. and E. Sykova.** Extracellular space structure revealed by diffusion analysis. *Trends Neurosci* - 21: 207-215, 1998.
65. **Kaila K and Chesler M.** Activity-evoked changes in extracellular pH. In: *pH and Brain Function*, edited by Kaila K and Ransom BR. Wiley Liss, 1998, p. 309-338.
66. **Chesler, M. and K. Kaila.** Modulation of pH by neuronal activity. *Trends Neurosci* - 15: 396-402, 1992.
67. **Ransom, B.R.** Glial modulation of neural excitability mediated by extracellular pH: a hypothesis. *Prog Brain Res* - 94: 37-46, 1992.
68. **Somjen, G.G. and G.C. Tombaugh.** pH modulation of neuronal excitability and central nervous system functions. In: *pH and Brain Function*, edited by Kaila K and Ransom BR. Wiley Liss, 1998, p. 373-394.
69. **Tombaugh, G.C. and G.G. Somjen.** pH modulation of voltage-gated ion channels. In: *pH and Brain Function*, edited by Kaila K and Ransom BR. Wiley Liss, 1998, p. 395-416.
70. **Traynelis, S.F.** pH modulation of ligand-gated ion channels. In: *pH and Brain Function*, edited by Kaila K and Ransom BR. Wiley Liss, 1998, p. 417-446.
71. **Tombaugh, G.C. and G.G. Somjen.** Effects of extracellular pH on voltage-gated Na⁺, K⁺ and Ca²⁺ currents in isolated rat CA1 neurons. *J Physiol* - 493 (Pt 3): 719-732, 1996.
72. **Coulter, K.L., F. Perier, C.M. Radeke, and C.A. Vandenberg.** Identification and molecular localization of a pH-sensing domain for the inward rectifier potassium channel HIR. *Neuron* - 15: 1157-1168, 1995.

73. **Tombaugh, G.C. and G.G. Somjen.** Differential sensitivity to intracellular pH among high- and low-threshold Ca^{2+} currents in isolated rat CA1 neurons. *J Neurophysiol* - 77: 639-653, 1997.
74. **Krishek, B.J., A. Amato, C.N. Connolly, S.J. Moss, and T.G. Smart.** Proton sensitivity of the GABA(A) receptor is associated with the receptor subunit composition. *J Physiol* - 492 (Pt 2): 431-443, 1996.
75. **Traynelis, S.F., M. Hartley, and S.F. Heinemann.** Control of proton sensitivity of the NMDA receptor by RNA splicing and polyamines. *Science* - 268: 873-876, 1995.
76. **Waldmann, R. and M. Lazdunski.** H^{+} -gated cation channels: neuronal acid sensors in the NaC/DEG family of ion channels. *Curr Opin Neurobiol* - 8: 418-424, 1998.
77. **Spray D.C. and Scemes E.** Effects of intracellular pH (and Ca^{2+}) on gap junction channels. In: *pH and Brain Function*, edited by Kaila K and Ransom BR. Wiley Liss, 1998, p. 477-490.
78. **Ballanyi K and Kaila K.** Activity evoked changes in intracellular pH. In: *pH and Brain Function*, edited by Kaila K and Ransom BR. Wiley Liss, 1998, p. 291-308.
79. **Billups, B., D. Rossi, and D. Attwell.** Anion conductance behavior of the glutamate uptake carrier in salamander retinal glial cells. *J Neurosci* - 16: 6722-6731, 1996.
80. **Billups, B. and D. Attwell.** Modulation of non-vesicular glutamate release by pH. *Nature* - 379: 171-174, 1996.
81. **Bevensee, M.O. and W.F. Boron.** pH regulation in mammalian neurons. In: *pH and Brain Function*, edited by Kaila K and Ransom BR. Wiley Liss, 1998, p. 211-232.
82. **Rose, C.R. and Ransom B.R.** pH regulation in mammalian glia. In: *pH and Brain Function*, edited by Kaila K and Ransom BR. Wiley Liss, 1998, p. 253-276.
83. **Trapp, S., M. Luckermann, K. Kaila, and K. Ballanyi.** Acidosis of hippocampal neurones mediated by a plasmalemmal $\text{Ca}^{2+}/\text{H}^{+}$ pump. *Neuroreport* - 7: 2000-2004, 1996.
84. **Schmitt, B.M., U.V. Berger, R.M. Douglas, M.O. Bevensee, M.A. Hediger, G.G. Haddad, and W.F. Boron.** Na/HCO_3 cotransporters in rat brain: expression in glia, neurons, and choroid plexus. *J Neurosci* - 20: 6839-6848, 2000.
85. **Grichtchenko, I.I. and M. Chesler.** Depolarization-induced alkalization of astrocytes in gliotic hippocampal slices. *Neuroscience* - 62: 1071-1078, 1994.
86. **Grichtchenko, I.I. and M. Chesler.** Depolarization-induced acid secretion in gliotic hippocampal slices. *Neuroscience* - 62: 1057-1070, 1994.
87. **Pappas, C.A. and B.R. Ransom.** Depolarization-induced alkalization (DIA) in rat hippocampal astrocytes. *J Neurophysiol* - 72: 2816-2826, 1994.

88. Counillon, L. and J. Pouyssegur. The expanding family of eucaryotic Na⁺/H⁺ exchangers. *J Biol Chem* - 275: 1-4, 2000.
89. Numata, M., K. Petrecca, N. Lake, and J. Orlowski. Identification of a mitochondrial Na⁺/H⁺ exchanger. *J Biol Chem* - 273: 6951-6959, 1998.
90. Numata, M. and J. Orlowski. Molecular cloning and characterization of a novel (Na⁺,K⁺)/H⁺ exchanger localized to the trans-Golgi network. *J Biol Chem* - 276: 17387-17394, 2001.
91. Orlowski, J. and S. Grinstein. Na⁺/H⁺ exchangers of mammalian cells. *J Biol Chem* - 272: 22373-22376, 1997.
92. Wakabayashi, S., M. Shigekawa, and J. Pouyssegur. Molecular physiology of vertebrate Na⁺/H⁺ exchangers. *Physiol Rev* - 77: 51-74, 1997.
93. Putney, L.K., S.P. Denker, and D.L. Barber. THE CHANGING FACE OF THE Na⁺/H⁺ EXCHANGER, NHE1: Structure, Regulation, and Cellular Actions. *Annu Rev Pharmacol Toxicol* - 42: 527-552, 2002.
94. Iannuzzi, P. Delineation of Structural Domains of the Na⁺/H⁺ Exchanger Isoform 1. 2000.
(GENERIC)
Ref Type: Thesis/Dissertation
95. Khadilkar, A., P. Iannuzzi, and J. Orlowski. Identification of sites in the second exomembrane loop and ninth transmembrane helix of the mammalian Na⁺/H⁺ exchanger important for drug recognition and cation translocation. *J Biol Chem* - 276: 43792-43800, 2001.
96. Wakabayashi, S., T. Pang, X. Su, and M. Shigekawa. A novel topology model of the human Na⁺/H⁺ exchanger isoform 1. *J Biol Chem* - 275: 7942-7949, 2000.
97. Biemesderfer, D., B. DeGray, and P.S. Aronson. Membrane topology of NHE3. Epitopes within the carboxyl-terminal hydrophilic domain are exoplasmic. *J Biol Chem* - 273: 12391-12396, 1998.
98. Williams, K.A. Three-dimensional structure of the ion-coupled transport protein NhaA. *Nature* - 403: 112-115, 2000.
99. Fafournoux, P., J. Noel, and J. Pouyssegur. Evidence that Na⁺/H⁺ exchanger isoforms NHE1 and NHE3 exist as stable dimers in membranes with a high degree of specificity for homodimers. *J Biol Chem* - 269: 2589-2596, 1994.
100. Fliegel, L., R.S. Haworth, and J.R. Dyck. Characterization of the placental brush border membrane Na⁺/H⁺ exchanger: identification of thiol-dependent transitions in apparent molecular size. *Biochem J* - 289 (Pt 1): 101-107, 1993.
101. Counillon, L., J. Pouyssegur, and R.A. Reithmeier. The Na⁺/H⁺ exchanger NHE-1 possesses N- and O-linked glycosylation restricted to the first N-terminal extracellular domain. *Biochemistry* - 33: 10463-10469, 1994.

102. **Tse, C.M., S.A. Levine, C.H. Yun, S. Khurana, and M. Donowitz.** Na⁺/H⁺ exchanger-2 is an O-linked but not an N-linked sialoglycoprotein. *Biochemistry* - 33: 12954-12961, 1994.
103. **Orlowski, J.** Heterologous expression and functional properties of amiloride high affinity (NHE-1) and low affinity (NHE-3) isoforms of the rat Na/H exchanger. *J Biol Chem* - 268: 16369-16377, 1993.
104. **Yu, F.H., G.E. Shull, and J. Orlowski.** Functional properties of the rat Na/H exchanger NHE-2 isoform expressed in Na/H exchanger-deficient Chinese hamster ovary cells. *J Biol Chem* - 268: 25536-25541, 1993.
105. **Aronson, P.S., M.A. Suhm, and J. Nee.** Interaction of external H⁺ with the Na⁺-H⁺ exchanger in renal microvillus membrane vesicles. *J Biol Chem* - 258: 6767-6771, 1983.
106. **Paris, S. and J. Pouyssegur.** Biochemical characterization of the amiloride-sensitive Na⁺/H⁺ antiport in Chinese hamster lung fibroblasts. *J Biol Chem* - 258: 3503-3508, 1983.
107. **Aronson, P.S.** Kinetic properties of the plasma membrane Na⁺-H⁺ exchanger. *Annu Rev Physiol* - 47: 545-560, 1985.
108. **Aronson, P.S., J. Nee, and M.A. Suhm.** Modifier role of internal H⁺ in activating the Na⁺-H⁺ exchanger in renal microvillus membrane vesicles. *Nature* - 299: 161-163, 1982.
109. **Bookstein, C., M.W. Musch, A. DePaoli, Y. Xie, K. Rabenau, M. Villereal, M.C. Rao, and E.B. Chang.** Characterization of the rat Na⁺/H⁺ exchanger isoform NHE4 and localization in rat hippocampus. *Am.J.Physiol.Cell Physiol.* 271: C1629-C1638, 1996.
110. **Counillon, L., W. Scholz, H.J. Lang, and J. Pouyssegur.** Pharmacological characterization of stably transfected Na⁺/H⁺ antiporter isoforms using amiloride analogs and a new inhibitor exhibiting anti-ischemic properties. *Mol.Pharmacol.* 44: 1041-1045, 1993.
111. **Kleyman, T.R. and E.J.J. Cragoe.** Amiloride and its analogs as tools in the study of ion transport. *J Membr Biol* - 105: 1-21, 1988.
112. **Orlowski, J. and R.A. Kandasamy.** Delineation of transmembrane domains of the Na⁺/H⁺ exchanger that confer sensitivity to pharmacological antagonists. *J.Biol.Chem.* 271: 19922-19927, 1996.
113. **Karmazyn, M., X.T. Gan, R.A. Humphreys, H. Yoshida, and K. Kusumoto.** The myocardial Na(+)-H(+) exchange: structure, regulation, and its role in heart disease. *Circ Res* - 85: 777-786, 1999.
114. **Scholz, W., U. Albus, L. Counillon, H. Gögelein, H.-J. Lang, W. Linz, A. Weichert, and B.A. Schölkens.** Protective effects of HOE642, a selective sodium-hydrogen exchange subtype 1 inhibitor, on cardiac ischaemia and reperfusion. *Cardiovasc.Res.* 29: 260-268, 1995.
115. **Karmazyn, M.** Role of sodium-hydrogen exchange in cardiac hypertrophy and heart failure: a novel and promising therapeutic target. *Basic Res Cardiol* - 96: 325-328, 2001.

116. Fischer, H., A. Seelig, N. Beier, P. Raddatz, and J. Seelig. New drugs for the Na⁺/H⁺ exchanger. Influence of Na⁺ concentration and determination of inhibition constants with a microphysiometer. *J Membr Biol* - 168: 39-45, 1999.
117. Lorrain, J., V. Briand, E. Favennec, N. Duval, A. Grosset, P. Janiak, C. Hoornaert, G. Cremer, C. Latham, and S.E. O'Connor. Pharmacological profile of SL 59.1227, a novel inhibitor of the sodium/hydrogen exchanger. *Br J Pharmacol* - 131: 1188-1194, 2000.
118. Knight, D.R., A.H. Smith, D.M. Flynn, J.T. MacAndrew, S.S. Ellery, J.X. Kong, R.B. Marala, R.T. Wester, A. Guzman-Perez, R.J. Hill, W.P. Magee, and W.R. Tracey. A novel sodium-hydrogen exchanger isoform-1 inhibitor, zoniporide, reduces ischemic myocardial injury in vitro and in vivo. *J Pharmacol Exp Ther* - 297: 254-259, 2001.
119. Kawamoto, T., H. Kimura, K. Kusumoto, S. Fukumoto, M. Shiraishi, T. Watanabe, and H. Sawada. Potent and selective inhibition of the human Na⁺/H⁺ exchanger isoform NHE1 by a novel aminoguanidine derivative T-162559. *Eur J Pharmacol* - 420: 1-8, 2001.
120. Schwark, J.R., H.W. Jansen, H.J. Lang, W. Krick, G. Burckhardt, and M. Hropot. S3226, a novel inhibitor of Na⁺/H⁺ exchanger subtype 3 in various cell types. *Pflugers Arch* - 436: 797-800, 1998.
121. Counillon, L., A. Franchi, and J. Pouyssegur. A point mutation of the Na⁺/H⁺ exchanger gene (NHE1) and amplification of the mutated allele confer amiloride resistance upon chronic acidosis. *Proc.Natl.Acad.Sci. USA* 90: 4508-4512, 1993.
122. Wang, D., D.F. Balkovetz, and D.G. Warnock. Mutational analysis of transmembrane histidines in the amiloride-sensitive Na⁺/H⁺ exchanger. *Am J Physiol* - 269: C392-C402, 1995.
123. Touret, N., P. Poujeol, and L. Counillon. Second-site revertants of a low-sodium-affinity mutant of the Na⁺/H⁺ exchanger reveal the participation of TM4 into a highly constrained sodium-binding site. *Biochemistry* - 40: 5095-5101, 2001.
124. Denker, S.P., D.C. Huang, J. Orlowski, H. Furthmayr, and D.L. Barber. Direct binding of the Na⁺-H exchanger NHE1 to ERM proteins regulates the cortical cytoskeleton and cell shape independently of H(+) translocation. *Mol Cell* - 6: 1425-1436, 2000.
125. Bell, S.M., C.M. Schreiner, P.J. Schultheis, M.L. Miller, R.L. Evans, C.V. Vorhees, G.E. Shull, and W.J. Scott. Targeted disruption of the murine Nhe1 locus induces ataxia, growth retardation, and seizures. *Am J Physiol* - 276: C788-C795, 1999.
126. Cox, G.A., C.M. Lutz, C.L. Yang, D. Biemesderfer, R.T. Bronson, A. Fu, P.S. Aronson, J.L. Noebels, and W.N. Frankel. Sodium/hydrogen exchanger gene defect in slow-wave epilepsy mutant mice. *Cell* - 91: 139-148, 1997.
127. Bookstein, C., Y. Xie, K. Rabenau, M.W. Musch, R.L. McSwine, M.C. Rao, and E.B. Chang. Tissue distribution of Na⁺/H⁺ exchanger isoforms NHE2 and NHE4 in rat intestine and kidney. *Am J Physiol* - 273: C1496-C1505, 1997.

128. **Malakooti, J., R.Y. Dahdal, L. Schmidt, T.J. Layden, P.K. Dudeja, and K. Ramaswamy.** Molecular cloning, tissue distribution, and functional expression of the human Na(+)/H(+) exchanger NHE2. *Am J Physiol* - 277: G383-G390, 1999.
129. **Wang, Z., J. Orlowski, and G.E. Shull.** Primary structure and functional expression of a novel gastrointestinal isoform of the rat Na/H exchanger. *J Biol Chem* - 268: 11925-11928, 1993.
130. **Chow, C.W., M. Woodside, N. Demaurex, F.H. Yu, P. Plant, D. Rotin, S. Grinstein, and J. Orlowski.** Proline-rich motifs of the Na+/H+ exchanger 2 isoform. Binding of Src homology domain 3 and role in apical targeting in epithelia. *J Biol Chem* - 274: 10481-10488, 1999.
131. **Schultheis, P.J., L.L. Clarke, P. Meneton, M. Harline, G.P. Boivin, G. Stemmermann, J.J. Duffy, T. Doetschman, M.L. Miller, and G.E. Shull.** Targeted disruption of the murine Na⁺/H⁺ exchanger isoform 2 gene causes reduced viability of gastric parietal cells and loss of net acid secretion. *J.Clin.Invest.* 101: 1243-1253, 1998.
132. **Orlowski, J., R.A. Kandasamy, and G.E. Shull.** Molecular cloning of putative members of the Na/H exchanger gene family. cDNA cloning, deduced amino acid sequence, and mRNA tissue expression of the rat Na/H exchanger NHE-1 and two structurally related proteins. *J Biol Chem* - 267: 9331-9339, 1992.
133. **Schultheis, P.J., L.L. Clarke, P. Meneton, M.L. Miller, M. Soleimani, L.R. Gawenis, T.M. Riddle, J.J. Duffy, T. Doetschman, T. Wang, G. Giebisch, P.S. Aronson, J.N. Lorenz, and G.E. Shull.** Renal and intestinal absorptive defects in mice lacking the NHE3 Na⁺/H⁺ exchanger. *Nature Genet.* 19: 282-285, 1998.
134. **Pizzonia, J.H., D. Biemesderfer, A.K. Abu-Alfa, M.S. Wu, M. Exner, P. Isenring, P. Igarashi, and P.S. Aronson.** Immunochemical characterization of Na+/H+ exchanger isoform NHE4. *Am J Physiol* - 275: F510-F517, 1998.
135. **Roussa, E., S.L. Alper, and F. Thevenod.** Immunolocalization of anion exchanger AE2, Na(+)/H(+) exchangers NHE1 and NHE4, and vacuolar type H(+)-ATPase in rat pancreas. *J Histochem Cytochem* - 49: 463-474, 2001.
136. **Chambrey, R., P.L. St John, D. Eladari, F. Quentin, D.G. Warnock, D.R. Abrahamson, R.A. Podevin, and M. Paillard.** Localization and functional characterization of Na+/H+ exchanger isoform NHE4 in rat thick ascending limbs. *Am J Physiol Renal Physiol* - 281: F707-F717, 2001.
137. **Peti-Peterdi, J., R. Chambrey, Z. Bebok, D. Biemesderfer, P.L. St John, D.R. Abrahamson, D.G. Warnock, and P.D. Bell.** Macula densa Na(+)/H(+) exchange activities mediated by apical NHE2 and basolateral NHE4 isoforms. *Am J Physiol Renal Physiol* - 278: F452-F463, 2000.
138. **Moor, A.N. and L. Fliegel.** Protein kinase-mediated regulation of the Na(+)/H(+) exchanger in the rat myocardium by mitogen-activated protein kinase-dependent pathways. *J Biol Chem* - 274: 22985-22992, 1999.

139. **Takahashi, E., J. Abe, and B.C. Berk.** Angiotensin II stimulates p90rsk in vascular smooth muscle cells. A potential Na(+)-H+ exchanger kinase. *Circ Res* - 81: 268-273, 1997.
140. **Takahashi, E., J. Abe, B. Gallis, R. Aebersold, D.J. Spring, E.G. Krebs, and B.C. Berk.** p90(RSK) is a serum-stimulated Na+/H+ exchanger isoform-1 kinase. Regulatory phosphorylation of serine 703 of Na+/H+ exchanger isoform-1. *J Biol Chem* - 274: 20206-20214, 1999.
141. **Tominaga, T. and D.L. Barber.** Na-H exchange acts downstream of RhoA to regulate integrin-induced cell adhesion and spreading. *Mol Biol Cell* - 9: 2287-2303, 1998.
142. **Yan, W., K. Nehrke, J. Choi, and D.L. Barber.** The Nck-interacting kinase (NIK) phosphorylates the Na+-H+ exchanger NHE1 and regulates NHE1 activation by platelet-derived growth factor. *J Biol Chem* - 276: 31349-31356, 2001.
143. **Wakabayashi, S., B. Bertrand, T. Ikeda, J. Pouyssegur, and M. Shigekawa.** Mutation of calmodulin-binding site renders the Na+/H+ exchanger (NHE1) highly H(+)-sensitive and Ca2+ regulation-defective. *J Biol Chem* - 269: 13710-13715, 1994.
144. **Bertrand, B., S. Wakabayashi, T. Ikeda, J. Pouyssegur, and M. Shigekawa.** The Na+/H+ exchanger isoform 1 (NHE1) is a novel member of the calmodulin-binding proteins. Identification and characterization of calmodulin-binding sites. *J Biol Chem* - 269: 13703-13709, 1994.
145. **Wakabayashi, S., B. Bertrand, M. Shigekawa, P. Fafournoux, and J. Pouyssegur.** Growth factor activation and "H(+)-sensing" of the Na+/H+ exchanger isoform 1 (NHE1). Evidence for an additional mechanism not requiring direct phosphorylation. *J Biol Chem* - 269: 5583-5588, 1994.
146. **Pang, T., X. Su, S. Wakabayashi, and M. Shigekawa.** Calcineurin homologous protein as an essential cofactor for Na+/H+ exchangers. *J Biol Chem* - 276: 17367-17372, 2001.
147. **Kurashima, K., F.H. Yu, A.G. Cabado, E.Z. Szabo, S. Grinstein, and J. Orlowski.** Identification of sites required for down-regulation of Na+/H+ exchanger NHE3 activity by cAMP-dependent protein kinase. phosphorylation-dependent and -independent mechanisms. *J Biol Chem* - 272: 28672-28679, 1997.
148. **Weinman, E.J., D. Steplock, Y. Wang, and S. Shenolikar.** Characterization of a protein cofactor that mediates protein kinase A regulation of the renal brush border membrane Na(+)-H+ exchanger. *J Clin Invest* - 95: 2143-2149, 1995.
149. **Weinman, E.J., D. Steplock, M. Donowitz, and S. Shenolikar.** NHERF associations with sodium-hydrogen exchanger isoform 3 (NHE3) and ezrin are essential for cAMP-mediated phosphorylation and inhibition of NHE3. *Biochemistry* - 39: 6123-6129, 2000.
150. **Yun, C.H., S. Oh, M. Zizak, D. Steplock, S. Tsao, C.M. Tse, E.J. Weinman, and M. Donowitz.** cAMP-mediated inhibition of the epithelial brush border Na+/H+ exchanger, NHE3, requires an associated regulatory protein. *Proc Natl Acad Sci U S A* - 94: 3010-3015, 1997.

151. **Attapitaya, S., K. Nehrke, and J.E. Melvin.** Acute inhibition of brain-specific Na(+)/H(+) exchanger isoform 5 by protein kinases A and C and cell shrinkage. *Am J Physiol Cell Physiol* - 281: C1146-C1157, 2001.
152. **Hall, R.A., L.S. Ostedgaard, R.T. Premont, J.T. Blitzer, N. Rahman, M.J. Welsh, and R.J. Lefkowitz.** A C-terminal motif found in the beta2-adrenergic receptor, P2Y1 receptor and cystic fibrosis transmembrane conductance regulator determines binding to the Na+/H+ exchanger regulatory factor family of PDZ proteins. *Proc Natl Acad Sci U S A* - 95: 8496-8501, 1998.
153. **Fanning, A.S. and J.M. Anderson.** Protein modules as organizers of membrane structure. *Curr Opin Cell Biol* - 11: 432-439, 1999.
154. **D'Souza, S., A. Garcia-Cabado, F. Yu, K. Teter, G. Lukacs, K. Skorecki, H.P. Moore, J. Orlowski, and S. Grinstein.** The epithelial sodium-hydrogen antiporter Na+/H+ exchanger 3 accumulates and is functional in recycling endosomes. *J Biol Chem* - 273: 2035-2043, 1998.
155. **Chow, C.W., S. Khurana, M. Woodside, S. Grinstein, and J. Orlowski.** The epithelial Na(+)/H(+) exchanger, NHE3, is internalized through a clathrin-mediated pathway. *J Biol Chem* - 274: 37551-37558, 1999.
156. **Kurashima, K., E.Z. Szabo, G. Lukacs, J. Orlowski, and S. Grinstein.** Endosomal recycling of the Na+/H+ exchanger NHE3 isoform is regulated by the phosphatidylinositol 3-kinase pathway. *J Biol Chem* - 273: 20828-20836, 1998.
157. **Kurashima, K., S. D'Souza, K. Szaszi, R. Ramjeesingh, J. Orlowski, and S. Grinstein.** The apical Na(+)/H(+) exchanger isoform NHE3 is regulated by the actin cytoskeleton. *J Biol Chem* - 274: 29843-29849, 1999.
158. **Bubb, M.R., A.M. Senderowicz, E.A. Sausville, K.L. Duncan, and E.D. Korn.** Jasplakinolide, a cytotoxic natural product, induces actin polymerization and competitively inhibits the binding of phalloidin to F-actin. *J Biol Chem* - 269: 14869-14871, 1994.
159. **Spector, I., N.R. Shochet, D. Blasberger, and Y. Kashman.** Latrunculins--novel marine macrolides that disrupt microfilament organization and affect cell growth: I. Comparison with cytochalasin D. *Cell Motil Cytoskeleton* - 13: 127-144, 1989.
160. **MacLean-Fletcher, S. and T.D. Pollard.** Mechanism of action of cytochalasin B on actin. *Cell* - 20: 329-341, 1980.
161. **Gottlieb, T.A., I.E. Ivanov, M. Adesnik, and D.D. Sabatini.** Actin microfilaments play a critical role in endocytosis at the apical but not the basolateral surface of polarized epithelial cells. *J Cell Biol* - 120: 695-710, 1993.
162. **Brown, D. and I. Sabolic.** Endosomal pathways for water channel and proton pump recycling in kidney epithelial cells. *J Cell Sci Suppl* - 17: 49-59, 1993.

163. **Courtois-Coutry, N., D. Roush, V. Rajendran, J.B. McCarthy, J. Geibel, M. Kashgarian, and M.J. Caplan.** A tyrosine-based signal targets H/K-ATPase to a regulated compartment and is required for the cessation of gastric acid secretion. *Cell* - 90: 501-510, 1997.
164. **Donowitz, M., A. Janecki, S. Akhter, M.E. Cavet, F. Sanchez, G. Lamprecht, M. Zizak, W.L. Kwon, S. Khurana, C.H. Yun, and C.M. Tse.** Short-term regulation of NHE3 by EGF and protein kinase C but not protein kinase A involves vesicle trafficking in epithelial cells and fibroblasts. *Ann N Y Acad Sci* - 915: 30-42, 2000.
165. **O'Neill, W.C.** Physiological significance of volume-regulatory transporters. *Am J Physiol* - 276: C995-C1011, 1999.
166. **Kapus, A., S. Grinstein, S. Wasan, R. Kandasamy, and J. Orlowski.** Functional characterization of three isoforms of the Na⁺/H⁺ exchanger stably expressed in Chinese hamster ovary cells. ATP dependence, osmotic sensitivity, and role in cell proliferation. *J Biol Chem* - 269: 23544-23552, 1994.
167. **Grinstein, S., M. Woodside, C. Sardet, J. Pouyssegur, and D. Rotin.** Activation of the Na⁺/H⁺ antiporter during cell volume regulation. Evidence for a phosphorylation-independent mechanism. *J Biol Chem* - 267: 23823-23828, 1992.
168. **Grinstein, S., M. Woodside, T.K. Waddell, G.P. Downey, J. Orlowski, J. Pouyssegur, D.C. Wong, and J.K. Foskett.** Focal localization of the NHE-1 isoform of the Na⁺/H⁺ antiport: assessment of effects on intracellular pH. *EMBO J* - 12: 5209-5218, 1993.
169. **Ma, E. and G.G. Haddad.** Expression and localization of Na⁺/H⁺ exchangers in rat central nervous system. *Neuroscience* 79: 591-603, 1997.
170. **Douglas, R.M., B.M. Schmitt, Y. Xia, M.O. Bevensee, D. Biemesderfer, W.F. Boron, and G.G. Haddad.** Sodium-hydrogen exchangers and sodium-bicarbonate co-transporters: ontogeny of protein expression in the rat brain. *Neuroscience* - 102: 217-228, 1992.
171. **Wiemann, M., J.R. Schwark, U. Bonnet, H.W. Jansen, S. Grinstein, R.E. Baker, H.J. Lang, K. Wirth, and D. Bingmann.** Selective inhibition of the Na⁺/H⁺ exchanger type 3 activates CO₂/H⁺-sensitive medullary neurones. *Pflugers Arch* - 438: 255-262, 1999.
172. **Klanke, C.A., Y.R. Su, D.F. Callen, Z. Wang, P. Meneton, N. Baird, R.A. Kandasamy, J. Orlowski, B.E. Otterud, and M. Leppert.** Molecular cloning and physical and genetic mapping of a novel human Na⁺/H⁺ exchanger (NHE5/SLC9A5) to chromosome 16q22.1. *Genomics* - 25: 615-622, 1995.
173. **Pouyssegur, J., C. Sardet, A. Franchi, G. L'Allemain, and S. Paris.** A specific mutation abolishing Na⁺/H⁺ antiport activity in hamster fibroblasts precludes growth at neutral and acidic pH. *Proc Natl Acad Sci U S A* - 81: 4833-4837, 1984.
174. **Demaurex, N., J. Orlowski, G. Brisseau, M. Woodside, and S. Grinstein.** The mammalian Na⁺/H⁺ antiporters NHE-1, NHE-2, and NHE-3 are electroneutral and voltage independent, but can couple to an H⁺ conductance. *J Gen Physiol* - 106: 85-111, 1995.

175. **Attapitaya, S., K. Park, and J.E. Melvin.** Molecular cloning and functional expression of a rat Na⁺/H⁺ exchanger (NHE5) highly expressed in brain. *J Biol Chem* - 274: 4383-4388, 1999.
176. **Baird, N.R., J. Orlowski, E.Z. Szabo, H.C. Zaun, P.J. Schultheis, A.G. Menon, and G.E. Shull.** Molecular cloning, genomic organization, and functional expression of Na⁺/H⁺ exchanger isoform 5 (NHE5) from human brain. *J Biol Chem* - 274: 4377-4382, 1999.
177. **Chien, C.T., P.L. Bartel, R. Sternglanz, and S. Fields.** The two-hybrid system: a method to identify and clone genes for proteins that interact with a protein of interest. *Proc Natl Acad Sci U S A* - 88: 9578-9582, 1991.
178. **Borgese, F., M. Malapert, B. Fievet, J. Pouyssegur, and R. Motais.** The cytoplasmic domain of the Na⁺/H⁺ exchangers (NHEs) dictates the nature of the hormonal response: behavior of a chimeric human NHE1/trout beta NHE antiporter. *Proc Natl Acad Sci U S A* - 91: 5431-5435, 1994.
179. **Cabado, A.G., F.H. Yu, A. Kapus, G. Lukacs, S. Grinstein, and J. Orlowski.** Distinct structural domains confer cAMP sensitivity and ATP dependence to the Na⁺/H⁺ exchanger NHE3 isoform. *J Biol Chem* - 271: 3590-3599, 1996.
180. **Wakabayashi, S., T. Ikeda, J. Noel, B. Schmitt, J. Orlowski, J. Pouyssegur, and M. Shigekawa.** Cytoplasmic domain of the ubiquitous Na⁺/H⁺ exchanger NHE1 can confer Ca²⁺ responsiveness to the apical isoform NHE3. *J Biol Chem* - 270: 26460-26465, 1995.
181. **Eisenberg, D., E. Schwarz, M. Komaromy, and R. Wall.** Analysis of membrane and surface protein sequences with the hydrophobic moment plot. *J Mol Biol* - 179: 125-142, 1984.
182. **Kozak, M.** Compilation and analysis of sequences upstream from the translational start site in eukaryotic mRNAs. *Nucleic Acids Res* - 12: 857-872, 1984.
183. **Chen, C. and H. Okayama.** High-efficiency transformation of mammalian cells by plasmid DNA. *Mol Cell Biol* - 7: 2745-2752, 1987.
184. **Traynelis, S.F. and S.G. Cull-Candy.** Proton inhibition of N-methyl-D-aspartate receptors in cerebellar neurons. *Nature* - 345: 347-350, 1990.
185. **Zhai, J., R.W. Peoples, and C. Li.** Proton inhibition of GABA-activated current in rat primary sensory neurons. *Pflugers Arch* - 435: 539-545, 1998.
186. **Church, J., K.A. Baxter, and J.G. McLarnon.** pH modulation of Ca²⁺ responses and a Ca²⁺-dependent K⁺ channel in cultured rat hippocampal neurones. *J Physiol* - 511 (Pt 1): 119-132, 1998.
187. **Kiss, L. and S.J. Korn.** Modulation of N-type Ca²⁺ channels by intracellular pH in chick sensory neurons. *J Neurophysiol* - 81: 1839-1847, 1999.
188. **Tombaugh, G.C. and G.G. Somjen.** Effects of extracellular pH on voltage-gated Na⁺, K⁺ and Ca²⁺ currents in isolated rat CA1 neurons. *J Physiol* - 493 (Pt 3): 719-732, 1996.

189. **Tombaugh, G.C. and G.G. Somjen.** Differential sensitivity to intracellular pH among high- and low-threshold Ca^{2+} currents in isolated rat CA1 neurons. *J Neurophysiol* - 77: 639-653, 1997.
190. **Rorig, B., G. Klaus, and B. Sutor.** Intracellular acidification reduced gap junction coupling between immature rat neocortical pyramidal neurones. *J Physiol* - 490 (Pt 1): 31-49, 1996.
191. **Babinski, K., K.T. Le, and P. Seguela.** Molecular cloning and regional distribution of a human proton receptor subunit with biphasic functional properties. *J Neurochem* - 72: 51-57, 1999.
192. **Brookes, N.** Intracellular pH as a regulatory signal in astrocyte metabolism. *Glia* - 21: 64-73, 1997.
193. **Takahashi, K.I. and D.R. Copenhagen.** Modulation of neuronal function by intracellular pH. *Neurosci Res* - 24: 109-116, 1996.
194. **Baxter, K.A. and J. Church.** Characterization of acid extrusion mechanisms in cultured fetal rat hippocampal neurones. *J Physiol* - 493 (Pt 2): 457-470, 1996.
195. **Raley-Susman, K.M., E.J. Cragoe, Jr., R.M. Sapolsky, and R.R. Kopito.** Regulation of intracellular pH in cultured hippocampal neurons by an amiloride-insensitive Na^+/H^+ exchanger. *J.Biol.Chem.* 266: 2739-2745, 1991.
196. **Raley-Susman, K.M., R.M. Sapolsky, and R.R. Kopito.** $\text{Cl}^-/\text{HCO}_3^-$ exchange function differs in adult and fetal rat hippocampal neurons. *Brain Res.* 614: 308-314, 1993.
197. **Ritucci, N.A., L. Chambers-Kersh, J.B. Dean, and R.W. Putnam.** Intracellular pH regulation in neurons from chemosensitive and nonchemosensitive areas of the medulla. *Am.J.Physiol.Regul.Integr.Comp.Physiol.* 275: R1152-R1163, 1998.
198. **Tolkovsky, A.M. and C.D. Richards.** Na^+/H^+ exchange is the major mechanism of pH regulation in cultured sympathetic neurons: measurements in single cell bodies and neurites using a fluorescent pH indicator. *Neuroscience* 22: 1093-1102, 1987.
199. **Gaillard, S. and J.L. Dupont.** Ionic control of intracellular pH in rat cerebellar Purkinje cells maintained in culture. *J Physiol* - 425: 71-83, 1990.
200. **Jean, T., C. Frelin, P. Vigne, P. Barbry, and M. Lazdunski.** Biochemical properties of the Na^+/H^+ exchange system in rat brain synaptosomes. Interdependence of internal and external pH control of the exchange activity. *J.Biol.Chem.* 260: 9678-9684, 1985.
201. **Boyarsky, G., B. Ranson, W.-R. Schlue, M.B.E. Davis, and W.F. Boron.** Intracellular pH regulation in single cultured astrocytes from rat forebrain. *GLIA* 8: 241-248, 1993.
202. **Boussouf, A., R.C. Lambert, and S. Gaillard.** Voltage-dependent $\text{Na}^+-\text{HCO}_3^-$ cotransporter and Na^+/H^+ exchanger are involved in intracellular pH regulation of cultured mature rat cerebellar oligodendrocytes. *GLIA* 19: 74-84, 1997.

203. Benos, D.J., S. McPherson, B.H. Hahn, M.A. Chaikin, and E.N. Benveniste. Cytokines and HIV envelope glycoprotein gp120 stimulate Na^+/H^+ exchange in astrocytes. *J.Biol.Chem.* 269: 13811-13816, 1994.
204. Rotin, D. and S. Grinstein. Impaired cell volume regulation in Na^+/H^+ exchange-deficient mutants. *Am.J.Physiol.* 257: C1158-C1165, 1989.
205. Franchi, A., D. Perucca-Lostanlen, and J. Pouyssegur. Functional expression of a human Na^+/H^+ antiporter gene transfected into antiporter-deficient mouse L cells. *Proc Natl Acad Sci USA* - 83: 9388-9392, 1986.
206. Thomas, J.A., R.N. Buchsbaum, A. Zimniak, and E. Racker. Intracellular pH measurements in Ehrlich ascites tumor cells utilizing spectroscopic probes generated in situ. *Biochemistry* - 18: 2210-2218, 1979.
207. Lazdunski, M., C. Frelin, and P. Vigne. The sodium/hydrogen exchange system in cardiac cells: its biochemical and pharmacological properties and its role in regulating internal concentrations of sodium and internal pH. *J.Mol.Cell.Cardiol.* 17: 1029-1042, 1985.
208. Ives, H.E., V.J. Yee, and D.G. Warnock. Mixed type inhibition of the renal Na^+/H^+ antiporter by Li^+ and amiloride. Evidence for a modifier site. *J.Biol.Chem.* 258: 9710-9716, 1983.
209. Levine, S.A., M.H. Montrose, C.M. Tse, and M. Donowitz. Kinetics and regulation of three cloned mammalian Na^+/H^+ exchangers stably expressed in a fibroblast cell line. *J.Biol.Chem.* 268: 25527-25535, 1993.
210. Chambrey, R., J.M. Achard, and D.G. Warnock. Heterologous expression of rat NHE4: a highly amiloride-resistant Na^+/H^+ exchanger isoform. *Am J Physiol* - 272: C90-C98, 1997.
211. Chambrey, R., J.M. Achard, P.L. St John, D.R. Abrahamson, and D.G. Warnock. Evidence for an amiloride-insensitive Na^+/H^+ exchanger in rat renal cortical tubules. *Am.J.Physiol.* 273: C1064-C1074, 1997.
212. Lenox, R.H., R.K. McNamara, R.L. Papke, and H.K. Manji. Neurobiology of lithium: an update. *J Clin Psychiatry* - 59 Suppl 6: 37-47, 1998.
213. Otsu, K., J.L. Kinsella, E. Koh, and J.P. Froehlich. Proton dependence of the partial reactions of the sodium-proton exchanger in renal brush border membranes. *J.Biol.Chem.* 267: 8089-8096, 1992.
214. Boyarsky, G., M.B. Ganz, E.J.J. Cragoe, and W.F. Boron. Intracellular-pH dependence of Na^+/H^+ exchange and acid loading in quiescent and arginine vasopressin-activated mesangial cells. *Proc Natl Acad Sci U S A* 87: 5921-5924, 1990.
215. Burns, K.D., T. Homma, and R.C. Harris. Regulation of Na^+/H^+ exchange by ATP depletion and calmodulin antagonism in renal epithelial cells. *Am.J.Physiol.* 261: F607-F616, 1991.

216. **Cassel, D., M. Katz, and M. Rotman.** Depletion of cellular ATP inhibits the Na^+/H^+ antiport in cultured human cells. Modification of the regulatory effect of intracellular protons on antiporter activity. *J.Biol.Chem.* 261: 5460-5466, 1986.
217. **Little, P.J., P.L. Weissberg, E.J. Cragoe, Jr., and A. Bobik.** Dependence of Na^+/H^+ antiport activation in cultured rat aortic smooth muscle on calmodulin, calcium, and ATP. Evidence for the involvement of calmodulin-dependent kinases. *J.Biol.Chem.* 263: 16780-16786, 1988.
218. **Wakabayashi, S., P. Fafournoux, C. Sardet, and J. Pouyssegur.** The Na^+/H^+ antiporter cytoplasmic domain mediates growth factor signals and controls " H^+ -sensing". *Proc.Natl.Acad.Sci.USA* 89: 2424-2428, 1992.
219. **Goss, G.G., M. Woodside, S. Wakabayashi, J. Pouyssegur, T. Waddell, G.P. Downey, and S. Grinstein.** ATP dependence of NHE-1, the ubiquitous isoform of the Na^+/H^+ antiporter. Analysis of phosphorylation and subcellular localization. *J.Biol.Chem.* 269: 8741-8748, 1994.
220. **Ikeda, T., B. Schmitt, J. Pouyssegur, S. Wakabayashi, and M. Shigekawa.** Identification of cytoplasmic subdomains that control pH-sensing of the Na^+/H^+ exchanger (NHE1): pH-maintenance, ATP-Sensitive, and flexible loop domains. *J.Biochem.(Tokyo)* 121: 295-303, 1997.
221. **Aharonovitz, O., N. Demaurex, M. Woodside, and S. Grinstein.** ATP dependence is not an intrinsic property of Na^+/H^+ exchanger NHE1: requirement for an ancillary factor. *Am.J.Physiol.Cell Physiol.* 276: C1303-C1311, 1999.
222. **Demaurex, N., R.R. Romanek, J. Orlowski, and S. Grinstein.** ATP dependence of Na^+/H^+ exchange. Nucleotide specificity and assessment of the role of phospholipids. *J Gen Physiol* - 109: 117-128, 1997.
223. **Kandasamy, R.A., F.H. Yu, R. Harris, A. Boucher, J.W. Hanrahan, and J. Orlowski.** Plasma membrane Na^+/H^+ exchanger isoforms (NHE-1, -2, and -3) are differentially responsive to second messenger agonists of the protein kinase A and C pathways. *J Biol Chem* - 270: 29209-29216, 1995.
224. **Szabo, E.Z., M. Numata, G.E. Shull, and J. Orlowski.** Kinetic and pharmacological properties of human brain Na^+/H^+ exchanger isoform 5 stably expressed in Chinese hamster ovary cells. *J Biol Chem* - 275: 6302-6307, 2000.
225. **Gietz, R.D., R.H. Schiestl, A.R. Willems, and R.A. Woods.** Studies on the transformation of intact yeast cells by the LiAc/SS-DNA/PEG procedure. *Yeast* - 11: 355-360, 1995.
226. **Davies, S.P., D. Carling, and D.G. Hardie.** Tissue distribution of the AMP-activated protein kinase, and lack of activation by cyclic-AMP-dependent protein kinase, studied using a specific and sensitive peptide assay. *Eur J Biochem* - 186: 123-128, 1989.
227. **Cheung, P.C., I.P. Salt, S.P. Davies, D.G. Hardie, and D. Carling.** Characterization of AMP-activated protein kinase gamma-subunit isoforms and their role in AMP binding. *Biochem J* - 346 Pt 3: 659-669, 2000.

228. Gao, G., J. Widmer, D. Stapleton, T. Teh, T. Cox, B.E. Kemp, and L.A. Witters. Catalytic subunits of the porcine and rat 5'-AMP-activated protein kinase are members of the SNF1 protein kinase family. *Biochim Biophys Acta* - 1266: 73-82, 1995.
229. Gao, G., C.S. Fernandez, D. Stapleton, A.S. Auster, J. Widmer, J.R. Dyck, B.E. Kemp, and L.A. Witters. Non-catalytic beta- and gamma-subunit isoforms of the 5'-AMP-activated protein kinase. *J Biol Chem* - 271: 8675-8681, 1996.
230. Stapleton, D., K.I. Mitchelhill, G. Gao, J. Widmer, B.J. Michell, T. Teh, C.M. House, C.S. Fernandez, T. Cox, L.A. Witters, and B.E. Kemp. Mammalian AMP-activated protein kinase subfamily. *J Biol Chem* - 271: 611-614, 1996.
231. Stapleton, D., E. Woollatt, K.I. Mitchelhill, J.K. Nicholl, C.S. Fernandez, B.J. Michell, L.A. Witters, D.A. Power, G.R. Sutherland, and B.E. Kemp. AMP-activated protein kinase isoenzyme family: subunit structure and chromosomal location. *FEBS Lett* - 409: 452-456, 1997.
232. Thornton, C., M.A. Snowden, and D. Carling. Identification of a novel AMP-activated protein kinase beta subunit isoform that is highly expressed in skeletal muscle. *J Biol Chem* - 273: 12443-12450, 1998.
233. Woods, A., I. Salt, J. Scott, D.G. Hardie, and D. Carling. The alpha1 and alpha2 isoforms of the AMP-activated protein kinase have similar activities in rat liver but exhibit differences in substrate specificity in vitro. *FEBS Lett* - 397: 347-351, 1996.
234. Salt, I., J.W. Celler, S.A. Hawley, A. Prescott, A. Woods, D. Carling, and D.G. Hardie. AMP-activated protein kinase: greater AMP dependence, and preferential nuclear localization, of complexes containing the alpha2 isoform. *Biochem J* - 334 (Pt 1): 177-187, 1998.
235. Dale, S., W.A. Wilson, A.M. Edelman, and D.G. Hardie. Similar substrate recognition motifs for mammalian AMP-activated protein kinase, higher plant HMG-CoA reductase kinase-A, yeast SNF1, and mammalian calmodulin-dependent protein kinase I. *FEBS Lett* - 361: 191-195, 1995.
236. Kemp, B.E., K.I. Mitchelhill, D. Stapleton, B.J. Michell, Z.P. Chen, and L.A. Witters. Dealing with energy demand: the AMP-activated protein kinase. *Trends Biochem Sci* - 24: 22-25, 1999.
237. Dyck, J.R., G. Gao, J. Widmer, D. Stapleton, C.S. Fernandez, B.E. Kemp, and L.A. Witters. Regulation of 5'-AMP-activated protein kinase activity by the noncatalytic beta and gamma subunits. *J Biol Chem* - 271: 17798-17803, 1996.
238. Hardie, D.G., D. Carling, and M. Carlson. The AMP-activated/SNF1 protein kinase subfamily: metabolic sensors of the eukaryotic cell? *Annu Rev Biochem* - 67: 821-855, 1998.
239. Hallows, K.R., V. Raghuram, B.E. Kemp, L.A. Witters, and J.K. Foskett. Inhibition of cystic fibrosis transmembrane conductance regulator by novel interaction with the metabolic sensor AMP-activated protein kinase. *J Clin Invest* - 105: 1711-1721, 2000.

240. **Turnley, A.M., D. Stapleton, R.J. Mann, L.A. Witters, B.E. Kemp, and P.F. Bartlett.** Cellular distribution and developmental expression of AMP-activated protein kinase isoforms in mouse central nervous system. *J Neurochem* - 72: 1707-1716, 1999.
241. **Hardie, D.G. and S.A. Hawley.** AMP-activated protein kinase: the energy charge hypothesis revisited. *Bioessays* - 23: 1112-1119, 2001.
242. **Salt, I.P., G. Johnson, S.J. Ashcroft, and D.G. Hardie.** AMP-activated protein kinase is activated by low glucose in cell lines derived from pancreatic beta cells, and may regulate insulin release. *Biochem J* - 335 (Pt 3): 533-539, 1998.
243. **Krupnick, J.G. and J.L. Benovic.** The role of receptor kinases and arrestins in G protein-coupled receptor regulation. *Annu Rev Pharmacol Toxicol* - 38: 289-319, 1998.
244. **Ferguson, S.S.** Evolving concepts in G protein-coupled receptor endocytosis: the role in receptor desensitization and signaling. *Pharmacol Rev* - 53: 1-24, 2001.
245. **Pierce, K.L. and R.J. Lefkowitz.** Classical and new roles of beta-arrestins in the regulation of G-protein-coupled receptors. *Nat Rev Neurosci* - 2: 727-733, 2001.
246. **Luttrell, L.M., S.S. Ferguson, Y. Daaka, W.E. Miller, S. Maudsley, R.G. Della, F. Lin, H. Kawakatsu, K. Owada, D.K. Luttrell, M.G. Caron, and R.J. Lefkowitz.** Beta-arrestin-dependent formation of beta2 adrenergic receptor-Src protein kinase complexes. *Science* - 283: 655-661, 1999.
247. **Luttrell, L.M., F.L. Roudabush, E.W. Choy, W.E. Miller, M.E. Field, K.L. Pierce, and R.J. Lefkowitz.** Activation and targeting of extracellular signal-regulated kinases by beta-arrestin scaffolds. *Proc Natl Acad Sci U S A* - 98: 2449-2454, 2001.
248. **McDonald, P.H., C.W. Chow, W.E. Miller, S.A. Laporte, M.E. Field, F.T. Lin, R.J. Davis, and R.J. Lefkowitz.** Beta-arrestin 2: a receptor-regulated MAPK scaffold for the activation of JNK3. *Science* - 290: 1574-1577, 2000.
249. **Miller, W.E. and R.J. Lefkowitz.** Expanding roles for beta-arrestins as scaffolds and adapters in GPCR signaling and trafficking. *Curr Opin Cell Biol* - 13: 139-145, 2001.
250. **Gurevich, V.V., S.B. Dion, J.J. Onorato, J. Ptasienski, C.M. Kim, R. Sterne-Marr, M.M. Hosey, and J.L. Benovic.** Arrestin interactions with G protein-coupled receptors. Direct binding studies of wild type and mutant arrestins with rhodopsin, beta 2-adrenergic, and m2 muscarinic cholinergic receptors. *J Biol Chem* - 270: 720-731, 1995.
251. **Goodman, O.B.J., J.G. Krupnick, F. Santini, V.V. Gurevich, R.B. Penn, A.W. Gagnon, J.H. Keen, and J.L. Benovic.** Beta-arrestin acts as a clathrin adaptor in endocytosis of the beta2-adrenergic receptor. *Nature* - 383: 447-450, 1996.
252. **Laporte, S.A., R.H. Oakley, J. Zhang, J.A. Holt, S.S. Ferguson, M.G. Caron, and L.S. Barak.** The beta2-adrenergic receptor/betaarrestin complex recruits the clathrin adaptor AP-2 during endocytosis. *Proc Natl Acad Sci U S A* - 96: 3712-3717, 1999.

253. **Anborgh, P.H., J.L. Seachrist, L.B. Dale, and S.S. Ferguson.** Receptor/beta-arrestin complex formation and the differential trafficking and resensitization of beta2-adrenergic and angiotensin II type 1A receptors. *Mol Endocrinol* - 14: 2040-2053, 2000.
254. **Bremnes, T., J.D. Paasche, A. Mehllum, C. Sandberg, B. Bremnes, and H. Attramadal.** Regulation and intracellular trafficking pathways of the endothelin receptors. *J Biol Chem* - 275: 17596-17604, 2000.
255. **McConalogue, K., O. Dery, M. Lovett, H. Wong, J.H. Walsh, E.F. Grady, and N.W. Bunnett.** Substance P-induced trafficking of beta-arrestins. The role of beta-arrestins in endocytosis of the neurokinin-1 receptor. *J Biol Chem* - 274: 16257-16268, 1999.
256. **Oakley, R.H., S.A. Laporte, J.A. Holt, L.S. Barak, and M.G. Caron.** Association of beta-arrestin with G protein-coupled receptors during clathrin-mediated endocytosis dictates the profile of receptor resensitization. *J Biol Chem* - 274: 32248-32257, 1999.
257. **Trejo, J. and S.R. Coughlin.** The cytoplasmic tails of protease-activated receptor-1 and substance P receptor specify sorting to lysosomes versus recycling. *J Biol Chem* - 274: 2216-2224, 1999.
258. **Zhang, J., L.S. Barak, P.H. Anborgh, S.A. Laporte, M.G. Caron, and S.S. Ferguson.** Cellular trafficking of G protein-coupled receptor/beta-arrestin endocytic complexes. *J Biol Chem* - 274: 10999-11006, 1999.
259. **Barak, L.S., S.S. Ferguson, J. Zhang, and M.G. Caron.** A beta-arrestin/green fluorescent protein biosensor for detecting G protein-coupled receptor activation. *J Biol Chem* - 272: 27497-27500, 1997.
260. **Krupnick, J.G., F. Santini, A.W. Gagnon, J.H. Keen, and J.L. Benovic.** Modulation of the arrestin-clathrin interaction in cells. Characterization of beta-arrestin dominant-negative mutants. *J Biol Chem* - 272: 32507-32512, 1997.
261. **Orsini, M.J. and J.L. Benovic.** Characterization of dominant negative arrestins that inhibit beta2-adrenergic receptor internalization by distinct mechanisms. *J Biol Chem* - 273: 34616-34622, 1998.
262. **Hirsch, J.A., C. Schubert, V.V. Gurevich, and P.B. Sigler.** The 2.8 Å crystal structure of visual arrestin: a model for arrestin's regulation. *Cell* - 97: 257-269, 1999.
263. **Pinna, L.A. and M. Ruzzene.** How do protein kinases recognize their substrates? *Biochim Biophys Acta* - 1314: 191-225, 1996.
264. **Brunati, A.M., O. Marin, A. Folda, F. Meggio, and L.A. Pinna.** Possible implication of the Golgi apparatus casein kinase in the phosphorylation of vesicle docking protein p115 Ser-940: a study with peptide substrates. *Biochem Biophys Res Commun* - 284: 817-822, 2001.
265. **Kuenzel, E.A., J.A. Mulligan, J. Sommercorn, and E.G. Krebs.** Substrate specificity determinants for casein kinase II as deduced from studies with synthetic peptides. *J Biol Chem* - 262: 9136-9140, 1987.

266. **Litchfield, D.W., A. Arendt, F.J. Lozeman, E.G. Krebs, P.A. Hargrave, and K. Palczewski.** Synthetic phosphopeptides are substrates for casein kinase II. *FEBS Lett* - 261: 117-120, 1990.
267. **Fredericks, Z.L., J.A. Pitcher, and R.J. Lefkowitz.** Identification of the G protein-coupled receptor kinase phosphorylation sites in the human beta2-adrenergic receptor. *J Biol Chem* - 271: 13796-13803, 1996.
268. **Pitcher, J.A., N.J. Freedman, and R.J. Lefkowitz.** G protein-coupled receptor kinases. *Annu Rev Biochem* - 67: 653-692, 1998.
269. **Budd, D.C., J.E. McDonald, and A.B. Tobin.** Phosphorylation and regulation of a Gq/11-coupled receptor by casein kinase 1alpha. *J Biol Chem* - 275: 19667-19675, 2000.
270. **Hanyaloglu, A.C., M. Vrecl, K.M. Kroeger, L.E. Miles, H. Qian, W.G. Thomas, and K.A. Eidne.** Casein kinase II sites in the intracellular C-terminal domain of the thyrotropin-releasing hormone receptor and chimeric gonadotropin-releasing hormone receptors contribute to beta-arrestin-dependent internalization. *J Biol Chem* - 276: 18066-18074, 2001.
271. **Zhang, J., L.S. Barak, K.E. Winkler, M.G. Caron, and S.S. Ferguson.** A central role for beta-arrestins and clathrin-coated vesicle-mediated endocytosis in beta2-adrenergic receptor resensitization. Differential regulation of receptor resensitization in two distinct cell types. *J Biol Chem* - 272: 27005-27014, 1997.
272. **Menard, L., S.S. Ferguson, J. Zhang, F.T. Lin, R.J. Lefkowitz, M.G. Caron, and L.S. Barak.** Synergistic regulation of beta2-adrenergic receptor sequestration: intracellular complement of beta-adrenergic receptor kinase and beta-arrestin determine kinetics of internalization. *Mol Pharmacol* - 51: 800-808, 1997.
273. **Grady, E.F., A.M. Garland, P.D. Gamp, M. Lovett, D.G. Payan, and N.W. Bunnett.** Delineation of the endocytic pathway of substance P and its seven-transmembrane domain NK1 receptor. *Mol Biol Cell* - 6: 509-524, 1995.
274. **Krueger, K.M., Y. Daaka, J.A. Pitcher, and R.J. Lefkowitz.** The role of sequestration in G protein-coupled receptor resensitization. Regulation of beta2-adrenergic receptor dephosphorylation by vesicular acidification. *J Biol Chem* - 272: 5-8, 1997.
275. **Flanigan, K., K. Gardner, K. Alderson, B. Galster, B. Otterud, M.F. Leppert, C. Kaplan, and L.J. Ptacek.** Autosomal dominant spinocerebellar ataxia with sensory axonal neuropathy (SCA4): clinical description and genetic localization to chromosome 16q22.1. *Am J Hum Genet* - 59: 392-399, 1996.
276. **Zoghbi, H.Y. and H.T. Orr.** Glutamine repeats and neurodegeneration. *Annu Rev Neurosci* - 23: 217-247, 2000.